NASA CONTRACTOR REPORT

NASA CR-1473

INVESTIGATION OF THE MIXING AND COMBUSTION OF TURBULENT, COMPRESSIBLE FREE JETS

by Leonard S. Cohen and Roy N. Guile

Prepared by
UNITED AIRCRAFT RESEARCH LABORATORIES
East Hartford, Conn.
for Langley Research Center

NATIONAL AERONAUTICS AND SPACE ADMINISTRATION • WASHINGTON, D. C. • DECEMBER 1969

NASA CR-1473

INVESTIGATION OF THE MIXING AND COMBUSTION OF TURBULENT, COMPRESSIBLE FREE JETS

By Leonard S. Cohen and Roy N. Guile

Prepared under Contract No. NAS 1-7255 by
UNITED AIRCRAFT RESEARCH LABORATORIES
East Hartford, Conn.

for Langley Research Center

NATIONAL AERONAUTICS AND SPACE ADMINISTRATION

For sale by the Clearinghouse for Federal Scientific and Technical Information
Springfield, Virginia 22151 – Price $3.00

INVESTIGATION OF THE MIXING AND COMBUSTION OF TURBULENT, COMPRESSIBLE FREE JETS*

By Leonard S. Cohen
and Roy N. Guile
United Aircraft Research Laboratories

SUMMARY

The effect of combustion on the mixing of axisymmetric, supersonic, turbulent free jets was investigated experimentally using cooled probes, an Ebert spectrophotometer, high-speed motion pictures, and schlieren, infrared and ultraviolet photographs. Results of this work including detailed Mach number, temperature, and species concentration profiles are presented for the mixing of a Mach 1.46 central jet of cold hydrogen with a vitiated Mach 1.86 concentric outer jet. The flow conditions in the high temperature vitiated jet flow were adjusted to provide two different values of oxygen concentration in an effort to identify the separate effects of mixing vis-a-vis combustion. Static temperatures of the vitiated streams exceeded the H_2/O_2 autoignition value of 1000°K. Pressures in both jets were matched at approximately 0.91×10^5-N/m^2(0.9-atm). Samples aspirated from the flow through quenching probes were analyzed for species concentrations by employing an on-line gas chromatograph. Water concentration and local static temperature were also measured spectrophotometrically for comparison with the probe measurements. A comparison of mixing rates in equivalent combusting and inert jet flows showed little difference for the conditions studied. The data were also used to evaluate eddy viscosity models and provide information on ignition times and flamespreading angles. An eddy viscosity model which includes the effect of preturbulence and the variation of density through the mixing layer generates predictions which are in agreement with the test measurements.

*Information previously released in condensed form as AIAA Paper No. 69-538, "Measurements in Free Jet Mixing/Combusting Flows," at the AIAA 5th Propulsion Joint Specialist Conference, Colorado, June 9-13, 1969.

INTRODUCTION

Widespread interest in advanced air-breathing propulsion devices such as the supersonic combustion ramjet (scramjet) and the ducted rocket has motivated numerous analytical studies of the mixing and combustion of compressible, turbulent streams. These analyses are basically either of the integral type (Refs. 1 and 2) in which the conservation equations are satisfied over every cross section normal to the flow direction, or the detailed computational type in which the partial differential equations describing the physics of the flow field are solved directly along streamlines using numerical techniques (Refs. 3, 4, and 5). Whichever type is employed, a certain amount of empiricism must be introduced in order to specify the rate of mixing of fuel and air streams. The validity of any of the analyses is limited, therefore, by the extent and accuracy of available experimental information on jet mixing rates and/or kinematic eddy viscosities. Since high-temperature flow facilities and suitable instrumentation for use in supersonic combusting flows have only recently become available, these analyses have not, in general, been subjected to experimental confirmation.

The objective of the present work was to obtain detailed experimental data including pitot pressures, temperatures, and species concentrations throughout equivalent constant pressure inert and chemically reactive jet flow fields. This data was to be sufficiently definitive to reflect any significant influence of chemical heat release on mixing rates and to allow the characterization of the perturbed mixing rates with a suitable formulation for the kinematic eddy viscosity. In addition, special instrumentation techniques for use in combustion test environments including on-line gas chromatographic analysis and spectrophotometric determination of temperature and water concentration in axisymmetric flows, were to be employed and evaluated.

SYMBOLS

a	spectral absorptivity
b	transverse extent of mixing layer, m
B	line width, cm^{-1}/atm
c	sound speed, m/sec
C_1	$(2\pi)(\text{speed of light})^2 \times \text{Planck's constant} = 3.8139 \times 10^{-17}$ kg-m^3/sec
C_2	Planck's constant × speed of light/Boltzman's constant = 0.014838 m^oK

ER	equivalence ratio, $kgH_2/(kgH_2$-stoichiometric)
f_{H_2}	fraction of hydrogen unreacted
F	correlating parameter or "history," see Fig. 30
F'	history adjusted for intermixing effect, see Eq. (6)
Ie	gas spectral emission intensity per unit volume, $kg\text{-}m\text{-}sec^{-1}/m^3$
K	rate constant, cgs units-various
L	length of enclosure, m
m	ratio of vitiated stream velocity to centerline velocity
m_1	value of m at which preturbulence mechanism becomes important
M_j	mass fraction of species j
M	Mach number
n	ratio of vitiated stream density to centerline density
n_1	value of n at which preturbulence mechanism becomes important
p	partial pressure, N/m^2 (atm)
P	pressure, N/m^2 (atm)
PP	pitot pressure, N/m^2 (atm)
r_i	centerbody radius, cm
$r_{\frac{1}{2}}$	half-thickness of mixing layer determined using Eq. (17), m
R	gas constant, $cm^3\text{-}atm\text{-}{}^oK^{-1}/(gm\text{-}mole)$
S	line strength, cm/gm
T	temperature, ^oK
u	longitudinal velocity, m/sec
$\bar{u}$	average longitudinal velocity over computational segment, m/sec

v	transverse velocity, m/sec
W	mass flow rate, kg/sec
X	longitudinal distance from nozzle exit plane, cm
X_1	axial station at which preturbulence mechanism becomes important, cm
ΔX	length of computational segment, cm
Y_j	mole fraction of species j
Z	transverse distance from centerline, cm
δ	slit half-width, cm^{-1}
ϵ	kinematic eddy viscosity, m^2/sec
η	weighting factor, see Table VIII
θ	time, sec unless otherwise specified
κ	universal constant in mixing models
λ	wavelength, m
μ	molecular weight, gm/(gm-mole)
ν	frequency, sec^{-1}
ρ	density, kg/m^3
τ_{ID}	ignition delay time, sec
τ_R	reaction time, sec
$\Delta\tau$	residence time, sec
ϕ	$\equiv (M-M_a)/(M_\ell - M_a)$

Subscripts

a	vitiated stream
ℓ	centerline

i hydrogen jet

j species designation

k segment designation

n radial zone

o streamtube bounded by streamlines q and q + 1

q streamline designation

r resonant

t stagnation condition

EXPERIMENTAL STUDY

Discussion

An investigation of the effect of combustion on mixing requires the collection of and comparison between comparable measurements made in equivalent inert and reacting jet flows. To facilitate the acquisition of suitable data and the ultimate analytical treatment of the problem, a coaxial free jet system was chosen in which to produce such equivalent flows. The system consists of a central hydrogen jet surrounded by a high temperature annular jet containing various (adjustable) quantities of oxygen, nitrogen and water; a less reactive flow is simply produced by replacing most of the oxygen in the annular stream with nitrogen.

A high temperature is required in the annular jet to insure the rapid autoignition of hydrogen in the mixing layer formed between the jets. Heating of the annular jet is accomplished by the method variously referred to as vitiation or preburning. Hydrogen and air are combusted in a vitiation chamber to produce a high temperature gas flow, and additional make-up oxygen and/or nitrogen is added to obtain the desired weight flow and oxygen concentration. It is possible, in principle, to burn out all the oxygen in the air during vitiation to produce an inert flow containing only nitrogen and water. Alternatively, make-up oxygen may be added to yield any desired reactive flow.

Vitiation was selected over alternative heating methods including the use of a pebble bed (Ref. 6), arc jet (Ref. 7), shock tube (Ref. 8), or rocket (Ref. 9)

since associated run times can be relatively long depending on fuel and make-up gas storage capacity. Typical run times achieved ranged from 30-50 minutes. As a result of vitiation, water and various intermediate species such as H, O, and OH will be present in the annular jet. The effect of these contaminants, as discussed later in this paper, must be considered when treating the chemical reaction between the annular jet and hydrogen jet.

Test Apparatus

The experiments were conducted using the water-cooled UARL mixing and combustion test rig shown schematically in Fig. 1. High-pressure air is admitted at the upstream end of the rig and passed through a 2.54-cm diameter bellmouth flowmeter into the injection section where it is mixed with either make-up oxygen or nitrogen injected through flat-face rings. The resulting flow is then mixed and burned with hydrogen in the vitiation section. In tests requiring a reactive flow comparable to air, i.e., vitiated air, sufficient oxygen is injected so that it comprises approximately 21 volume percent of the resulting, high enthalpy vitiated stream. The total temperature of a vitiated air stream is typically 2000°K. The same temperature may be obtained for an inert (nitrogen) vitiated flow by reacting the oxygen in the air with hydrogen, and making up the desired total weight flow with additional nitrogen injection. In either case, the resulting vitiated flow is passed successively through a conical reducing section, a temperature measurement section, and an annular converging-diverging nozzle. The inner surface of the nozzle is formed by a centerbody held in place by three equispaced oval struts. Hydrogen introduced into the centerbody via the support struts is brought into contact with the vitiated stream at the exit of the nozzle section. The vitiated stream and central hydrogen jet mix (and burn) in the following free jet test region and ultimately exhaust into a large ejector duct where excess hydrogen is totally reacted prior to discharge to the atmosphere. Figure 2 is a photograph of the test facility.

Nozzle centerbody. - The nickel centerbody and support struts, shown detailed in the Fig. 3 drawing of the nozzle test section, are coated with 0.410-mm of insulating material to provide thermal protection. The insulation consists of three layers including: (1) a 651C nickel titanium 0.037-mm undercoat, (2) a 0.053-mm gradecoat of a 50-50 mixture of 651C nickel titanium and stabilized zirconia, and (3) a 0.32-mm zirconia outercoat. With this arrangement, no cooling other than that provided by the hydrogen is required. Four passages in each strut channel the hydrogen into a collection chamber from whence it is directed onto the aft end of the centerbody to provide impingement cooling. A pitot tube and thermocouple built into the centerbody facilitate measurement of hydrogen flow conditions before expansion through the supersonic exhaust nozzle. The nozzle lip has a thickness of 0.54-mm, of which 0.13-mm is nickel and 0.41-mm is insulation.

During the course of the experimental program it was found that the hydrogen temperature increased approximately 55°K in passing through the struts and centerbody. Boundary layer calculations indicated nominal centerbody surface temperatures of 670-830°K for this temperature rise.

Annular nozzle. - The copper annular nozzle for the UARL mixing/combustion test rig is cooled by 1.81-kg/sec of water which flows through two circumferential cooling slots; delivery pressure of the water is 1.35×10^6 - N/m^2 (13.5-atm). The nozzle is designed for uniform, parallel, shock-free flow at a nominal Mach number of 1.80. A method of characteristics, computerized design analysis (Ref. 10) was employed to determine the appropriate contour for the outer wall of the annular nozzle passage. Subsequently, the predicted contour was used as input to the flow computer program of Ref. 11 to independently verify that the flow field within the nozzle is shock-free. After the inviscid design was established the "Energy Deficit Method," an up-dated version of work presented in Ref. 12, was utilized to determine a correction for the contour to account for boundary layer effects. This method predicted very small negative displacement thickness corrections, e.g., -0.55-mm at the nozzle throat and -0.32-mm at the nozzle exit. In support of the computations, it is of interest to note that the predicted overall nozzle heat flux was found to agree to within ten percent of the heat flux subsequently measured in the experiments.

Tests were conducted with the nozzle section installed at the UARL mixing and combustion test rig to evaluate the annular nozzle design. The measured pitot pressure profile at the nozzle exit plane, shown in Fig. 4, displays the expected flat regions in the jet flow field away from solid boundaries. The edge of the centerbody and annular nozzle are designated by bars on the ordinate of the figure. A Mach number distribution obtained from these data, Fig. 5, indicates that the inviscid annular nozzle flow is uniform at a Mach number of 1.86; a constant Mach number of 1.46 appears to be characteristic of the centerbody flow. Mach numbers in Fig. 5 computed from both the pitot-to-total pressure ratio and the measured static-to-pitot pressure ratio are identical, thereby confirming that the flow leaving the nozzle is shock-free. Boundary layer thicknesses at the nozzle exit plane on the inner and outer surfaces of the centerbody and on the annular nozzle, determined using the "Energy Deficit Method," are indicated in both Figs. 4 and 5.

Instrumentation

A variety of instrumentation was utilized to establish a detailed description of the free jet mixing flow at various test conditions. Pitot pressures and species concentrations are determined with the use of water-cooled probes. Aspirating temperature probes are also water-cooled except for their precious metal immersion tips. Probes disturb the flow so it is of interest to compare probe measurements with temperatures and water concentrations found optically with the Ebert spectrophotometer. Photographs and motion pictures taken during the test program are

also useful for characterizing the mixing and combustion of supersonic free jets by providing information on ignition lengths, flame shapes and flame speeds.

Water-cooled probe rake. - A rake containing two pitot probes and two gas-sampling (quenching) probes, Fig. 6, was constructed for this investigation. In the external design of the rake, probe-to-probe spacing and probe dimensions were chosen to insure that conical shocks off adjacent probe tips coalesced far downstream of the probe tips and that the stand-off distance of the strut bow shock was much less than the probe length. On the basis of these considerations, the pitot probes were made with a 30-deg half-angle stainless steel tip and mounted on the strut with a tip-to-tip separation of 19.5-mm; the hole in the pitot probe tip has a 1.15-mm diameter. The gas sampling probes have 20-deg half-angle tips constructed from TD nickel, and a tip-to-tip separation of 19.0-mm. A distance of 37.2-mm separates the upper sampling probe from the lower pitot probe. A cooling water flow rate of 0.12-kg/sec is supplied to each probe at a pressure of 1.365×10^6 - N/m^2 (13.5-atm). After a circuit through the probe, the water is dumped into the strut cooling water which is at a pressure of 4.05×10^5 - N/m^2 (4.0-atm); the strut water flow rate is 1.0-kg/sec. The strut is supported top and bottom in a yoke-like structure to prevent deflection of the probe due to loading by the flow. The probe rake is coupled to traversing mechanisms to allow both vertical and horizontal positioning throughout the free jet flow field.

The internal design of the quenching probe was achieved through a parametric study of the governing geometrical and flow parameters for the most severe environmental conditions expected. Area variations, wall friction, and heat transfer were all considered in the analysis through the use of influence coefficients, as given in Ref. 13. The following were to be accomplished by the design:

1. swallow probe bow shock when aspirating gas samples from the free jet flow,

2. inhibit chemical reaction of gas samples injected into the probe by aerodynamic expansion and convective cooling,

3. prevent choking of the flow in the probe, and

4. delay shocking down of the flow until the total temperature is reduced below the autoignition limit of approximately 1000°K.

The resulting probe, Fig. 7, has a length of 89-mm and an inlet hole diameter of 0.61-mm. The water jacket surrounding the gas sample tube consists of a counter flow region, an impingement flow region for the conical tip of the probe, and a parallel flow region for cooling the outer wall of the probe. The gas sample tube consists of a divergent conical nozzle having a 5-deg half-angle followed by a 1.88-mm diameter duct.

The ignition parameter for a coolant water flow rate of 0.12-kg/sec is also given in Fig. 7. This parameter, which is the summation of the ratio of gas residence time to chemical ignition delay time (see Ref. 4), equals unity at ignition. For a gas sample initially at Mach 1.50, total temperature of 2220°K, and containing a stoichiometric mixture of hydrogen and oxygen, no ignition occurs within the probe, at least on a one-dimensional basis. The possibility of chemical reaction in the wall boundary layer of the sample tube cannot, however, be discounted on the basis of this analysis. At the end of the probe, the ingested gas sample must flow through a 90-deg bend and shocking down of the flow will occur. Nevertheless, chemical reaction will not be initiated since the total temperature of the flow has been reduced to about 450°K which is 550°K below the autoignition limit. The calculations also indicated that the Mach number of the gas sample within the probe, for the design of Fig. 7, is maintained near a value of 2.20 as the result of a trade-off between wall friction and cooling effects.

Gas chromatograph. - During a gas sampling test, vacuum pumps connected to the quenching probes continuously aspirate material from the free jet mixing region into the probes. After a purge time of about 15-sec, a portion of the gas mixture from the probe is injected via a remotely actuated valve into a gas chromatograph (GC) for on-line determination of the concentrations of H_2, O_2, H_2O, and N_2. Lines from the probe to the GC are heated to prevent condensation of water. Each of the two quenching probes has an associated GC so that two analyses can occur simultaneously.

Figure 8(a) shows a schematic diagram of the GC system employed. It consists of a carrier gas flow system, a sample injection valve, a separation column, a temperature control system, a detector, and a read-out device to record results of the analysis, see Fig. 8(b). Actually, two separation stages are used since no one column material was found that could separate the four gaseous constituents rapidly. Poropak R (50-80 mesh) is packed into Column (1) to separate H_2, O_2, and N_2 from H_2O, and 40-50 Mesh Molecular Sieve 13X is used in Column (2), after elimination of H_2O, to effect a separation between H_2, O_2, and N_2. The columns are constructed from 6.33-mm O.D. stainless steel tubing; Column (1) is 0.61-m long and Column (2) is 1.525-m long. Drying of the gas mixture occurs in the first 0.3-m of Column (2) wherein water is retained by the Molecular Sieve material. Hot-wire thermal conductivity cells are employed as detectors. The GC carrier gas consisting of a mixture of 91.5% He - 8.5% H_2, is passed through the system at a pressure of 3.37×10^5 - N/m^2 (3.33-atm) and a volumetric flow rate of 6.7×10^{-6} - m^3/sec. This carrier gas is a special mixture used for analysis of samples containing H_2 since pure He carrier gives uninterpretable H_2 results. The entire GC unit (Fig. 9) is enclosed in an oven heated to 410°K.

The recorder traces of Fig. 8(b) show the order and time of elution of the gaseous components. A complete analysis is completed in less than 60-sec, after which the probe rake may be moved to a new position to repeat the purge-analysis procedure.

The on-line gas chromatographs must be calibrated to relate the time integrated output signal to the partial pressure of the gas being analyzed, and thereby allow the conversion of GC output, as recorded on strip charts, into gas concentrations. Calibrations were conducted before and after each test series (about once a day), although only minor variations were found.

For the calibration of nitrogen and oxygen, an air sample at atmospheric pressure is injected into the GC to obtain the output signals associated with corresponding partial pressures calculated from the known composition of air and the barometric pressure. In a similar manner, the sensitivity of the GC to hydrogen is determined with three prepared hydrogen/nitrogen mixtures containing 20%, 50%, and 80% hydrogen by volume. Calibrations for water vapor are carried out utilizing the apparatus shown in Fig. 10. To begin the calibration procedure, the system is evacuated through two vacuum pumps with Valve No. 1 closed. Subsequently, both vacuum pumps are shut off, using Valves Nos. 2 and 3, and Valve No. 1 is re-opened to allow water vapor from the heated air-free vessel to escape into the heated lines of the calibration system. When a desired pressure is attained within the calibration system, as indicated on a digital voltmeter, Valve No. 1 is closed and water vapor is injected into the GC for analysis. This procedure is repeated for several levels of water vapor pressure by maintaining Valve No. 1 in the open position for different lengths of time.

For the gases of interest, the recorded signals were found to approximate symmetrical Gaussian distributions and, therefore, the areas under the output curves may be taken equal to the product of the maximum height of the Gaussian and the width at half-height. The lengths required could be read accurately from the strip charts as signal to noise ratios were typically greater than 15. This information and applicable electronic attenuation factors are used with the calibration curves to determine the partial pressures of H_2, N_2, O_2, and H_2O present in the original gas sample. The volume fraction of any constituent gas is determined from the ratio of its partial pressure to the sum of the partial pressures of all the gases in the sample.

Aspirating temperature probes. - Total temperatures at the entrance to the nozzle section of the experimental rig and in the inert free jet flow field are measured by employing water-cooled aspirating probes with immersion sections constructed of precious metal (see Ref. 14 for details). Platinum-tipped probes containing a platinum, platinum-10% rhodium thermocouple are used up to 1900°K. At higher temperatures, in the 1900-2150°K range, an iridium-tipped probe (Fig. 11) with an iridium, iridium-40% rhodium thermocouple is required. The thermocouple junction in these probes is situated within two concentric radiation shields. The gas flow whose temperature is to be measured is aspirated through 4.76-mm hole into the probe, conducted past the thermocouple junction, and exhausted through the water-cooled support member. As demonstrated in Ref. 14, this probe design yields data which require no correction for radiation losses. A

zirconium oxide coating is applied to the immersion section of the probes to inhibit catalytic action.

Ebert spectrophotometer. - The spectrophotometer system shown in Fig. 12 was used to obtain local temperatures and H_2O concentrations from infrared emission and absorption measurements. It consists of a light-source unit, an optical collection system, a wave length scanning monochromator, a detector unit, and photometric circuitry. The system has all mirror optics along with several sources, diffraction gratings, and detectors, required to permit the measurement of both emission and absorption spectra throughout the wavelength range from 0.25 to 6 microns in a number of segments. Provision is made for absolute calibration of the system from a black-body source or a Bureau of Standards-traceable source of spectral radiance. In addition, dry nitrogen purging of the entire optical system is provided to eliminate atmospheric water vapor and carbon dioxide absorption when working in the infrared portion of the spectrum. The arrangement of mirrors shown in Fig. 12 produces a collimated beam, permitting any desired working space. The entire system can be traversed as a unit over a 0.3-m horizontal path to obtain data at various axial locations along the jet flow. In order to take measurements at different radial locations, the height of the base stands which support the light source unit, collection system and monochromator must be varied; base stand jack screws are provided for this purpose.

During IR operation, a beam from the Nernst glower light source (SI) in Fig. 12 impinges on an off-axis parabola (MP3) from whence it is directed to flat folding mirror (MF2) and thence through the test area. The beam cross section is approximately a rectangle 6.34-mm × 3.17-mm with the longer sides normal to the flow direction. The collimated beam is collected and focused on the monochromator entrance slit by parabolic mirror (MP2) via mirror (MF4). The 1.22-m focal length, f/8 Ebert monochromator is equipped with a 3.00-micron grating which is utilized for the infrared emission and absorption measurements. The grating has 300-grooves/mm, a ruled area height and width of 102-mm (each dimension), a first order wavelength range of 1.4 to 4.5-microns, first order dispersion of 50.8-Å/mm, a theoretical resolution of 16,100 and a scanning rate of 56 to 500-Å/sec. At the exit of the monochromator the beam impinges on a lead sulfide detector (DE2). Additional details regarding the spectrophotometer and associated instrumentation may be found in Ref. 15. A photograph of the device is reproduced in Fig. 13.

Measurements taken with the spectrophotometer include the gas spectral emission intensity per unit volume, $Ie(\lambda)$, and the spectral absorptivity, $a(\lambda)$. All data are obtained at a selected wavelength $\lambda = \lambda^*$ in the (H_2O) 2.7-micron region where thick emission and absorption lines are found. In the present work, the CO_2-free ν_3 line at $\lambda^{-1} = 3837.85$ cm^{-1}, the strongest emitter in the 2.7-micron region, was chosen.

All data obtained from the axisymmetric flame are reduced by an Abel integral computer program (Ref. 16) which corrects for self-absorption to yield the radial-zone quantities Ie_n and a_n. The program then computes the zonal Planck-Kirchoff temperature which is essentially the translational temperature at local thermodynamic equilibrium:

$$T_n = C_2 \left[\lambda^* \ \ell n \left\{ 1 + \frac{C_1 a_n(\lambda^*)}{\lambda^{*5} Ie_n(\lambda^*)} \right\} \right]^{-1} \qquad (1)$$

Equation (1), following Plass (Ref. 17) and Tourin (Ref. 18), is based on the observation that a gas radiates energy as a grey body for a narrow region in the molecular spectrum. Derivation of Eq. (1) is covered in Ref. 16. Water partial pressures within a radial zone of unit depth are computed from the expression

$$P_n = \left(\frac{RT_n}{\mu_n} \right) \frac{\delta^2 a_n^2}{4 S_n B_n P_n} \qquad (2)$$

which was derived for a thick line and a constant slit function in Ref. 17. Equation (2) results when the frequency-dependent absorptivity from the Beer-Bouger-Lambert law is weighted with a rectangular slit function and integrated to determine the integrated line absorption. Line parameters S and B are obtained by applying temperature and pressure corrections to the tabulated values of Ref. 19. For completeness, the vibrational-rotational correction for the ν_3 line (Ref. 20) is also applied to the line strength, S. The slit half-width, δ, is a property of the spectrophotometer, see Ref. 15.

During a typical data acquistion test a continuous signal is recorded as the spectrophotometer is traversed a distance of 0.3-m from the nozzle exit plane while in the absorption mode, and then returned to the nozzle exit in the emission mode. Calibrations for the reference no-absorption intensity signal and the black body emission signals at various temperatures are obtained before and after each test. The total time between calibrations is noted as are the test start and test completion times to permit determination of linear-time-corrected calibration signals.

Photographs and motion pictures. - The system employed for the acquisition of spark schlieren photographs, Fig. 14, consists of a collimated double-pass mirror schlieren with an FX-12 flash lamp of 4-μsec duration serving as the light source for exposure. The field diameter is 0.203-m with f/8 optics. A 70-mm camera is used to record the image on ASA 320 black and white panchromatic film. Steady illumination for monitoring the schlieren image on a closed circuit television system is provided by a mercury arc lamp. This arrangement facilitates the adjustment of a remotely-controlled motorized knife edge for optimum flow visualization. During photographic recording the monitoring system is interrupted for approximately 0.1 sec.

A modified 35-mm camera having a special 50-mm focal length ultraviolet transmitting lens and filter combination is employed to photograph the emission of the combusting flows in the 2500-3260 Å region of the spectrum. The ASA 320 black and white film used is exposed for 0.02 sec at f/5.6. Emission in the 0.7 to 1.0-micron region of the spectrum is photographed with a 35-mm camera using high speed infrared negative film with an infrared passing filter over the lens. Exposure time is 0.02 sec at f/5.6.

A 16-mm intermittent framing camera is used to take high speed motion pictures of the flow. In this work, color reversal film (ASA 125) is exposed at f/1.9 with a 50-mm lens and a shutter duration of 0.0033 sec. Normal commercial processing is satisfactory for developing the film.

Provision is made for remote operation of all cameras.

Experimental Procedures

Pre-test. - A thorough inspection of the experimental apparatus and instrumentation is conducted prior to each test to verify that water supply hoses and pressure measuring lines are properly installed, and that there is continuity in all electrical lines including thermocouple leads. The gas delivery lines are pressurized with nitrogen, and water is introduced into the rig and probe cooling passages for a complete system leak-check. If the apparatus is found to be leak-tight, the gas lines are vented and the various gas supplies are connected into the gas delivery systems. Hydrogen is supplied from trailers, each holding up to 3100 standard-m^3. The hydrogen supply pressure is regulated to approximately 65.8×10^5 - N/m^2 (65-atm) before the flow for the vitiation chamber is separated from the flow for the centerbody. Once separated, these hydrogen flows are independently regulated and their flow rates are independently measured with the use of choked venturis. The flow rate of the make-up gas, either nitrogen or oxygen, is also determined with a choked venturi. The gases are taken from manifolded gas cylinders having total capacities of 850 and 1750 standard m^3 for nitrogen and oxygen, respectively. All gas systems are monitored and controlled from an engineering operations room which is adjacent to the test area. When the gas chromatograph is to be used, carrier gas is

fed into the system, compressed air is supplied for actuation of the sample valves and all vacuum pumps are started.

Start-up. - Compressed air is available to the test facility at pressures and flow rates up to 27.3×10^5 - N/m^2 (27-atm) and 4.54 - kg/sec, respectively. At the start of a test, the air is admitted into the experimental rig until a desired weight flow is attained; the air pressure and temperature upstream of the (calibrated) choked bellmouth is monitored for this purpose. Hydrogen is then brought into the centerbody from whence it ultimately flows into the exhaust duct where it is ignited with an oxygen-hydrogen torch. Delivery pressure of the centerbody hydrogen at this stage is essentially that which will be required for the test, 17.7×10^5 - N/m^2 (17-atm). The flame in the exhaust duct is held on a cooled flameholder constructed from steel pipe. The flame is quite unstable and usually will go out after the torch is removed unless the vitiation chamber is immediately ignited. Therefore, hydrogen is admitted into the vitiation chamber after the exhaust duct ignition and immediately spark-ignited. All gas flows are then brought to desired levels. The free jets studied in the present program appear steady to the eye during the entire course of a test.

Data acquisition. - Fifteen pressures and thirty temperatures are monitored during the course of a test. Venturi total and throat pressures displayed on digital voltmeters are continually scanned by the test engineer so that any deviation in gas flow rates can be detected and immediately corrected. Certain critical cooling water temperatures are also displayed.

After a few minutes, once the various temperatures and pressures reach steady levels, schlieren photographs may be taken by depressing a button which simultaneously activates the flash lamp, camera shutter and deflection mirror (see Fig. 14). Improved picture quality is achieved by moving the motorized knife edge and observing the result on a T.V. monitor. Other cameras can also be controlled from a remote station in the engineering operations room for infrared and ultraviolet photographs, and high speed motion pictures.

Probes may be brought to any position in the free jet flow by successively activating the horizontal and vertical traversing mechanisms until calibrated position indicators are at desired settings. Once a probe is positioned, pitot pressures are read from precision gages, total temperatures are read from calibrated potentiometers and GC output signals are recorded for subsequent analysis. The amplitude of the GC signal may be changed on-line by manipulating the sensitivity controls of the GC power supply to (1) allow the measurement of small concentrations of gases, and (2) improve the accuracy of H_2 concentration measure-measurement since the detector sensitivity for H_2 with the present system is approximately 3 percent of that for N_2. In fact, H_2 mole fractions less than about 0.05 cannot be determined with confidence.

Output signals obtained with the scanning Ebert spectrophotometer are read out on a recorder. Absorption measurements are made during a 65-sec downstream traverse at some pre-set vertical position relative to the jet centerline, while emission measurements are recorded during the return, upstream traverse. As a result of vibrations within the test cell, realignment of optics or other adjustments are typically required after each test.

Post-test. - Hydrogen flows to the vitiation chamber and centerbody are terminated in sequence to commence the shutdown procedure. Following this, the hydrogen system is vented and the air and make-up gas systems are closed. The test area may now be entered to collect exposed film and prepare for post-test calibrations for the GC and spectrophotometer.

Initial Conditions

A precise knowledge of initial conditions is essential in an experimental fluid mechanics study. In fact, much of the equipment design for the experiment is concerned with producing a flow field with certain required flow properties and physical properties at the entrance to the test section where data are to be taken. The desired properties of the entering stream are usually dictated by those phenomena the experimentalist wishes to induce or avoid within the test area. Thus stringent physical and mechanical restrictions are imposed on the apparatus which, often, cannot be fully achieved.

The perfect experimental rig for the present study would feature:

1. complete combustion in the vitiation heater,
2. uniform, parallel shock-free flow delivered by the annular nozzle and centerbody,
3. uniform static pressure at the nozzles exit plane at a value of 1-atm,
4. no boundary layers,
5. zero centerbody wall thickness at the nozzles exit.

If Items (1) through (5) above could be attained, the initial flow conditions could be characterized exactly. Furthermore, the influence of the apparatus on the downstream jet mixing and chemical reaction would be eliminated. There would then be some hope of achieving a full and detailed analytical description of the flow in the test section.

Establishment of test conditions. - At the start of the test program an attempt was made to produce equivalent inert and reactive flows for the study

of the influence of chemical heat release on mixing rates. It was assumed, at that time, that 100 percent combustion efficiency could be achieved in the vitiation chamber at all conditions. However, this assumption was not verified by the temperature measurements taken at the 10-cm diameter nozzle entrance, Fig. 15. Temperatures found for the vitiated stream containing make-up oxygen were approximately 200 to 400°K higher than corresponding temperatures in the vitiated stream containing make-up nitrogen. Note that the fuel flow rate and the total flow are almost identical for these two vitiated flows; equilibrium calculations yield identical reaction temperatures. Attempts to achieve higher temperatures in the stream containing make-up nitrogen by injection of up to 10 percent more hydrogen were unsuccessful. Thus combustion in the flow with excess inert diluent is probably limited by (1) mixing, so that parts of the flow are too fuel-rich to ignite and (2) chemical kinetics. The kinetically limiting effect was investigated analytically using a UARL computer program, the Chemical Kinetics Program, which numerically integrates the coupled system of reaction kinetic, gas dynamic and state equations to give the time variation of conditions in a reacting one-dimensional flow. Two equivalent pre-mixed streams, each containing 0.0454-kg/sec of H_2 and having a total weight flow of 2.65-kg/sec, were chosen for the computation: a nitrogen-rich stream initially contained a stoichiometric concentration of O_2 and 2.24-kg/sec of N_2; an oxygen-rich stream initially contained 0.655-kg/sec of O_2 above that required for stoichiometric combustion plus 1.59-kg/sec of N_2. Both streams had an initial temperature of 1050°K and an initial pressure of 5.58×10^5 - N/m^2 (5.51-atm). The calculations, reproduced in Fig. 16, indicate that significantly more time is required by the nitrogen-rich stream to burn completely, but at typical combustor velocities of 30 to 100-m/s sufficient length of vitiation heater is available to achieve high efficiencies. It may be concluded, therefore, that the loss of combustion efficiency indicated by the temperature measurements in Fig. 15 is primarily due to incomplete mixing.

The attainment of 100 percent combustion efficiency for flows containing excess nitrogen is clearly not possible with the present apparatus. Hence completely inert, oxygen-free streams cannot be produced, and some concentration of oxygen in the flow must be tolerated. Furthermore, the establishment of suitable equivalent flows to study the coupling between mixing and chemical reaction can only be accomplished empirically, through the examination of data. Accordingly, calibration tests were conducted to determine two sets of equivalent flows. One set of flows with an exhaust static temperature slightly greater than the autoignition value was designated the low temperature set. The (other) high temperature set, with an exhaust static temperature approximately 10 percent higher than the low temperature set, has an associated ignition delay time 0.3 to 0.5 that of the low temperature set (depending on which of the many available ignition delay expressions is used for the calculation). Each set contains a (reactive) vitiated air flow with an oxygen volume concentration of approximately 21 percent, and an "inert" vitiated nitrogen flow with an oxygen volume

concentration of approximately 5 percent. In the course of the calibration tests, fluid flow rates were varied until the total temperature profiles at the nozzles exit plane were essentially the same for both vitiated nitrogen and vitiated air, at each of two temperature levels, see Fig. 17. Gas flow rates corresponding to these results appear in Table I. The vitiated streams exhausted from the annular nozzle at a static pressure of 0.91×10^5 - N/m^2 (0.9-atm), for all the conditions of Table I. This slight under-expansion had to be accepted in order to obtain gas flow rates which were consistent with the capabilities of the gas storage facilities to provide realistic run times. The very weak wave which results from the mismatch with cell pressure has an associated angle which is only 1 deg larger than the Mach wave angle corresponding to a perfect match of the flow field pressure.

The flow delivered by the nozzles. - Shocks which emanate from a poorly-designed nozzle propagate downstream to influence the entire flow field. Large variations in static conditions caused by these waves result in complex fluid mechanical and chemical effects that are not well understood. Great care must be taken in the design of nozzles, therefore, to insure that shocks will not form within the nozzle. In addition, when coaxial supersonic jets are under study, the exhaust static pressures of the jets must be matched to avoid shock formation. The success of the present effort to minimize shock-related effects on the mixing and combusting flows may be gaged by examining schlieren photographs of the jets issuing from the nozzles, for each of the four test conditions listed in Table I. The photographs, Figs. 18 and 19, verify that shockless flow is delivered by the nozzles. The waves starting at the centerbody and extending into both the vitiated stream and H_2 stream are essentially Mach waves whose influence on the flow is not expected to be important.

Boundary layer thicknesses at the nozzles exit plane on the outer and inner centerbody surfaces were calculated to be 1.85-mm and 1.15-mm, respectively. These boundary layers and the 0.54-mm centerbody lip constitute a 3.54-mm thick ring which will appear as a wake in the free jet flow. Velocities in a wake are lower than in the surrounding fluid and fluid residence times may be very large. Longer residence times can, in turn, result in shorter ignition lengths if the fluid in the wake consists of a combustible mixture of fuel and air at a temperature exceeding the autoignition value. However, mixing, the very process which brings fuel and high temperature air together, also rapidly increases wake velocities. If wake velocities are increased significantly before proper concentrations of fuel and oxident can be brought together or before the wake temperatures are raised to 1000°K, then the effect of the wake on ignition will not be important. From computations made with the mixing and combustion analysis, described in a later section of this report, this appears to be the case for the present experiments.

Vitiation combustion efficiencies. - Maximum total temperatures from Fig. 17 and concentrations at the nozzles exit plane, see Fig. 20 for typical data, were compared to equilibrium chemistry calculations to establish combustion efficiencies for the conditions in Table I. The calculational procedure of Ref. 21 was employed. All reactants were initially at 284°K and the vitiation chamber pressure was taken as 5.62×10^5 - N/m^2 (5.55-atm). Computations were made assuming that various fractions of the available hydrogen between 0.7 and 1.0 were consumed during vitiation. Following vitiation, each of the resulting product streams was expanded through a Mach 1.86 nozzle to a static pressure of 0.91×10^5 - N/m^2 (0.9-atm). Frozen and equilibrium expansions downstream of the nozzle throat were found to yield identical concentrations for the molecular species. The combustion efficiency, defined as the percent of available hydrogen consumed, was determined by matching the calculated nozzle exhaust conditions with the data. The results of this comparison are presented in Table II. As seen from this table, the calculated combustion efficiency which best agrees with the data was 95 percent for both vitiated air test conditions, 83 percent for the high temperature vitiated nitrogen test condition, and 73 percent for the low temperature vitiated nitrogen test condition. Note that the low temperature vitiated nitrogen stream contains about 70 percent more inert diluent than the high temperature vitiated nitrogen stream.

Photographic Study

High speed motion pictures. - High speed (128 fps) color motion pictures were taken at all test conditions, although only the luminous jet flows for the vitiated air conditions could be recorded. Examination of the films revealed an unsteady but cyclical behavior of the flame in the free jet flow field. During a typical cycle of 0.020 to 0.024 sec, the brightly burning flame disappeared and then reappeared, ultimately regaining its initial luminosity. High speed black and white motion pictures at 500 fps were also taken to verify the flame variations. Ten frames of this film, about one flame cycle, are reproduced in Fig. 21. Note that combustion occurs downstream of the probe strut even in those frames where no upstream flame is in evidence.

In an attempt to determine the origin of the flame instability, high frequency response pressure transducers were placed on all gas supply lines and on the upstream air bellmouth pressure, the mixing section pressure, the vitiation chamber pressure and the nozzle exit pressure. Recordings were made of all pressures during the course of several vitiated air tests. No fluctuations were detected in any of the gas supply pressures, or in the plenum pressure upstream of the airflow bellmouth. However, a sinusoidal pressure fluctuation was found in the mixing section and the vitiation chamber; the pressure variations had a frequency of about 42 cps and an amplitude of 1.38×10^4 - N/m^2 (0.136-atm). Very slight variations were also evident on close inspection of the record of the nozzle exahust pressure. It must be concluded therefore that the cyclical

instabilities are produced in the cavity of the experimental apparatus downstream of the air bellmouth.

If it assumed that a constant weight flow is maintained through the mixing and combustion test rig, then combustion temperature fluctuations must accompany the variations in vitiation chamber pressure. Since the vitiation chamber pressure is

$$P_{ta} = 5.55 \pm 0.136 \text{ atm}$$

fluctuations of $\pm 75^{\circ}K$ and $\pm 83^{\circ}K$ are required for the low and high temperature conditions, respectively. Corresponding exhaust static temperatures are

$$T_a = 1029 \pm 50^{\circ}K \qquad \text{low temperature}$$

and

$$T_a = 1140 \pm 56^{\circ}K \qquad \text{high temperature}$$

The effect of such temperature variations on ignition characteristics are profound at temperatures close to the autoignition limit. Thus the changing luminosity of the flame, and even the apparent extinguishment during each flame cycle, are not surprising.

The findings discussed above suggest that the pressure fluctuations are associated with vibrations of the gas mass within the test rig downstream of the bellmouth. While exact calculation of the resonant frequency of the test rig is made difficult by uncertainties in end corrections and the inhomogeneous nature of the gas, a crude estimate can be made from the expression

$$\nu_r = \frac{c}{4L} \tag{3}$$

which applies to a tube with one opened end (Ref. 22). In Eq. (3), c is the sound speed and L is the length of the enclosure. The sound speed of the combustion gases is approximately 800-m/s and that of the gas approaching the vitiation chamber is 330-m/s. Using a length-averaged sound speed of 610-m/s,

$$\nu_r = \frac{610}{(4)\ 3.32} = 46 \text{ cps}$$

or roughly the experimental value. The contribution of the nozzle section was not included in the calculation.

The time to make any given measurement generally encompasses several cycles of flame fluctuations so that some averaged effect is manifested. It is expected that the "averaged" conditions measured show a greater influence of combustion than would be found in a comparable steady flame situation, since reaction rates are largely exponential functions of temperature (see Shelkin's argument regarding large scale turbulence, Ref. 23).

Infrared and ultraviolet photographs. - Ultraviolet and infrared photographs of the free jet region are presented ($\frac{1}{2}$ scale) for the high and low temperature vitiated air conditions in Figs. 22 and 23, respectively. No flame was observed in the photographs for the vitiated nitrogen conditions for either the infrared or ultraviolet portion of the spectrum. The exposure time of 0.02 sec utilized for these photographs was sufficient to include a complete cycle of flame fluctuations.

Figures 22 and 23 are quite similar and display essentially the same characteristics, i.e., very shallow flame angles and ignition lengths less than 3-cm. Flame half-angles measured from the photographs are 2 to 3 degrees.

The thicknesses of the UV emitting OH zones are somewhat larger than the zones containing water which are observed in the corresponding infrared photographs. This is consistent with H_2/O_2 flame chemistry in that large concentrations of OH must build up before combustion with attendant formation of water can occur. Thus significant concentrations of OH may be present in portions of the flow where no water has yet been produced. It has been assumed here that the IR emission is from H_2O and the UV emission is due to OH. For completeness it must be pointed out that a definitive spectral scan was not conducted so that the presence of impurities which emit in either the IR or UV bands cannot be discounted.

Local Conditions Throughout the Free Jet Flow Fields

Table III summarizes the test conditions for which profile measurements were acquired during the test program. A detailed listing of all probe data is given in Table IV; a compilation of the spectrophotometer data is given in Tables V and VI.

Pitot pressure profiles. - The development of pitot pressure with downstream distance for the high temperature vitiated N_2 condition, shown in Fig. 24 is representative of this type of data. The initial, step-function profile (also see Fig. 4), is gradually eroded by momentum transport between the various streams until a typical mixing layer profile is achieved at the 35.6-cm station.

A comparison between pitot profiles for the high temperature air and N_2 conditions at X = 35.6-cm in Fig. 25 discloses small differences which are confined to a 2.5-cm radius circular region about the jet centerline.

Temperature profiles. - The total temperature profile at X = 0.33-cm for the vitiated nitrogen test conditions (Fig. 26) displays a temperature plateau of about 1700°K. As mixing proceeds, the cold ambient stream and central hydrogen jet penetrate into the vitiated stream. A temperature peak of 1840°K which occurs in the mixing layer between the vitiated flow and the hydrogen stream results from some combustion of the oxygen carried in the vitiated nitrogen stream. A similar temperature peak was found in the low temperature nitrogen data. Attempts on two occasions to measure downstream jet temperatures for the vitiated air conditions were aborted due to probe burn-out, so that no temperature data is available for these cases.

Also shown in Fig. 26 are temperatures calculated from spectrophotometer data. The overall quantitative agreement between the two types of measurements is only fair with the spectrophotometer-determined values averaging 200-300°K less than the probe values at X = 0.33 and 10.2-cm, and 500°K less at X = 25.4-cm. It should be noted that although complete scans were taken with the spectrophotometer, a portion of the data was lost due to equipment malfunction.

A compilation of all temperatures ultimately obtained with the spectrophotometer in Table V reveals that measured temperatures at the edge of the flame region, i.e., Z = 1.90-cm, are lower for the high temperature air conditions than the high temperature N_2 conditions. The reason for this inconsistent result is not known, although it is suspected that the underlying assumption of local thermodynamic equilibrium used in the spectrophotometer data analysis breaks down in combusting portions of the flow.

Species concentration profiles. - The sharply defined concentration distributions at the nozzle exit plane noted in Fig. 20 for the high temperature nitrogen case, are changed through intermixing into the smoothly varying profiles of Fig. 27. By the X = 35.6-cm location, significant nitrogen, oxygen and water from the vitiated stream have penetrated through the central hydrogen stream to the jet centerline. Some spreading of hydrogen beyond the centerbody lip location is also clearly indicated. The presence of a water "bump" verifies that some combustion takes place for the vitiated nitrogen conditions, as was previously suggested by the total temperature profiles presented in Fig. 26.

Profiles measured at X = 35.6-cm for the high temperature air conditions, Fig. 28, are similar to those for the nitrogen case. The water bump is somewhat more prominent, suggesting that additional significant combustion has occurred. However, the centerline hydrogen concentration is about the same. In fact, the variation of the centerline hydrogen and nitrogen concentration with downstream

distance (Fig. 29) is identical for both high temperature conditions when a proper normalization is used to reflect different initial concentrations. Thus any influence of combustion on mixing rates which may be present in these experiments does not appear to be dramatic.

Water concentrations from spectrophotometer measurements are compared to the corresponding probe measurements in Table VII. The spectrophotometer concentrations are larger in all but one case, but the same trends are indicated in both sets of data.

ANALYTICAL STUDY

Mixing and Combustion Analysis

An analytical study of the simultaneous trubulent mixing and chemical reaction of free,axially directed, supersonic gas streams was conducted using the computer program described in Ref. 4. Local conditions along streamlines in a constant pressure, free jet flow field are obtained from a numerical solution of the boundary layer form of the conservation equations in the von Mises coordinate system. Nonequilibrium chemical reaction effects are included in the analysis by employing a correlation of the ignition and reaction time-history of the $H_2/Air/H_2O$ system. The mixing rate is introduced through the specification of a formulation for the kinematic eddy viscosity.

The static pressure and the distributions of velocity (or Mach number), temperature and species concentrations in the gas streams at the nozzles exit plane constitute the required input for this computer program. The operation of the computer program may be briefly described as follows. Mixing and combustion between the vitiated stream and central hydrogen jet is treated by dividing the flow field into a large number of small segments, and solving the conservation equations in the manner of an initial value problem with the conditions at the end of one segment becoming the initial conditions for the following segment. Within each segment mixing is assumed to proceed independently of any chemical reaction effects. Therefore, when equations describing the conservation of mass, momentum, species concentrations, and energy are written for the segment, terms involving the generation of heat and the production or loss of reactive species are omitted. After the fluid within the segment has mixed, chemical reaction effects are introduced on the basis of average conditions within the segment. Conditions are subsequently adjusted within the segment to reflect heat release and species chemical conversions before proceeding to the adjacent downstream segment. In this procedure it is assumed that the gases obey the perfect gas law and the flow is shock-free. The turbulent Lewis number and turbulent Prandtl number are taken equal to unity.

The application of the boundary layer equations to mixing situations in which the characteristics of the two streams are significantly different has been criticized by Ferri in Ref. 24. Certainly, the assumption of constant static pressure throughout a combusting flow is questionable since mass conservation considerations require that the flow turn away from the centerline as the flame front is approached. In the present experiments, however, the flame angle and hence the deflection angle of the flow upstream of the flame are small, and the use of a constant-pressure turning approximation is reasonable.

Chemical Model

The fraction of hydrogen fuel entering a given segment of the flow which remains unreacted in its passage through the segment is required as input to the analysis. Thus a suitable correlation for the unreacted fuel fraction, f_{H_2}, as a function of local flow conditions and species concentrations, and the time to traverse the segment, i.e., the residence time $\Delta\tau = \Delta X/\bar{u}$, must be provided.

This "history" of the combustion of H_2 was obtained by employing the reaction mechanism and reaction rate constants set forth in Table VIII in a one-dimensional, constant pressure kinetics computer program. The initiation reaction, Reaction 1 of Table VIII, with the three chain-branching Reactions 2, 3, and 4, have been found to yield induction times which are in excellent agreement with measurements in shock tubes (Refs. 34 and 35). Initial conditions for the computer computations, including temperature and concentrations of all important species (i.e., H, OH, O, H_2O, H_2, N_2, and O_2) were taken from the vitiation-nozzle exhaust calculations described earlier. As expected, relatively large initial concentrations of the free radicals H and OH are present as a result of the preburning. In the absence of preburning comparable free radical concentrations would be attained only after a "production" time which may not be insignificant compared to the ignition delay time. Therefore, since free radicals play an important role in the ignition process (cf., Ref. 36) it is anticipated that shorter ignition times would be observed for the combustion of a vitiated stream than for one pre-heated by a pebble bed. This supposition was verified analytically by computing reaction-time histories for test cases which were identical in all respects except that their initial concentrations of free radicals differed. Ignition delay times found for the cases with zero initial free radical concentrations were two to five times longer than those for comparable cases with concentrations of initial free radical representative of the present experiments.

Time histories with the initial conditions listed in Table IX were correlated in the form shown in Fig. 30, giving the fraction of unburned hydrogen as a function of the time, θ, temperature, T, and equivalence ratio, ER. The curve drawn through the correlated kinetics information in Fig. 30 was introduced into the mixing computer program in tabular form.

The chemical reaction history of Fig. 30 can ideally be divided into three distinct time periods: (1) an isothermal preignition period of length τ_{ID} during which molecular species concentrations remain unchanged, (2) a reaction period of length τ_R during which significant changes occur with time, and (3) an equilibrium period. The preignition period is defined as the time required for f_{H_2} to fall noticeably below unity. Referring to Fig. 30, this time may be located at a value of the correlating parameter F = 0.076. Thus

$$\tau_{ID} = 8.1 \times 10^{-10} \left[T \times 10^{-4} \right]^{-3.60} \qquad (4)$$

This expression is used with an ignition criterion to describe the chemistry in the preignition period. Ignition is said to occur on any streamline q bounding a particular segment of the flow at the axial location X_k where the following condition is satisfied:

$$\sum_{X=0}^{X=X_k} \left(\frac{\Delta\tau}{\tau_{ID}} \right)_{X_k} \geq 1.0 \qquad (5)$$

If ignition has already occurred on streamline q upstream of the segment in question, then the extent of chemical reaction, i.e., the degree of water formation and heat release, is determined by employing the correlating curve of Fig. 30. Conditions of the flow leaving the segment are then adjusted to reflect chemical reaction effects. It is assumed in this that the extent of combustion in any segment is small so that changes in velocity and static pressure can be ignored. Note that the correlation factor or "history" F is accumulated on streamline q following ignition just as the ratio $\Delta\tau/\tau_{ID}$ is summed prior to ignition.

One additional problem which must be considered is the intermixing of packets of fluid with different reaction-time histories. Consider a fluid flowing at the rate W_o with history F_o between the streamlines q and q + 1 in any given segment ΔX. In the passage through the segment, an amount ΔW of the fluid with history F_o passes across the streamlines and an equal flow of fluid, ΔW, mixes in from the adjacent regions to replace it. The portion of ΔW flowing into the segment bounded by streamlines q and q + 1 across streamline q has a history F_q, and that moving across streamline q + 1 has a history F_{q+1}. At the end of the segment ΔX, a new history F'_o of the fluid may be determined from the mass-averaged relationship,

$$F'_o = F_o \left(1 - \frac{\Delta W}{W_o} \right) + F_q \frac{\Delta W_q}{W_o} + F_{q+1} \frac{\Delta W_{q+1}}{W_o} \qquad (6)$$

where

$$\Delta W = \Delta W_q + \Delta W_{q+1} \tag{7}$$

Either fractional weight flow, say $\Delta W_q/W_o$, may also be written as

$$\frac{\Delta W_q}{W_o} = \frac{Z_q \ \Delta X \ (\rho_q/\rho_o)}{Z_{q+\frac{1}{2}} (Z_{q+1} - Z_q)} \left(\frac{v_q}{u_o}\right) \tag{8}$$

in which the ratio of characteristic transverse and longitudinal velocities, (v_q/u_o), is essentially the tangent of the flame angle, i.e., the flame spread. Experimental evidence to support such a dependence of flame spread on turbulence level for low speed turbulent jets at nearly equal velocities is given by Lefebvre and Reid (Ref. 37). Thus

$$\frac{\Delta W}{W_o} \approx 0.05 \ \frac{\Delta X}{(Z_{q+1} - Z_q)} \left[\frac{Z_q}{Z_{q+\frac{1}{2}}} \left(\frac{\rho_q}{\rho_o}\right) + \frac{Z_{q+1}}{Z_{q+\frac{1}{2}}} \left(\frac{\rho_{q+1}}{\rho_o}\right)\right] \tag{9}$$

for the present experiments. The transverse distance $Z_{q+\frac{1}{2}}$, was set equal to $\frac{1}{2}(Z_q+Z_{q+1})$ in the present analysis.

Mixing Model

The mixing and combustion computer program can be used to generate a detailed flow field for given initial conditions and appropriate boundary conditions, once a kinematic eddy viscosity distribution has been specified. In any general formulation of the kinematic eddy viscosity, it is necessary to consider the turbulence initially present in the jets, i.e., the "preturbulence," as well as the turbulence produced as a result of the interactions between the jets. When the velocity ratio $m \equiv u_a/u_\zeta$ differs significantly from unity, the growth of the mixing layer is controlled by jet interaction since shearing stresses of large magnitude occur which induce high intensity turbulent activity. As m

approaches unity, however, the preturbulence contribution may become the dominant factor. Thus in a jet mixing situation where m (X = 0) << 1, the initial spread of the mixing layer depends on jet-induced turbulence, while far downstream, after appreciable decay of the centerline velocity, the effect of preturbulence may become important. Thus the flow displays a "memory," in that mixing far downstream is controlled by a turbulence level which is initially present in the jets. To a significant degree this turbulence level is a function of the experimental apparatus so that the value of m ($=m_1$) at which preturbulence becomes important is a characteristic of the system under consideration. While a value of m_1 close to unity may be obtained, in theory, in a very carefully designed experiment, values of m_1 between 0.4 and 0.6 are found to be representative of a major portion of the existing mixing data (cf., Ref. 38 and Figs. 5 and 7 of Ref. 39).

Classically, the constant exchange coefficient hypothesis of Prandtl has been used for the turbulence contribution from jet interaction. This formulation for the kinematic eddy viscosity may be written as

$$\epsilon = \kappa (1 - m)\, b u_{\ell} \tag{10}$$

where κ is a universal constant in each region of the jet for a given geometry, e.g., κ = 0.00764 in the core region and 0.0089 in the developed region of an axisymmetric jet, see Ref. 39. In Eq. (10) b is the transverse extent of the mixing layer.

An extension of the above expression to jet flows in which density varies through the mixing layer was derived in Ref. 39 in the form

$$\epsilon = \kappa \left(\frac{1 + n}{2} \right)^{0.8} (1 - m)\, b u_{\ell} \tag{11}$$

The parameter n is the ratio of densities, ρ_a / ρ_{ℓ}.

At some longitudinal distance $X = X_1$ the preturbulence mechanism becomes dominant and a different eddy viscosity model must be employed. This problem was treated in Ref. 39 with the result for the region of the flow downstream of X_1:

$$\epsilon = \kappa \left(\frac{1 + n_1}{2} \right)^{0.8} (1 - m_1)\, b u_{\ell} \left[\left(\frac{1 + n_1}{1 + n} \right) \left(\frac{1 + mn}{1 + m_1 n_1} \right) \right] \tag{12}$$

Deviation of Eq. (12) depends on the assumption that the shear flow induced by the preturbulence is self-preserving, i.e., the distribution of the nondimensional turbulent shear stress across the mixing layer is similar at any cross section. Verification of such behavior is provided by the measurements in Ref. 40 for plane jets in most of the developed region. Furthermore, it is interesting to note that Eq. (12) closely corresponds to the expression describing the mixing of an incompressible submerged jet since the factor in the square brackets is only a slowly varying function of m and n.

As a practical matter eddy viscosity formulations have historically been applied to both inert and reactive jet flows. This practice, while still widely followed, has lately been the subject of renewed study. The work of Eschenroeder (Ref. 41) has provided the stimulus for these recent efforts which seek to discover the influence of chemical heat release on mixing rates. Malte in Ref. 42 shows that if chemical reaction is taking place, then the density fluctuations and corresponding acoustic pressure fluctuations couple in such a manner as to intensify the vorticity and turbulent kinetic energy of a flow. Combustion therefore increases the turbulent intensity in a turbulent shear flow, and this increase should be reflected by an augmented eddy viscosity. The correction derived for the eddy viscosity in Ref. 42 was based on the global reaction rate given in Ref. 4 which was determined for zero initial concentrations of O, H, and OH. A suitable correction applicable to a given experiment may be derived, if needed, by following the method of Ref. 42 but using a more appropriate reaction-time history.

DISCUSSION OF RESULTS

Experimental Results

Consistency calculation. - The total (integrated) hydrogen flow rate was computed at several axial stations for both vitiated nitrogen test conditions as an overall check of the dependability of the species concentration, pitot pressure, and temperature measurements. The resulting weight flows, presented in Fig. 31, are compared to the delivered weight flow which was measured using a venturi in the H_2 supply line. The primary cause of the deviations which appear in the figure may be traced to inaccuracies in the temperature measurements which, unfortunately, accrue from the particular construction of the aspirating temperature probes. Fluid whose temperature is to be measured is aspirated through a 0.476-cm diameter hole that serves as the inlet to the probe. The averaging which must occur over the inlet hole area precludes the determination of true local temperatures when gradients exist in the flow, and no accurate determination of integrated weight flows can be made. It is of interest to

note, however, that the error in the integrated weight flows is the same at almost all axial locations.

Profile similarity. - Nondimensional nitrogen concentration profiles at the three downstream stations, X = 17.8, 25.4, and 35.6-cm for high temperature vitiated air and high temperature vitiated nitrogen conditions are presented in Fig. 32. The nondimensional concentration used is the difference between local and vitiated stream mass fractions divided by the difference between centerline and vitiated stream mass fractions. Radial position is nondimsionalized with the radius of the centerbody. The results in Fig. 32 indicate that profile similarity is achieved for both the reactive and "inert" jet flows. A curve of the form

$$\phi = \exp\left\{-0.693\ (Z/r_1)^2\right\} \tag{13}$$

gives a good representation of all the data.

Comparison of Analytical Predictions with Data

The velocity ratios, u_a/u_i, for the conditions tested, varied from 0.698 to 0.749 suggesting that mixing was controlled exclusively by the preturbulence mechanism, i.e., $X_1 = 0$. Accordingly, the kinematic eddy viscosity model given by Eq. (12) was utilized with the mixing and combustion computer program to generate detailed flow properties at a constant static pressure of 0.91×10^5 - N/m^2 (0.9-atm) for comparison with the measurements. For these calculations the extent of the mixing layer, b, was taken as the transverse distance between the points in the flow at which

$$(u - u_a) = 0.95\ (u_\ell - u_a) \tag{14}$$

and

$$(u - u_a) = 0.05\ (u_\ell - u_a) \tag{15}$$

The value of m_1 used in all calculations was 0.60; n_1 was taken as 2.69 for the high temperature conditions and 2.98 for the low temperature conditions. Step profiles were used as input to start the analytical calculations; the vitiated flow was assumed to be infinite in extent.

Species concentration, total temperature and Mach number predictions are compared to the data from the high temperature vitiated nitrogen experiments in Figs. 33 through 36. The trends of the data are reproduced accurately and, to a significant degree, good quantitative agreement is achieved. It is particularly notable that the observed bumps in the water concentration profiles, see Figs. 33 and 34, are also generated by the analysis.

The flat peaks of the measured temperature distributions of Fig. 35 result from the averaging by the aspirating probes. In fact, this averaging results in an overall broadening which destroys the sharp delineation found in the predicted profiles. Temperatures in the peak portion of the profiles were computed assuming local equilibrium. This was done since the temperature probes employed cannot quench reactions which may occur in the aspirated flow. Thus the predicted peaks in Fig. 35 represent maximum achievable temperatures which are probably more appropriate for comparison with the data than the "frozen" peak temperatures which are about 200°K lower.

One interesting feature of the Mach number calculations shown in Fig. 36 is the presence of a cusp in the vicinity of the centerbody lip location due to local burning at X = 10.2-cm. The data for high temperature vitiated air in part (b) of the figure clearly follows this trend, but not to the same degree as the computed results. The ultimate disappearance of this profile feature downstream implies that the rate of heat input from chemical reaction is not large enough to sustain the temperature at the centerbody lip location against the gradient-smoothing process of turbulent transport. This effect is nicely illustrated by the axial variation of (frozen) peak total temperature in Fig. 37, calculated with the mixing combustion computer program. The peak jet temperature for the vitiated air condition rises dramatically to a maximum in the vicinity of X = 10-cm reflecting rapid chemical heat release. The rate of decrease in peak temperature downstream of the maximum is initially large, although a very gradual change is observed thereafter when the rate of chemical heat release is sufficient to maintain a fairly constant temperature. Figure 37 contains additional significant information and will be referred to again after comparisons of theory and data for the high temperature vitiated air conditions have been examined.

As pointed out earlier, flow property information was computed for the vitiated air conditions with the identical kinematic eddy viscosity employed for the vitiated N_2 conditions. As seen in Figs. 38, 39, 40, the use of this mixing model leads to results which are predictive of the experimentally determined species concentration profiles. The theoretical water profile bump at X = 10.2-cm is properly placed according to the data, but insufficient data was obtained in this critical region of the bump to properly define it. Considerably better delineation of the water profile bump is achieved at the other downstream stations shown, i.e., at X = 17.8 and 25.4-cm. It is noted that the predicted centerline concentrations for the vitiated air conditions are not as faithful to the data as those for the vitiated nitrogen conditions. Nevertheless, the overall agreement is fully as satisfactory as that achieved for the nitrogen test conditions.

It follows from the above that mixing proceeds at essentially identical rates for the vitiated nitrogen and vitiated air test conditions notwithstanding the substantial differences in heat release rate and total heat evolved for these cases. These differences between the conditions are further exemplified by the calculated peak temperatures presented earlier in Fig. 37. It is seen that the local temperature increases, i.e., $T_t - T_{t_a}$, maintained in the jet for the vitiated air conditions are 2 to 10 times larger than those for the vitiated nitrogen conditions.

It is noted that combustion is initiated earlier for the nitrogen case than for the air case. This is due to the very low equivalence ratios in the vicinity of the centerbody lip location which persist in the air case for the initial portion of the free jet flow field. This problem of low initial equivalence ratios is similarly experienced for the low temperature vitiated air conditions, except with a more dramatic result. According to the mixing and combustion analysis, ignition never occurs for this condition since temperatures are reduced below autoignition before sufficient hydrogen can be mixed with the oxygen in the vitiated stream. Evidentally, without the temperature fluctuations in the vitiated flow, no combustion effects would have been observed for the low temperature reactive jet.

Figures 41 through 44 verify that agreement between the analysis using Eq. (12) and the low temperature data is also very satisfactory, with the exception that no burning and hence no water formation is predicted for the vitiated air conditions. However, very little water is actually formed in the low temperature case so that the effect of chemical reaction on the concentration profiles is small.

Evaluation of Chemistry Model

An interesting exercise was conducted with the mixing and combustion computer program to determine how the predicted chemistry for the high temperature air conditions was affected by using the unadjusted history F rather than F', see Eq. (6). This work is shown in Fig. 45. The use of the unadjusted history results in increased chemical activity and, significantly, a deterioration in the accuracy of prediction.

Evaluation of Kinematic Eddy Viscosity Models

The various comparisons of data and theory already presented have provided ample verification of the kinematic eddy viscosity model, Eq. (12), based on a preturbulence mechanism. However, it is also of interest to test other frequently used mixing models with the same data, as shown in Fig. 46 for the high temperature nitrogen conditions. Prandtl's original constant exchange coefficient of Eq. (10)

predicts very low rates of mixing for the almost equal velocity jets studies. Inclusion of a density correction as per Eq. (11) increases the mixing only slightly. Another extension of Prandtl's ideas to include the effect of density variation through the mixing layer was proposed by Ferri in Ref. 43. This model has the form

$$\rho\epsilon = 0.025\, r_{\frac{1}{2}} (\rho_a u_a - \rho_{\ell} u_{\ell}) \tag{16}$$

where $r_{\frac{1}{2}}$ is measured from one edge of the mixing layer to the position at which the local product of velocity and density, ρu, has an average value between the centerline value and the outer stream value, i.e.,

$$(\rho u)_{r_{\frac{1}{2}}} = 0.5 (\rho_{\ell} u_{\ell} + \rho_a u_a) \tag{17}$$

Application of Eq. (16) is seen to result in unrealistically high mixing rates.

CONCLUSIONS AND RECOMMENDATIONS

Detailed probe and optical measurements have been made in mixing and combusting free jets to obtain species concentrations, pitot pressures and temperatures. On the basis of this data and its subsequent application to the verification of analytical mixing and chemistry models, it is concluded that:

1. The use of a kinematic eddy viscosity formulation based on a preturbulence mechanism in a constant pressure mixing and combustion analysis allows the accurate prediction of local conditions in free jet flow fields. The contribution to the turbulent transport from the jet shear interaction mechanism is not of importance, therefore, when the velocity ratios of jets exceed about 0.60. This finding is of consequence in all jet mixing problems, at least when considering the region far downstream from the nozzles exit plane.

2. No major influence of chemical heat release on mixing rates exists at the conditions of the present investigation.

3. Temperatures and water concentrations measured spectrophotometrically using IR emission and absorption follow the same trends as comparable information obtained with probes, but only fair quantitative agreement is realized. Thus although the worth of spectrophotometric methods for the measurement of temperature and concentration data has been shown,

this approach is still in a state of evolution. Clearly, optical techniques offer the only hope of acquiring local temperature information in flows having total temperatures in excess of 2000°K.

4. The ability to aspirate representative samples of gas from a reaction zone into a probe, effectively quench the sample and finally conduct an on-line gas chromatographic analysis of the sample has been demonstrated.

Recommendations are listed below for future work to extend and compliment the present effort.

1. Higher temperature reactive vitiated flows should be investigated in the search for a coupling between chemical heat release and mixing rates. The liberation of sufficient chemical energy to significantly raise the overall enthalpy level of the flow would be desirable in a continuation study.

2. Additional verification of mixing models through the acquisition of detailed profile data for systematic variations in density and velocity ratios is highly desirable. A complete map of m and n values can be achieved with the use of different nozzle combinations and with the addition of an inert fluid to the centerbody fuel. The correlation of initial turbulence level with mixing rates for almost equal velocity jets is also worthy of future study.

3. The choice of hydrogen for the present work was predicated somewhat on the widespread interest in hydrogen-fueled ramjets, but more practically on the availability of reliable kinetics information. As such information becomes available for other (hydrocarbon) fuels, it would be of interest to broaden the study to include different fuels.

4. The present experiments have laid bare many problems in the design of combustion rigs and instrumentation. For example, it is apparent that acoustic damping must be provided to mitigate vibrations within the heaterburner, and that some special provision must be made for introducing diluents so as not to interfere with the preheat combustion. By far the most difficult instrumentation problem is that associated with the measurement of local temperature. Unfortunately, temperature probes cannot do the job. It is important therefore that the development of optical methods be continued and that a special effort is directed toward obtaining an understanding of flows which are not in local thermodynamic equilibrium.

United Aircraft Corporation
Research Laboratories
East Hartford, Connecticut, August 14, 1969

REFERENCES

1. Peters, C. E., W. J. Phares and T. H. M. Cunningham: Theoretical and Experimental Studies of Ducted Mixing and Burning of Coaxial Streams. AIAA Paper No. 69-85, presented at the AIAA 7th Aerospace Sciences Meeting, New York, New York, January 20-22, 1969.

2. Channapragada, R. S. and J. P. Woolley: Turbulent Mixing of Parallel Compressible Non-Isoenergetic Streams. Astronautica Acta, Vol. 13, No. 4, 1967.

3. Vasiliu, J.: Turbulent Mixing of a Rocket Exhaust with a Supersonic Stream, Including Chemical Reaction. J. of the Aerospace Sciences, January 1962.

4. Cohen, L. S.: An Analytical Study of the Mixing and Nonequilibrium Chemical Reaction of Coflowing Compressible Streams. AIAA Paper No. 66-617, presented at the Second Propulsion Joint Specialist Conference, Colorado Springs, Colorado, June 1966.

5. Edelman, R. and O. Fortune: An Analysis of Mixing and Combustion in Ducted Flows. AIAA paper No. 68-114, presented at the AIAA 6th Aerospace Sciences Meeting, New York, New York, January 22-24, 1968.

6. Penny, G. S.: Diffusion Controlled Supersonic Combustion Utilizing a High Enthalpy Blowdown System. Thesis, The Propulsion Department, The College of Aeronautics, Cranfield, Bedford, England, October 1967.

7. Casaccio, A. and R. L. Rupp: A Supersonic Combustion Test Program Utilizing Gas Sampling, Optical and Photographic Measuring Techniques. NASA Contract NAS1-6314 by Fairchild Hiller, Republic Aviation Division, NASA CR 66393, August 1967.

8. Heyman, R. J., R. J. Sanderson and P. C. Steel: Combustion in Compressible Mixing Flows. Paper No. 68-28, presented at the Fall Meeting of the Combustion Institute, Western States Section, Menlo Park, California, October 1968.

9. Cohen, L. S., D. J. McFarlin and I. W. Kay: Experimental Study and One-Dimensional Analysis of a Ducted Hydrogen-Liquid Oxygen Rocket. United Aircraft Research Laboratories Report E110118-1, July 1966.

10. Pratt & Whitney Aircraft Division, United Aircraft Corporation: Perfect Nozzle Deck; Pratt & Whitney Deck No. 1298 (analyst - Herbert Jeremias), 1968.

11. Pratt & Whitney Aircraft Division, United Aircraft Corporation: User's Manual for the General Supersonic Flow Deck. USAF Contract No. AF 33(615)-3128, September 1968.

12. Flaherty, R. J.: A Method for Estimating Turbulent Boundary Layers and Heat Transfer in an Arbitrary Pressure Gradient. UAC Research Laboratories Report UAR-G51, August 1968.

13. Shapiro, A. H.: The Dynamics and Thermodynamics of Compressible Fluid Flow, Vol. I. The Ronald Press Co., New York, 1953.

14. Glawe, G. E., F. S. Simmons and T. M. Stickney: Radiation and Recovery Corrections and Time Constants of Several Chromel-Alumel Thermocouple Probes in High-Temperature, High-Velocity Gas Streams. NACA TN-3766, October 1956.

15. Leighton, R. L. and F. Michael: Spectrophotometer for Temperature and Species Concentration Measurement. United Aircraft Research Laboratories Report G130367-2, December 1968.

16. Bogush, H. I., R. L. Leighton and F. Michael: A Computerized Analysis for the Calculation of Temperatures and Species Concentrations from Spectrophotometer Measurements in Axisymmetric Jets. United Aircraft Research Laboratories Report H110568-1, September 1969.

17. Plass, G. N.: Models for Spectral Bond Absorption. Journal of the Optical Society of America, Vol. 48, No. 10, October 1958.

18. Tourin, R. H.: Monochromatic Radiation Pyrometry of Hot Gases, Plasmas and Detonations. Temperature - Its Control in Science and Industry, Vol. 3, Part 2, Reinhold Publishing Corp., 1962.

19. Gates, D. M., R. F. Calfee, D. W. Hansen and W. S. Benedict: Line Parameters and Computed Spectra for Water Vapor Bands at 2.7. National Bureau of Standards Monograph 71, August 3, 1964.

20. Maclay, G. J.: Integrated Absorptances of Spectral Line Groups in the 2.7-Bands of Hot Water Vapor, Including Effects of Centrifugal Distortion. The Journal of Chemical Physics, Vol. 43, No. 1, July 1, 1965.

21. Brinkley, S. R.: Calculation of the Thermodynamic Properties of Multi-component Systems and Evaluation of Propellant Performance Parameters. In: Kinetics, Equilibrium, and Performance of High Temperature Systems, Proceedings of the First Conference, Edited by G. S. Bahn and E. E. Zukoski, Butterworths, Washington, 1960.

22. Wood, A. B.: A Textbook of Sound. Second Edition, G. Bell and Sons, Ltd., London, 1944.

23. Karlovitz, B.: Combustion Processes. Vol. II of High Speed Aerodynamics and Jet Propulsion, Editors: B. Lewis, R. N. Peace, H. S. Taylor, Princeton, New Jersey, Princeton University Press, 1956.

24. Ferri, A.: A Critical Review of Heterogeneous Mixing Problems. Astronautica Acta, Vol. 13, Nos. 5 and 6, 1968.

25. Ripley, D. L. and W. C. Gardiner: J. Chem. Phys., Vol. 44, 1966.

26. Fristrom, R. M. and A. A. Westenberg: Flame Structure. McGraw-Hill, New York, 1955.

27. Westenberg, A. A. and N. deHaas: J. Chem. Phys., Vol. 46, 1967.

28. Wilson, W. E.: Paper presented at the 1967 Spring Meeting, The Combustion Institute, Western States Section, La Jolla, California, April 1967.

29. Wilson, W. E. and J. T. O'Donovan: J. Chem. Phys., Vol. 47, 1967.

30. Schott, G. L. and P. F. Bird: J. Chem. Phys., Vol. 41, 1964.

31. Jacobs, T. A., R. R. Giedt and N. Cohen: J. Chem. Phys., Vol. 47, 1967.

32. Camac, M. and A. Vaughan: J. Chem. Phys., Vol. 34, 1961.

33. Getzinger, R. W. and G. L. Schott: J. Chem. Phys., Vol. 43, 1965.

34. Belles, F. E. and M. R. Lauver: Effects of Concentration and of Vibrational Relaxation on the Induction Period of the H_2-O_2 Reaction. Tenth Symposium (International) on Combustion, The Combustion Institute, 1965.

35. Asaba, T., W. C. Gardiner and R. F. Stubbeman: Shock-Tube Study of the Hydrogen-Oxygen Reaction. Tenth Symposium (International) on Combustion, The Combustion Institute, 1965.

36. Rubins, P. M. and R. P. Rhodes: Shock-Induced Combustion with Oblique Shocks: Comparison of Experiment and Kinetics Calculations. AIAA Journal, Vol. 1, No. 12, December 1963.

37. Lefebvre, A. H. and R. Reid: The Influence of Turbulence on the Structure and Propagation of Enclosed Flames. Combustion and Flame, Vol. 10, 1966.

38. Abramovich, G. N.: The Theory of Turbulent Jets. M.I.T. Press, Cambridge, Massachusetts, 1963.

39. Cohen, L. S.: A New Kinematic Eddy Viscosity Model. United Aircraft Research Laboratories Report G211709-1, January 1968.

40. Bradbury, L. J. S.: The Structure of a Self-Preserving Plane Jet. J. of Fluid Mechanics, Vol. 23, 1965.

41. Eschenroeder, A. O.: Intensification of Turbulence by Chemical Heat Release. Physics of Fluids, Vol. 7, 1964.

42. Malte, P. C.: Turbulent Transport in a Combusting Shear Flow. Paper No. 68-27, presented at the Fall Meeting of the Western States Section of the Combustion Institute, Menlo Park, California, October 1968.

43. Ferri, A., P. A. Libby and V. Zakkay: Theoretical and Experimental Investigation of Supersonic Combustion. Polytechnical Institute of Brooklyn, PIBAL Report No. 713, ARL 62-467 AD 291712, September 1962.

TABLE I

Gas Flow Rates - kg/sec

	Low Temperature Set $T_T \approx 1560^{\circ}K$		High Temperature Set $T_T \approx 1750^{\circ}K$	
	Vitiated Air	Vitiated N_2	Vitiated Air	Vitiated N_2
Air	2.354	1.933	2.059	2.076
N_2 or O_2	0.604	0.732	0.540	0.428
H_2 for vitiation	0.038	0.048	0.045	0.053
Total	2.996	2.713	2.644	2.557

TABLE II

Match of Data and Calculation at Nozzle Exit Plane
to Establish Combustion Efficiencies

	Low Temperature				High Temperature			
	Vitiated Air		Vitiated N_2		Vitiated Air		Vitiated N_2	
Mass Fractions	Data	Calculated	Data	Calculated	Data	Calculated	Data	Calculated
O_2	0.29	0.288	0.10	0.062	0.26	0.254	0.06	0.051
H_2O	0.09	0.108	0.10	0.118	0.15	0.146	0.12	0.153
N_2	0.62	0.595	0.80	0.804	0.59	0.597	0.82	0.780
Other	--	0.009	--	0.016	--	0.007	—	0.026
Total Temperature (^oK)	1570	1460	1550	1480	1760	1760	1740	1770
Combustion Efficiencies (%)	95		73		95		83	

TABLE III

Summary of the Data*

	Longitudinal Station (cm)					
Measurements	X = 0.33	5.1	10.2	17.8	25.4	35.6
Pitot Profiles	All	All	All	All	All	(1),(2)
Complete Concentration Profiles - Probe	All	All	All	All	All	(1),(2)
Temperature Profiles - Probe	All	(2),(4)	(2),(4)	(2),(4)	(2),(4)	--
Temperature Profiles - Spectrophotometer	(1),(2) (3)	(1),(2) (3)	(1),(2) (3)	(1),(2) (3)	(1),(2) (3)	--
H_2O Concentration Profiles - Spectrophotometer	(1),(2) (3)	(1),(2) (3)	(1),(2) (3)	(1),(2) (3)	(1),(2) (3)	--

* (1) = High temperature vitiated air conditions

(2) = High temperature vitiated N_2 conditions

(3) = Low temperature vitiated air conditions

(4) = Low temperature vitiated N_2 conditions

All = (1), (2), (3), (4)

TABLE IV. - PROBE DATA

HIGH TEMPERATURE VITIATED AIR

AXIAL LOCATION = 0.33 CM

Z-M	PP-N/M**2	Z-M	TT-DEG K	Z-M	Y-H2	Y-H2O	Y-N2	Y-O2
.000000	.308887+06	.000000	.192222+04	.317500-02	.100000+01	-.000000	-.000000	-.000000
.889000-03	.310266+06	.238760-01	.189444+04	.635000-02	.100000+01	-.000000	-.000000	-.000000
.586740-02	.311645+06	.266700-01	.186667+04	.996950-02	.100000+01	.000000	.000000	.000000
.723900-02	.310266+06	.330200-01	.174722+04	.101600-01	.100000+01	-.000000	-.000000	-.000000
.850900-02	.314403+06	.393700-01	.158889+04	.114300-01	.957000-00	.190000-01	.160000-01	.800000-02
.967740-02	.209602+06	.469900-01	.139444+04	.127000-01	-.000000	.346000-00	.458000-00	.196000-00
.977900-02	.320608+06	.495300-01	.133333+04	.139700-01	-.000000	.259000-00	.521000-00	.228000-00
.109474-01	.174436+06	.520700-01	.123333+04	.152400-01	-.000000	.233000-00	.546000-00	.221000-00
.122174-01	.255108+06	.546100-01	.110000+04	.177800-01	-.000000	.249000-00	.538000-00	.213000-00
.135890-01	.197191+06	.571500-01	.727778+03	.203200-01	-.000000	.250000-00	.547000-00	.203000-00
.153670-01	.412309+06	.000000	.000000	.218440-01	-.000000	.236000-00	.547000-00	.217000-00
.168910-01	.416446+06	.000000	.000000	.221234-01	-.000000	.217000-00	.580000-00	.204000-00
.185674-01	.426099+06	.000000	.000000	.252984-01	-.000000	.210000-00	.574000-00	.216000-00
.194310-01	.417825+06	.000000	.000000	.291084-01	-.000000	.195000-00	.583000-00	.222000-00
.219710-01	.419204+06	.000000	.000000	.303784-01	-.000000	.192000-00	.551000-00	.257000-00
.232410-01	.423341+06	.000000	.000000	.317500-01	-.000000	.199000-00	.573000-00	.224000-00
.245110-01	.425409+06	.000000	.000000	.329184-01	-.000000	.197000-00	.565000-00	.238000-00
.257810-01	.428167+06	.000000	.000000	.381000-01	-.000000	.254000-00	.512000-00	.234000-00
.270510-01	.431614+06	.000000	.000000	.457200-01	.000000	.155000-00	.604000-00	.241000-00
.288290-01	.430236+06	.000000	.000000	.571500-01	-.000000	.000000	.785000-00	.215000-00
.308610-01	.435751+06	.000000	.000000	.000000	.000000	.000000	.000000	.000000
.340360-01	.434372+06	.000000	.000000	.000000	.000000	.000000	.000000	.000000
.348234-01	.425409+06	.000000	.000000	.000000	.000000	.000000	.000000	.000000
.359410-01	.424720+06	.000000	.000000	.000000	.000000	.000000	.000000	.000000
.363474-01	.421962+06	.000000	.000000	.000000	.000000	.000000	.000000	.000000
.372110-01	.430236+06	.000000	.000000	.000000	.000000	.000000	.000000	.000000
.388874-01	.421272+06	.000000	.000000	.000000	.000000	.000000	.000000	.000000
.414274-01	.415067+06	.000000	.000000	.000000	.000000	.000000	.000000	.000000
.426974-01	.420583+06	.000000	.000000	.000000	.000000	.000000	.000000	.000000
.439674-01	.422651+06	.000000	.000000	.000000	.000000	.000000	.000000	.000000
.452374-01	.428857+06	.000000	.000000	.000000	.000000	.000000	.000000	.000000
.465074-01	.420583+06	.000000	.000000	.000000	.000000	.000000	.000000	.000000
.482854-01	.266139+06	.000000	.000000	.000000	.000000	.000000	.000000	.000000
.503174-01	.965272+05	.000000	.000000	.000000	.000000	.000000	.000000	.000000
.534924-01	.965272+05	.000000	.000000	.000000	.000000	.000000	.000000	.000000
.553974-01	.951482+05	.000000	.000000	.000000	.000000	.000000	.000000	.000000

HIGH TEMPERATURE VITIATED AIR

AXIAL LOCATION = 5.1 CM

Z-M	PP-N/M**2	Z-M	TT-DEG K	Z-M	Y-H2	Y-H2O	Y-N2	Y-O2
.000000	.296476+06	.000000	.361111+03	.317500-02	.100000+01	-.000000	-.000000	-.000000
.889000-03	.301303+06	.508000-02	.500000+03	.635000-02	.668000-00	.720000-01	.192000-00	.680000-01
.723900-02	.306129+06	.101600-01	.173333+04	.914400-02	.100000+01	.000000	.000000	.000000
.122174-01	.284066+06	.152400-01	.170000+04	.101600-01	.965000-00	.100000-01	.160000-01	.900000-02
.185674-01	.442646+06	.203200-01	.170000+04	.127000-01	.626000-00	.125000-00	.185000-00	.640000-01
.245110-01	.439888+06	.254000-01	.168889+04	.221234-01	.000000	.202000-00	.576000-00	.222000-00
.308610-01	.441957+06	.317500-01	.166111+04	.252984-01	.000000	.180000-00	.581000-00	.239000-00
.340360-01	.441957+06	.381000-01	.162222+04	.291084-01	.000000	.206000-00	.571000-00	.223000-00
.439674-01	.405414+06	.444500-01	.157222+04	.316484-01	.000000	.201000-00	.564000-00	.235000-00
.503174-01	.129622+06	.508000-01	.136111+04	.381000-01	.000000	.267000-00	.497000-00	.236000-00
.534924-01	.102043+06	.558800-01	.533333+03	.457200-01	.000000	.164000-00	.613000-00	.222000-00
.000000	.000000	.000000	.000000	.570484-01	.000000	.000000	.785000-00	.215000-00

HIGH TEMPERATURE VITIATED AIR

AXIAL LOCATION = 10.2 CM

Z-M	PP-N/M**2	Z-M	TT-DEG K	Z-M	Y-H2	Y-H2O	Y-N2	Y-O2
.000000	.297855+06	.000000	.427778+03	.127000-02	.100000+01	-.000000	-.000000	-.000000
.889000-03	.301992+06	.508000-02	.522222+03	.508000-02	.000000	-.000000	-.000000	-.000000
.723900-02	.306129+06	.101600-01	.150000+04	.660400-02	.100000+01	.000000	.000000	.000000
.122174-01	.259244+06	.152400-01	.222222+04	.762000-02	.975000-00	.130000-01	.700000-02	.500000-02
.153670-01	.417825+06	.203200-01	.175000+04	.101600-01	.900000-00	.570000-01	.320000-01	.110000-01
.168910-01	.427478+06	.254000-01	.168889+04	.127000-01	.671000-00	.124000+00	.148000-00	.560000-01
.185674-01	.432993+06	.317500-01	.167222+04	.152400-01	-.000000	.316000-00	.509000-00	.174000-00
.194310-01	.428857+06	.381000-01	.163333+04	.177800-01	-.000000	.261000-00	.531000-00	.208000-00
.219710-01	.427478+06	.444500-01	.160556+04	.202184-01	-.000000	.234000-00	.564000-00	.201000-00
.245110-01	.427478+06	.508000-01	.144444+04	.203200-01	-.000000	.251000-00	.550000-00	.199000-00
.308610-01	.424720+06	.584200-01	.722222+03	.240284-01	-.000000	.227000-00	.560000-00	.213000-00
.340360-01	.426099+06	.000000	.000000	.252984-01	-.000000	.208000-00	.567000-00	.225000-00
.348234-01	.424720+06	.000000	.000000	.265684-01	-.000000	.218000-00	.569000-00	.214000-00
.359410-01	.422651+06	.000000	.000000	.291084-01	-.000000	.216000-00	.569000-00	.215000-00
.363474-01	.421272+06	.000000	.000000	.316484-01	-.000000	.208000-00	.553000-00	.239000-00
.388874-01	.420583+06	.000000	.000000	.341884-01	-.000000	.228000-00	.556000-00	.217000-00
.414274-01	.407483+06	.000000	.000000	.367284-01	-.000000	.222000-00	.569000-00	.209000-00
.439674-01	.383351+06	.000000	.000000	.381000-01	.000000	.251000-00	.503000-00	.246000-00
.503174-01	.159959+06	.000000	.000000	.444500-01	.000000	.237000-00	.521000-00	.242000-00
.534924-01	.122727+06	.000000	.000000	.570484-01	-.000000	.340000-01	.752000-00	.214000-00
.553974-01	.106869+06	.000000	.000000	.633984-01	-.000000	.000000	.779000-00	.221000-00

TABLE IV. - PROBE DATA - CONTINUED

HIGH TEMPERATURE VITIATED AIR

AXIAL LOCATION = 17.8 CM

Z-M	PP-N/M**2	Z-M	TT-DEG K	Z-M	Y-H2	Y-H2O	Y-N2	Y-O2
.000000	.335087+06	.000000	.588889+03	.000000	.983000-00	.500000-02	.800000-02	.400000-02
.889000-03	.304061+06	.508000-02	.827778+03	.317500-02	.978000-00	.600000-02	.110000-01	.500000-02
.586740-02	.273034+06	.101600-01	.158889+04	.635000-02	.958000-00	.140000-01	.210000-01	.700000-02
.586740-02	.273724+06	.152400-01	.194444+04	.101600-01	.875000-00	.420000-01	.650000-01	.180000-01
.723900-02	.292340+06	.190500-01	.225000+04	.127000-01	.739000-00	.101000+00	.118000+00	.410000-01
.967740-02	.253039+06	.203200-01	.205556+04	.139700-01	.644000-00	.131000-00	.169000-00	.560000-01
.977900-02	.286824+06	.254000-01	.169444+04	.152400-01	.423000-00	.241000-00	.237000-00	.990000-01
.122174-01	.260623+06	.317500-01	.167778+04	.177800-01	.080000	.303000-00	.516000-00	.160000-00
.135890-01	.267518+06	.381000-01	.165000+04	.189484-01	-.000000	.250000-00	.547000-00	.203000-00
.135890-01	.270966+06	.444500-01	.160556+04	.202184-01	-.000000	.244000-00	.575000-00	.182000-00
.153670-01	.366114+06	.508000-01	.140000+04	.221234-01	-.000000	.204000-00	.576000-00	.220000-00
.168910-01	.399898+06	.571500-01	.104444+04	.252984-01	-.000000	.208000-00	.569000-00	.223000-00
.185674-01	.410241+06	.635000-01	.638889+03	.291084-01	.000000	.205000-00	.577000-00	.218000-00
.194310-01	.419204+06	.000000	.000000	.316484-01	-.000000	.200000-00	.565000-00	.235000-00
.219710-01	.424720+06	.000000	.000000	.329184-01	.000000	.203000-00	.576000-00	.221000-00
.232410-01	.427478+06	.000000	.000000	.341884-01	-.000000	.230000-00	.542000-00	.228000-00
.245110-01	.426788+06	.000000	.000000	.367284-01	-.000000	.226000-00	.553000-00	.221000-00
.270510-01	.427478+01	.000000	.000000	.381000-01	.000000	.202000-00	.482000-00	.216000-00
.276860-01	.427478+06	.000000	.000000	.444500-01	.000000	.208000-00	.547000-00	.245000-00
.308610-01	.426099+06	.000000	.000000	.570484-01	-.000000	.880000-01	.700000-00	.212000-00
.340360-01	.425409+06	.000000	.000000	.633984-01	-.000000	.390000-01	.743000-00	.218000-00
.348234-01	.419893+06	.000000	.000000	.000000	.000000	.000000	.000000	.000000
.359410-01	.416446+06	.000000	.000000	.000000	.000000	.000000	.000000	.000000
.363474-01	.415067+06	.000000	.000000	.000000	.000000	.000000	.000000	.000000
.372110-01	.419204+06	.000000	.000000	.000000	.000000	.000000	.000000	.000000
.388874-01	.393693+06	.000000	.000000	.000000	.000000	.000000	.000000	.000000
.414274-01	.339914+06	.000000	.000000	.000000	.000000	.000000	.000000	.000000
.426974-01	.355772+06	.000000	.000000	.000000	.000000	.000000	.000000	.000000
.439674-01	.293718+06	.000000	.000000	.000000	.000000	.000000	.000000	.000000
.465074-01	.262002+06	.000000	.000000	.000000	.000000	.000000	.000000	.000000
.471424-01	.244076+06	.000000	.000000	.000000	.000000	.000000	.000000	.000000
.503174-01	.170991+06	.000000	.000000	.000000	.000000	.000000	.000000	.000000
.534924-01	.139275+06	.000000	.000000	.000000	.000000	.000000	.000000	.000000
.553974-01	.124106+06	.000000	.000000	.000000	.000000	.000000	.000000	.000000
.566674-01	.120659+06	.000000	.000000	.000000	.000000	.000000	.000000	.000000
.639826-01	.106180+06	.000000	.000000	.000000	.000000	.000000	.000000	.000000

HIGH TEMPERATURE VITIATED AIR

AXIAL LOCATION = 25.4 CM

Z-M	PP-N/M**2	Z-M	TT-DEG K	Z-M	Y-H2	Y-H2O	Y-N2	Y-O2
.000000	.289582+06	.000000	.855556+03	.127000-02	.950000-00	.180000-01	.220000-01	.110000-01
.889000-03	.295097+06	.508000-02	.107222+04	.317500-02	.937000-00	.190000-01	.310000-01	.120000-01
.419100-02	.300613+06	.101600-01	.155556+04	.635000-02	.915000-00	.320000-01	.390000-01	.140000-01
.586740-02	.268897+06	.177800-01	.194444+04	.101600-01	.825000-00	.640000-01	.810000-01	.300000-01
.723900-02	.285445+06	.203200-01	.222222+04	.127000-01	.583000-00	.149000-00	.197000-00	.710000-01
.967740-02	.262002+06	.228600-01	.222222+04	.127000-01	.680000-00	.125000-00	.142000-00	.520000-01
.977900-02	.279929+06	.254000-01	.186667+04	.152400-01	.550000-00	.153000-00	.228000-00	.690000-01
.122174-01	.273034+06	.317500-01	.167222+04	.177800-01	.291000-00	.163000-00	.416000-00	.130000-00
.135890-01	.278550+06	.381000-01	.166667+04	.221234-01	-.000000	.278000-00	.524000-00	.198000-00
.152654-01	.337845+06	.444500-01	.164444+04	.252984-01	-.000000	.183000-00	.584000-00	.232000-00
.153670-01	.349566+06	.508000-01	.148333+04	.316484-01	-.000000	.191000-00	.577000-00	.231000-00
.168910-01	.377835+06	.571500-01	.117222+04	.381000-01	.000000	.231000-00	.528000-00	.246000-00
.185674-01	.384730+06	.635000-01	.838889+03	.444500-01	.000000	.198000-00	.564000-00	.238000-00
.194310-01	.413688+06	.685800-01	.644444+03	.508000-01	.000000	.141000-00	.615000-00	.244000-00
.194310-01	.409551+06	.000000	.000000	.570484-01	-.000000	.710000-01	.709000-00	.220000-00
.219710-01	.425409+06	.000000	.000000	.633984-01	-.000000	.500000-01	.746000-00	.204000-00
.245110-01	.425409+06	.000000	.000000	.000000	.000000	.000000	.000000	.000000
.245110-01	.431614+06	.000000	.000000	.000000	.000000	.000000	.000000	.000000
.270510-01	.432993+06	.000000	.000000	.000000	.000000	.000000	.000000	.000000
.276860-01	.432993+06	.000000	.000000	.000000	.000000	.000000	.000000	.000000
.308610-01	.426099+06	.000000	.000000	.000000	.000000	.000000	.000000	.000000
.340360-01	.413688+06	.000000	.000000	.000000	.000000	.000000	.000000	.000000
.348234-01	.402656+06	.000000	.000000	.000000	.000000	.000000	.000000	.000000
.359410-01	.392314+06	.000000	.000000	.000000	.000000	.000000	.000000	.000000
.363474-01	.386109+06	.000000	.000000	.000000	.000000	.000000	.000000	.000000
.372110-01	.388867+06	.000000	.000000	.000000	.000000	.000000	.000000	.000000
.388874-01	.344740+06	.000000	.000000	.000000	.000000	.000000	.000000	.000000
.388874-01	.379903+06	.000000	.000000	.000000	.000000	.000000	.000000	.000000
.414274-01	.299234+06	.000000	.000000	.000000	.000000	.000000	.000000	.000000
.439674-01	.266829+06	.000000	.000000	.000000	.000000	.000000	.000000	.000000
.439674-01	.291650+06	.000000	.000000	.000000	.000000	.000000	.000000	.000000
.465074-01	.253729+06	.000000	.000000	.000000	.000000	.000000	.000000	.000000
.471424-01	.244765+06	.000000	.000000	.000000	.000000	.000000	.000000	.000000
.503174-01	.177886+06	.000000	.000000	.000000	.000000	.000000	.000000	.000000
.534924-01	.153065+06	.000000	.000000	.000000	.000000	.000000	.000000	.000000
.553974-01	.131001+06	.000000	.000000	.000000	.000000	.000000	.000000	.000000
.566674-01	.136317+06	.000000	.000000	.000000	.000000	.000000	.000000	.000000
.639826-01	.117212+06	.000000	.000000	.000000	.000000	.000000	.000000	.000000
.703326-01	.105490+06	.000000	.000000	.000000	.000000	.000000	.000000	.000000
.834390-01	.100664+06	.000000	.000000	.000000	.000000	.000000	.000000	.000000

TABLE IV. - PROBE DATA - CONTINUED

HIGH TEMPERATURE VITIATED AIR

AXIAL LOCATION = 35.6 CM

Z-M	PP-N/M**2	Z-M	TT-DEG K	Z-M	Y-H2	Y-H2O	Y-N2	Y-O2
.000000	.280618+06	.000000	.855556+03	.127000-02	.915000-00	.340000-01	.350000-01	.160000-01
.889000-03	.269587+06	.508000-02	.107222+04	.330200-02	.880000-00	.400000-01	.610000-01	.200000-01
.586740-02	.258555+06	.101600-01	.155556+04	.635000-02	.874000-00	.480000-01	.930000-01	.240000-01
.723900-02	.277860+06	.152400-01	.186667+04	.101600-01	.743000-00	.880000-01	.130000-00	.390000-01
.967740-02	.267518+06	.203200-01	.213889+04	.127000-01	.722000-00	.950000-01	.144000-00	.390000-01
.977900-02	.273034+06	.254000-01	.222222+0.	.152400-01	.536000-00	.168000-00	.208000-00	.680000-01
.122174-01	.282687+06	.317500-01	.183333+04	.165100-01	.385800-00	.179000-00	.322000-00	.114000+00
.135890-01	.273724+06	.381000-01	.166667+04	.177800-01	.384000-00	.140000-00	.348000-00	.128000-00
.153670-01	.329571+06	.444500-01	.164444+04	.202184-01	.000000	.225000-00	.581000-00	.194000-00
.168910-01	.351635+06	.508000-01	.148333+04	.221234-01	.000000	.178000-00	.657000-00	.164000-00
.185674-01	.369561+06	.571500-01	.117222+04	.252984-01	.000000	.140000-00	.630000-00	.229000-00
.194310-01	.379903+06	.635000-01	.838889+03	.316484-01	.000000	.144000-00	.634000-00	.222000-00
.207010-01	.393004+06	.685800-01	.644444+03	.367284-01	.000000	.156000-00	.605000-00	.239000-00
.219710-01	.400588+06	.000000	.000000	.381000-01	.000000	.320000-00	.527000-00	.152000-00
.245110-01	.413688+06	.000000	.000000	.444500-01	.000000	.173000-00	.615000-00	.212000-00
.270510-01	.426788+06	.000000	.000000	.508000-01	.000000	.161000-00	.643000-00	.196000-00
.276860-01	.426788+06	.000000	.000000	.570484-01	.000000	.300000-01	.765000-00	.205000-00
.308610-01	.407483+06	.000000	.000000	.633984-01	.000000	.300000-01	.765000-00	.205000-00
.340360-01	.377635+06	.000000	.000000	.000000	.000000	.000000	.000000	.000000
.348234-01	.374368+06	.000000	.000000	.000000	.000000	.000000	.000000	.000000
.359410-01	.330261+06	.000000	.000000	.000000	.000000	.000000	.000000	.000000
.363474-01	.351635+06	.000000	.000000	.000000	.000000	.000000	.000000	.000000
.388874-01	.317161+06	.000000	.000000	.000000	.000000	.000000	.000000	.000000
.401574-01	.321298+06	.000000	.000000	.000000	.000000	.000000	.000000	.000000
.414274-01	.274413+06	.000000	.000000	.000000	.000000	.000000	.000000	.000000
.439674-01	.249592+06	.000000	.000000	.000000	.000000	.000000	.000000	.000000
.465074-01	231665+06	.000000	.000000	.000000	.000000	.000000	.000000	.000000
.471424-01	.224081+06	.000000	.000000	.000000	.000000	.000000	.000000	.000000
.503174-01	.177886+06	.000000	.000000	.000000	.000000	.000000	.000000	.000000
.535940-01	.155822+06	.000000	.000000	.000000	.000000	.000000	.000000	.000000
.553974-01	.140654+06	.000000	.000000	.000000	.000000	.000000	.000000	.000000
.639826-01	.121348+06	.000000	.000000	.000000	.000000	.000000	.000000	.000000
.703326-01	.113764+06	.000000	.000000	.000000	.000000	.000000	.000000	.000000
.834390-01	.979062+05	.000000	.000000	.000000	.000000	.000000	.000000	.000000

TABLE IV. - PROBE DATA - CONTINUED

HIGH TEMPERATURE VITIATED NITROGEN — AXIAL LOCATION = 0.33 CM

Z-M	PP-N/M**2	Z-M	TT-DEG K	Z-M	Y-H2	Y-H2O	Y-N2	Y-O2
.000000	.307508+06	.000000	.238889+03	.317500-02	.100000+01	.000000	.000000	.000000
.889000-03	.299234+06	.127000-02	.330556+03	.635000-02	.100000+01	.000000	.000000	.000000
.586740-02	.290961+06	.685800-02	.422222+03	.996950-02	.100000+01	.000000	.000000	.000000
.723900-02	.296476+06	.101600-01	.700000+03	.127000-01	.000000	.162000-00	.796000-00	.420000-01
.967740-02	.206844+06	.124460-01	.139444+04	.221234-01	.000000	.169000-00	.789000-00	.420000-01
.977900-02	.306129+06	.152400-01	.167778+04	.252984-01	.000000	.185000-00	.770000-00	.450000-01
.122174-01	.455057+05	.165100-01	.170556+04	.316484-01	.000000	.152000-00	.791000-00	.570000-01
.135890-01	.384730+06	.185420-01	.172222+04	.444500-01	.000000	.163000-00	.795000-00	.420000-01
.185674-01	.427478+06	.200660-01	.171667+04	.500126-01	.000000	.163000-00	.795000-00	.420000-01
.245110-01	.434372+06	.228600-01	.170556+04	.000000	.000000	.000000	.000000	.000000
.308610-01	.445404+06	.266700-01	.170556+04	.000000	.000000	.000000	.000000	.000000
.340360-01	.437130+06	.330200-01	.166667+04	.000000	.000000	.000000	.000000	.000000
.439674-01	.432993+06	.393700-01	.158889+04	.000000	.000000	.000000	.000000	.000000
.503174-01	.979062+05	.431800-01	.148889+04	.000000	.000000	.000000	.000000	.000000
.534924-01	.979062+05	.469900-01	.140556+04	.000000	.000000	.000000	.000000	.000000
.000000	.000000	.495300-01	.134444+04	.000000	.000000	.000000	.000000	.000000
.000000	.000000	.495300-01	.133333+04	.000000	.000000	.000000	.000000	.000000
.000000	.000000	.520700-01	.123889+04	.000000	.000000	.000000	.000000	.000000
.000000	.000000	.546100-01	.101667+04	.000000	.000000	.000000	.000000	.000000

HIGH TEMPERATURE VITIATED NITROGEN — AXIAL LOCATION = 5.1 CM

Z-M	PP-N/M**2	Z-M	TT-DEG K	Z-M	Y-H2	Y-H2O	Y-N2	Y-O2
.000000	.283376+06	.000000	.361111+03	.127000-02	.100000+01	.000000	.000000	.000000
.889000-03	.289582+06	.508000-02	.500000+03	.317500-02	.100000+01	.000000	.000000	.000000
.342900-02	.295787+06	.101600-01	.173333+04	.635000-02	.100000+01	.000000	.000000	.000000
.586740-02	.297855+06	.152400-01	.170000+04	.914400-02	.100000+01	.000000	.000000	.000000
.723900-02	.293029+06	.203200-01	.170000+04	.101600-01	.887000-00	.320000-01	.750000-01	.500000-02
.967740-02	.250281+06	.254000-01	.168889+04	.127000-01	.469000-00	.168000-00	.343000-00	.200000-01
.977900-02	.296476+06	.317500-01	.166111+04	.152400-01	.000000	.161000-00	.787000-00	.520000-01
.122174-01	.314403+06	.381000-01	.162222+04	.221234-01	.000000	.155000-00	.798000-00	.480000-01
.135890-01	.335087+06	.444500-01	.157222+04	.252984-01	.000000	.163000-00	.784000-00	.530000-01
.160274-01	.441957+06	.508000-01	.136111+04	.316484-01	.000000	.145000-00	.782000-00	.730000-01
.185674-01	.449541+06	.558800-01	.533333+03	.381000-01	.000000	.247000-00	.703000-00	.500000-01
.213360-01	.439888+06	.000000	.000000	.406400-01	.000000	.152000-00	.793000-00	.560000-01
.219710-01	.439199+06	.000000	.000000	.595884-01	.000000	.340000-01	.754000-00	.212000-00
.245110-01	.441957+06	.000000	.000000	.633984-01	.000000	.000000	.795000-00	.205000-00
.270510-01	.439888+06	.000000	.000000	.000000	.000000	.000000	.000000	.000000
.276860-01	.441267+06	.000000	.000000	.000000	.000000	.000000	.000000	.000000
.308610-01	.444715+06	.000000	.000000	.000000	.000000	.000000	.000000	.000000
.340360-01	.449541+06	.000000	.000000	.000000	.000000	.000000	.000000	.000000
.407924-01	.435062+06	.000000	.000000	.000000	.000000	.000000	.000000	.000000
.414274-01	.435062+06	.000000	.000000	.000000	.000000	.000000	.000000	.000000
.439674-01	.408862+06	.000000	.000000	.000000	.000000	.000000	.000000	.000000
.465074-01	.333708+06	.000000	.000000	.000000	.000000	.000000	.000000	.000000
.471424-01	.295097+06	.000000	.000000	.000000	.000000	.000000	.000000	.000000
.503174-01	.139275+06	.000000	.000000	.000000	.000000	.000000	.000000	.000000

HIGH TEMPERATURE VITIATED NITROGEN — AXIAL LOCATION = 10.2 CM

Z-M	PP-N/M**2	Z-M	TT-DEG K	Z-M	Y-H2	Y-H2O	Y-N2	Y-O2
.000000	.292340+06	.000000	.427778+03	.127000-02	.100000+01	-.000000	-.000000	-.000000
.889000-03	.293718+06	.508000-02	.522222+03	.317500-02	.100000+01	-.000000	-.000000	-.000000
.889000-03	.295097+06	.101600-01	.150000+04	.635000-02	.100000+01	-.000000	-.000000	-.000000
.586740-02	.298545+06	.152400-01	.175556+04	.762000-02	.100000+01	.000000	.000000	.000000
.723900-02	.304061+06	.203200-01	.170556+04	.127000-01	.778000-00	.320000-01	.172000-00	.170000-01
.967740-02	.266139+06	.254000-01	.168889+04	.152400-01	.262000-00	.149000-00	.551000-00	.380000-01
.977900-02	.295787+06	.317500-01	.167222+04	.165100-01	.000000	.188000-00	.768000-00	.450000-01
.122174-01	.327503+06	.381000-01	.163333+04	.202184-01	.000000	.132000-00	.819000-00	.490000-01
.135890-01	.321298+06	.444500-01	.160556+04	.221234-01	.000000	.125000-00	.808000-00	.670000-01
.153670-01	.430236+06	.508000-01	.144444+04	.252984-01	.000000	.144000-00	.815000-00	.410000-01
.168910-01	.437820+06	.584200-01	.722222+03	.316484-01	.000000	.121000+00	.818000-00	.610000-01
.185674-01	.438509+06	.000000	.000000	.341684-01	.000000	.119000+00	.817000-00	.640000-01
.185674-01	.430925+06	.000000	.000000	.367284-01	.000000	.118000+00	.840000-00	.420000-01
.194310-01	.439199+06	.000000	.000000	.381000-01	.000000	.158000-00	.784000-00	.580000-01
.207010-01	.431614+06	.000000	.000000	.570484-01	.000000	.490000-01	.781000-00	.170000-00
.219710-01	.437130+06	.000000	.000000	.633984-01	.000000	.000000	.788000-00	.212000-00
.245110-01	.434372+06	.000000	.000000	.000000	.000000	.000000	.000000	.000000
.266700-01	.430236+06	.000000	.000000	.000000	.000000	.000000	.000000	.000000
.270510-01	.430236+06	.000000	.000000	.000000	.000000	.000000	.000000	.000000
.308610-01	.432304+06	.000000	.000000	.000000	.000000	.000000	.000000	.000000
.340360-01	.432993+06	.000000	.000000	.000000	.000000	.000000	.000000	.000000
.348234-01	.432993+06	.000000	.000000	.000000	.000000	.000000	.000000	.000000
.363474-01	.432993+06	.000000	.000000	.000000	.000000	.000000	.000000	.000000
.388874-01	.432993+06	.000000	.000000	.000000	.000000	.000000	.000000	.000000
.401574-01	.428857+06	.000000	.000000	.000000	.000000	.000000	.000000	.000000
.414274-01	.421962+06	.000000	.000000	.000000	.000000	.000000	.000000	.000000
.439674-01	.375077+06	.000000	.000000	.000000	.000000	.000000	.000000	.000000
.461264-01	.321987+06	.000000	.000000	.000000	.000000	.000000	.000000	.000000
.465074-01	.308887+06	.000000	.000000	.000000	.000000	.000000	.000000	.000000
.486410-01	.432993+06	.000000	.000000	.000000	.000000	.000000	.000000	.000000
.503174-01	.163407+06	.000000	.000000	.000000	.000000	.000000	.000000	.000000
.534924-01	.124796+06	.000000	.000000	.000000	.000000	.000000	.000000	.000000
.553974-01	.113075+06	.000000	.000000	.000000	.000000	.000000	.000000	.000000
.589026-01	.102043+06	.000000	.000000	.000000	.000000	.000000	.000000	.000000

TABLE IV. - PROBE DATA - CONTINUED

HIGH TEMPERATURE VITIATED NITROGEN

AXIAL LOCATION = 17.8 CM

Z-M	PP-N/M**2	Z-M	TT-DEG K	Z-M	Y-H2	Y-H2O	Y-N2	Y-O2
.000000	.285445+06	.000000	.588889+03	.000000	.983000-00	.700000-02	.100000-01	.000000
.889000-03	.294408+06	.508000-02	.827778+03	.317500-02	.978000-00	.700000-02	.130000-01	.200000-02
.889000-03	.303371+06	.101600-01	.158889+04	.635000-02	.953000-00	.140000-01	.310000-01	.200000-02
.586740-02	.288203+06	.152400-01	.180556+04	.101600-01	.808000-00	.540000-01	.125000-00	.130000-01
.586740-02	.293718+06	.203200-01	.171667+04	.127000-01	.563000-00	.128000-00	.289000-00	.200000-01
.723900-02	.300613+06	.254000-01	.169444+04	.165100-01	.173000-00	.168000-00	.624000-00	.350000-01
.723900-02	.304750+06	.317500-01	.167778+04	.202184-01	.000000	.139000-00	.806000-00	.550000-01
.967740-02	.282687+06	.381000-01	.165000+04	.221234-01	.000000	.140000-00	.804000-00	.560000-01
.977900-02	.297855+06	.444500-01	.160556+04	.252984-01	.000000	.144000-00	.798000-00	.580000-01
.101600-01	.255108+06	.508000-01	.140000+04	.381000-01	.000000	.160000-00	.781000-00	.590000-01
.122174-01	.303371+06	.571500-01	.104444+04	.444500-01	.000000	.164000-00	.752000-00	.830000-01
.122174-01	.301992+06	.635000-01	.638889+03	.508000-01	.000000	.178000-00	.732000-00	.910000-01
.135890-01	.318540+06	.000000	.000000	.570484-01	.000000	.620000-01	.767000-00	.171000-00
.135890-01	.317850+06	.000000	.000000	.633984-01	.000000	.210000-01	.792000-00	.188000-00
.185674-01	.421272+06	.000000	.000000	.697484-01	.000000	.000000	.788000-00	.212000-00
.185674-01	.423341+06	.000000	.000000	.000000	.000000	.000000	.000000	.000000
.194310-01	.425409+06	.000000	.000000	.000000	.000000	.000000	.000000	.000000
.207010-01	.428857+06	.000000	.000000	.000000	.000000	.000000	.000000	.000000
.219710-01	.427478+06	.000000	.000000	.000000	.000000	.000000	.000000	.000000
.245110-01	.427478+06	.000000	.000000	.000000	.000000	.000000	.000000	.000000
.245110-01	.428167+06	.000000	.000000	.000000	.000000	.000000	.000000	.000000
.245110-01	.428857+06	.000000	.000000	.000000	.000000	.000000	.000000	.000000
.276860-01	.428857+06	.000000	.000000	.000000	.000000	.000000	.000000	.000000
.308610-01	.428857+06	.000000	.000000	.000000	.000000	.000000	.000000	.000000
.340360-01	.430236+06	.000000	.000000	.000000	.000000	.000000	.000000	.000000
.359410-01	.429546+06	.000000	.000000	.000000	.000000	.000000	.000000	.000000
.372110-01	.427478+06	.000000	.000000	.000000	.000000	.000000	.000000	.000000
.388874-01	.419204+06	.000000	.000000	.000000	.000000	.000000	.000000	.000000
.401574-01	.406793+06	.000000	.000000	.000000	.000000	.000000	.000000	.000000
.414274-01	.381972+06	.000000	.000000	.000000	.000000	.000000	.000000	.000000
.439674-01	.325435+06	.000000	.000000	.000000	.000000	.000000	.000000	.000000
.439674-01	.293718+06	.000000	.000000	.000000	.000000	.000000	.000000	.000000
.439674-01	.326814+06	.000000	.000000	.000000	.000000	.000000	.000000	.000000
.465074-01	.429546+06	.000000	.000000	.000000	.000000	.000000	.000000	.000000
.471424-01	.246144+06	.000000	.000000	.000000	.000000	.000000	.000000	.000000
.503174-01	.172370+06	.000000	.000000	.000000	.000000	.000000	.000000	.000000
.534924-01	.144101+06	.000000	.000000	.000000	.000000	.000000	.000000	.000000
.553974-01	.128243+06	.000000	.000000	.000000	.000000	.000000	.000000	.000000
.566674-01	.131001+06	.000000	.000000	.000000	.000000	.000000	.000000	.000000
.639826-01	.106180+06	.000000	.000000	.000000	.000000	.000000	.000000	.000000

HIGH TEMPERATURE VITIATED NITROGEN

AXIAL LOCATION = 25.4 CM

Z-M	PP-N/M**2	Z-M	TT-DEG K	Z-M	Y-H2	Y-H2O	Y-N2	Y-O2
.000000	.322677+06	.000000	.855556+03	.317500-02	.946000-00	.160000-01	.370000-01	.000000
.889000-03	.317161+06	.508000-02	.107222+04	.635000-02	.894000-00	.330000-01	.730000-01	.000000
.419100-02	.311645+06	.101600-01	.155556+04	.101600-01	.777000-00	.660000-01	.145000-00	.130000-01
.586740-02	.298545+06	.152400-01	.183889+04	.127000-01	.493000-00	.159000-00	.348000-00	.000000
.723900-02	.307508+06	.203200-01	.175000+04	.152400-01	.355000-00	.178000-00	.438000-00	.290000-01
.723900-02	.308887+06	.254000-01	.170000+04	.177800-01	.158000-00	.164000-00	.629000-00	.490000-01
.967740-02	.299234+06	.317500-01	.167222+04	.221234-01	.000000	.186000-00	.758000-00	.560000-01
.977900-02	.306129+06	.381000-01	.166667+04	.252984-01	.000000	.183000-00	.759000-00	.580000-01
.122174-01	.310266+06	.444500-01	.164444+04	.381000-01	.000000	.229000-00	.706000-00	.650000-01
.122174-01	.321298+06	.508000-01	.148333+04	.444500-01	.000000	.180000-00	.725000-00	.950000-01
.135890-01	.336466+06	.571500-01	.117222+04	.508000-01	.000000	.152000-00	.720000-00	.128000-00
.152654-01	.373698+06	.635000-01	.838889+03	.570484-01	.000000	.660000-01	.787000-00	.147000-00
.185674-01	.400588+06	.685800-01	.644444+03	.633984-01	.000000	.470000-01	.775000-00	.177000-00
.194310-01	.427478+06	.000000	.000000	.697484-01	.000000	.310000-01	.781000-00	.188000-00
.219710-01	.436441+06	.000000	.000000	.120650+00	.000000	.000000	.782000-00	.218000-00
.245110-01	.431614+06	.000000	.000000	.139598-00	.000000	.000000	.799000-00	.201000-00
.270510-01	.436441+06	.000000	.000000	.000000	.000000	.000000	.000000	.000000
.276860-01	.435751+06	.000000	.000000	.000000	.000000	.000000	.000000	.000000
.308610-01	.430925+06	.000000	.000000	.000000	.000000	.000000	.000000	.000000
.340360-01	.426099+06	.000000	.000000	.000000	.000000	.000000	.000000	.000000
.372110-01	.404035+06	.000000	.000000	.000000	.000000	.000000	.000000	.000000
.372110-01	.392314+06	.000000	.000000	.000000	.000000	.000000	.000000	.000000
.388874-01	.386798+06	.000000	.000000	.000000	.000000	.000000	.000000	.000000
.414274-01	.336466+06	.000000	.000000	.000000	.000000	.000000	.000000	.000000
.439674-01	.299234+06	.000000	.000000	.000000	.000000	.000000	.000000	.000000
.465074-01	.238560+06	.000000	.000000	.000000	.000000	.000000	.000000	.000000
.471424-01	.230286+06	.000000	.000000	.000000	.000000	.000000	.000000	.000000
.503174-01	.198570+06	.000000	.000000	.000000	.000000	.000000	.000000	.000000
.534924-01	.164096+06	.000000	.000000	.000000	.000000	.000000	.000000	.000000
.566674-01	.143412+06	.000000	.000000	.000000	.000000	.000000	.000000	.000000
.566674-01	.132380+06	.000000	.000000	.000000	.000000	.000000	.000000	.000000
.639826-01	.111086+06	.000000	.000000	.000000	.000000	.000000	.000000	.000000
.703326-01	.104111+06	.000000	.000000	.000000	.000000	.000000	.000000	.000000
.834390-01	.965272+05	.000000	.000000	.000000	.000000	.000000	.000000	.000000

TABLE IV. - PROBE DATA - CONTINUED

HIGH TEMPERATURE VITIATED NITROGEN

AXIAL LOCATION = 35.6 CM

Z-M	PP-N/M**2	Z-M	TT-DEG K	Z-M	Y-H2	Y-H2O	Y-N2	Y-O2
.000000	.313024+06	.000000	.855556+03	.317500-02	.905000-00	.260000-01	.650000-01	.400000-02
.889000-03	.306129+06	.508000-02	.107222+04	.635000-02	.887000-00	.260000-01	.820000-01	.500000-02
.586740-02	.299234+06	.101600-01	.155556+04	.101600-01	.727000-00	.970000-01	.168000-00	.900000-02
.723900-02	.306129+06	.152400-01	.186667+04	.127000-01	.701000-00	.290000-01	.256000-00	.140000-01
.723900-02	.313024+06	.203200-01	.177778+04	.252984-01	.000000	.106000+00	.792000-00	.102000+00
.967740-02	.315092+06	.254000-01	.170000+04	.291084-01	.000000	.163000-00	.742000-00	.960000-01
.977900-02	.314403+06	.317500-01	.167222+04	.316484-01	.000000	.119000+00	.793000-00	.880000-01
.122174-01	.332329+06	.381000-01	.166667+04	.341884-01	.000000	.165000-00	.735000-00	.100000+00
.122174-01	.335777+06	.444500-01	.164444+04	.346964-01	.000000	.132000-00	.770000-00	.970000-01
.135890-01	.335777+06	.508000-01	.148333+04	.367284-01	.000000	.128000-00	.742000-00	.130000-00
.185674-01	.404035+06	.571500-01	.117222+04	.633984-01	.000000	.510000-01	.777000-00	.172000-00
.194310-01	.412309+06	.635000-01	.838889+03	.697484-01	.000000	.550000-01	.706000-00	.238000-00
.214630-01	.421962+06	.685800-01	.644444+03	.000000	.000000	.000000	.000000	.000000
.219710-01	.426099+06	.000000	.000000	.000000	.000000	.000000	.000000	.000000
.245110-01	.427478+06	.000000	.000000	.000000	.000000	.000000	.000000	.000000
.270510-01	.428857+06	.000000	.000000	.000000	.000000	.000000	.000000	.000000
.276860-01	.428167+06	.000000	.000000	.000000	.000000	.000000	.000000	.000000
.308610-01	.408172+06	.000000	.000000	.000000	.000000	.000000	.000000	.000000
.340360-01	.377146+06	.000000	.000000	.000000	.000000	.000000	.000000	.000000
.372110-01	.336466+06	.000000	.000000	.000000	.000000	.000000	.000000	.000000
.388874-01	.330950+06	.000000	.000000	.000000	.000000	.000000	.000000	.000000
.409194-01	.284755+06	.000000	.000000	.000000	.000000	.000000	.000000	.000000
.414274-01	.294408+06	.000000	.000000	.000000	.000000	.000000	.000000	.000000
.439674-01	.242007+06	.000000	.000000	.000000	.000000	.000000	.000000	.000000
.465074-01	.228218+06	.000000	.000000	.000000	.000000	.000000	.000000	.000000
.471424-01	.226839+06	.000000	.000000	.000000	.000000	.000000	.000000	.000000
.503174-01	.173749+06	.000000	.000000	.000000	.000000	.000000	.000000	.000000
.534924-01	.151686+06	.000000	.000000	.000000	.000000	.000000	.000000	.000000
.566674-01	.139964+06	.000000	.000000	.000000	.000000	.000000	.000000	.000000
.639826-01	.119280+06	.000000	.000000	.000000	.000000	.000000	.000000	.000000
.703326-01	.108248+06	.000000	.000000	.000000	.000000	.000000	.000000	.000000
.834390-01	.979062+05	.000000	.000000	.000000	.000000	.000000	.000000	.000000

TABLE IV. - PROBE DATA - CONTINUED

LOW TEMPERATURE VITIATED AIR — AXIAL LOCATION = 0.33 CM

Z-M	PP-N/M**2	Z-M	TT-DEG K	Z-M	Y-H2	Y-H2O	Y-N2	Y-O2
.000000	.295097+06	.000000	.361111+03	.317500-02	.100000+01	-.000000	-.000000	-.000000
.889000-03	.295097+06	.508000-02	.455556+03	.635000-02	.100000+01	-.000000	-.000000	-.000000
.889000-03	.295097+06	.101600-01	.141111+04	.996950-02	.100000+01	.000000	.000000	.000000
.723900-02	.298545+06	.152400-01	.157222+04	.127000-01	.000000	.162000-00	.796000-00	.420000-01
.723900-02	.296476+06	.238760-01	.178333+04	.221234-01	.000000	.169000-00	.789000-00	.420000-01
.122174-01	.198570+06	.254000-01	.150000+04	.221234-01	.000000	.191000-00	.606000-00	.203000-00
.122174-01	.372319+06	.266700-01	.175556+04	.221234-01	.000000	.121000+00	.639000-00	.240000-00
.185674-01	.426090+06	.330200-01	.166667+04	.252984-01	.000000	.185000-00	.770000-00	.450000-01
.185674-01	.424720+06	.393700-01	.152222+04	.252984-01	.000000	.129000-00	.611000-00	.260000-00
.245110-01	.428857+06	.469900-01	.129444+04	.316484-01	.000000	.152000-00	.791000-00	.570000-01
.308610-01	.438509+06	.495300-01	.123333+04	.316484-01	.000000	.191000-00	.582000-00	.227000-00
.340360-01	.432993+06	.508000-01	.110000+04	.316484-01	.000000	.121000+00	.635000-00	.244000-00
.439674-01	.432993+06	.520700-01	.115556+04	.381000-01	.000000	.154000-00	.578000-00	.267000-00
.503174-01	.985956+05	.546100-01	.101111+04	.444500-01	.000000	.233000-00	.704000-00	.640000-01
.534924-01	.985956+05	.571500-01	.711111+03	.444500-01	.000000	.157000-00	.574000-00	.269000-00
.000000	.000000	.000000	.000000	.570484-01	.000000	.000000	.809000-00	.191000-00
.000000	.000000	.000000	.000000	.570484-01	.000000	.000000	.810000-00	.190000-00

LOW TEMPERATURE VITIATED AIR — AXIAL LOCATION = 5.1 CM

Z-M	PP-N/M**2	Z-M	TT-DEG K	Z-M	Y-H2	Y-H2O	Y-N2	Y-O2
.000000	.285445+06	.000000	.316667+03	.127000-02	.100000+01	-.000000	-.000000	-.000000
.889000-03	.289582+06	.609600-02	.444444+03	.317500-02	.100000+01	-.000000	-.000000	-.000000
.723900-02	.293718+06	.104140-01	.156111+04	.635000-02	.100000+01	-.000000	-.000000	-.000000
.122174-01	.259934+06	.152400-01	.155000+04	.914400-02	.100000+01	.000000	.000000	.000000
.153670-01	.445404+06	.203200-01	.153333+04	.127000-01	.616000-00	.780000-01	.220000-00	.860000-01
.168910-01	.446094+06	.254000-01	.151667+04	.152400-01	.000000	.174000-00	.582000-00	.244000-00
.185674-01	.448851+06	.317500-01	.143889+04	.177800-01	.000000	.162000-00	.592000-00	.246000-00
.194310-01	.443336+06	.381000-01	.136667+04	.202184-01	-.000000	.130000-00	.629000-00	.241000-00
.219710-01	.443336+06	.444500-01	.128333+04	.221234-01	-.000000	.132000-00	.610000-00	.258000-00
.245110-01	.444025+06	.508000-01	.100000+04	.252984-01	-.000000	.121000+00	.623000-00	.256000-00
.299974-01	.985956+05	.558800-01	.588889+03	.316484-01	-.000000	.122000+00	.617000-00	.261000-00
.308610-01	.446094+06	.000000	.000000	.341884-01	-.000000	.121000+00	.609000-00	.270000-00
.340360-01	.443336+06	.000000	.000000	.367284-01	-.000000	.113000+00	.633000-00	.254000-00
.348234-01	.442646+06	.000000	.000000	.381000-01	.000000	.156000-00	.581000-00	.264000-00
.359410-01	.444025+06	.000000	.000000	.444500-01	.000000	.151000-00	.582000-00	.267000-00
.363474-01	.441267+06	.000000	.000000	.570484-01	-.000000	.122000+00	.696000-00	.182000-00
.388874-01	.441267+06	.000000	.000000	.633984-01	-.000000	.240000-01	.776000-00	.200000-00
.414274-01	.435062+06	.000000	.000000	.000000	.000000	.000000	.000000	.000000
.439674-01	.408862+06	.000000	.000000	.000000	.000000	.000000	.000000	.000000
.503174-01	.144791+06	.000000	.000000	.000000	.000000	.000000	.000000	.000000

LOW TEMPERATURE VITIATED AIR — AXIAL LOCATION = 10.2 CM

Z-M	PP-N/M**2	Z-M	TT-DEG K	Z-M	Y-H2	Y-H2O	Y-N2	Y-O2
.000000	.307508+06	.000000	.511111+03	.127000-02	.100000+01	-.000000	-.000000	-.000000
.889000-03	.303371+06	.508000-02	.527778+03	.317500-02	.100000+01	-.000000	-.000000	-.000000
.889000-03	.299234+06	.101600-01	.118333+04	.584200-02	.100000+01	.000000	.000000	.000000
.723900-02	.295787+06	.147320-01	.205556+04	.635000-02	.978000-00	.900000-02	.800000-02	.500000-02
.723900-02	.306129+06	.203200-01	.158333+04	.152400-01	.000000	.231000-00	.555000-00	.215000-00
.122174-01	.295097+06	.254000-01	.151111+04	.177800-01	.000000	.200000-00	.568000-00	.233000-00
.122174-01	.277171+06	.317500-01	.150556+04	.202184-01	-.000000	.135000-00	.631000-00	.235000-00
.153670-01	.425409+06	.381000-01	.146667+04	.221234-01	-.000000	.144000-00	.602000-00	.255000-00
.168910-01	.438509+06	.444500-01	.143889+04	.252984-01	-.000000	.137000-00	.615000-00	.248000-00
.185674-01	.435062+06	.508000-01	.129444+04	.316484-01	-.000000	.146000-00	.601000-00	.253000-00
.185674-01	.442646+06	.584200-01	.733333+03	.341884-01	-.000000	.126000-00	.586000-00	.288000-00
.194310-01	.441267+06	.000000	.000000	.367284-01	-.000000	.131000-00	.598000-00	.270000-00
.219710-01	.437130+06	.000000	.000000	.381000-01	.000000	.196000-00	.557000-00	.248000-00
.245110-01	.424030+06	.000000	.000000	.570484-01	-.000000	.180000-01	.757000-00	.225000-00
.245110-01	.435062+06	.000000	.000000	.000000	.000000	.000000	.000000	.000000
.308610-01	.432993+06	.000000	.000000	.000000	.000000	.000000	.000000	.000000
.340360-01	.432993+06	.000000	.000000	.000000	.000000	.000000	.000000	.000000
.348234-01	.432993+06	.000000	.000000	.000000	.000000	.000000	.000000	.000000
.359410-01	.431614+06	.000000	.000000	.000000	.000000	.000000	.000000	.000000
.363474-01	.431614+06	.000000	.000000	.000000	.000000	.000000	.000000	.000000
.388874-01	.430236+06	.000000	.000000	.000000	.000000	.000000	.000000	.000000
.414274-01	.421962+06	.000000	.000000	.000000	.000000	.000000	.000000	.000000
.439674-01	.341982+06	.000000	.000000	.000000	.000000	.000000	.000000	.000000
.439674-01	.441267+06	.000000	.000000	.000000	.000000	.000000	.000000	.000000
.503174-01	.165475+06	.000000	.000000	.000000	.000000	.000000	.000000	.000000
.534924-01	.125485+06	.000000	.000000	.000000	.000000	.000000	.000000	.000000

TABLE IV. - PROBE DATA - CONTINUED

LOW TEMPERATURE VITIATED AIR

AXIAL LOCATION = 17.8 CM

Z-M	PP-N/M**2	Z-M	TT-DEG K	Z-M	Y-H2	Y-H2O	Y-N2	Y-O2
.000000	.317161+06	.000000	.522222+03	.000000	.978000-00	.600000-02	.110000-01	.500000-02
.889000-03	.290271+06	.508000-02	.100000+04	.317500-02	.968000-00	.400000-02	.190000-01	.900000-02
.586740-02	.263381+06	.104140-01	.131111+04	.635000-02	.928000-00	.900000-02	.440000-01	.180000-01
.723900-02	.284066+06	.152400-01	.177778+04	.127000-01	.726000-00	.810000-01	.134000-00	.590000-01
.122174-01	.272345+06	.190500-01	.208333+04	.189484-01	-.000000	.172000-00	.586000-00	.242000-00
.135890-01	.263381+06	.203200-01	.188889+04	.221234-01	-.000000	.157000-00	.599000-00	.245000-00
.185674-01	.412309+06	.259080-01	.152222+04	.252984-01	-.000000	.150000-00	.594000-00	.255000-00
.245110-01	.423341+06	.317500-01	.150556+04	.316484-01	-.000000	.160000-00	.586000-00	.254000-00
.308610-01	.419204+06	.381000-01	.147778+04	.381000-01	.000000	.129000-00	.575000-00	.296000-00
.340360-01	.420583+06	.444500-01	.151111+04	.444500-01	-.000000	.114000+00	.599000-00	.287000-00
.372110-01	.417825+06	.513080-01	.135556+04	.508000-01	-.000000	.820000-01	.646000-00	.271000-00
.439674-01	.315782+06	.571500-01	.103333+04	.570484-01	-.000000	.150000-00	.652000-00	.198000-00
.503174-01	.178575+06	.637540-01	.811111+03	.633984-01	-.000000	.160000-00	.649000-00	.191000-00
.534924-01	.142722+06	.000000	.000000	.000000	.000000	.000000	.000000	.000000

LOW TEMPERATURE VITIATED AIR

AXIAL LOCATION = 25.4 CM

Z-M	PP-N/M**2	Z-M	TT-DEG K	Z-M	Y-H2	Y-H2O	Y-N2	Y-O2
.000000	.296476+06	.000000	.655556+03	.000000	.948000-00	.120000-01	.280000-01	.130000-01
.889000-03	.297166+06	.508000-02	.727778+03	.317500-02	.940000-00	.160000-01	.300000-01	.140000-01
.292100-02	.297855+06	.101600-01	.100000+04	.635000-02	.921000-00	.210000-01	.410000-01	.170000-01
.586740-02	.271655+06	.152400-01	.151667+04	.101600-01	.773000-00	.580000-01	.117000+00	.520000-01
.723900-02	.288203+06	.177800-01	.177778+04	.127000-01	.692000-00	.910000-01	.152000-00	.650000-01
.967740-02	.268897+06	.203200-01	.205556+04	.152400-01	.398000-00	.160000-00	.311000-00	.131000-00
.977900-02	.278550+06	.228600-01	.205556+04	.221234-01	.000000	.182000-00	.618000-00	.199000-00
.122174-01	.288203+06	.254000-01	.170000+04	.252984-01	.000000	.123000+00	.618000-00	.258000-00
.135890-01	.281308+06	.317500-01	.154444+04	.291084-01	.000000	.101000+00	.620000-00	.279000-00
.165354-01	.351635+06	.381000-01	.150556+04	.341884-01	.000000	.109000+00	.627000-00	.264000-00
.185674-01	.406793+06	.444500-01	.139444+04	.381000-01	.000000	.169000-00	.593000-00	.238000-00
.213360-01	.423341+06	.508000-01	.113889+04	.444500-01	.000000	.179000-00	.582000-00	.239000-00
.219710-01	.426099+06	.571500-01	.827778+03	.508000-01	.000000	.129000-00	.622000-00	.250000-00
.245110-01	.435751+06	.635000-01	.555556+03	.570484-01	.000000	.560000-01	.707000-00	.238000-00
.270510-01	.438509+06	.000000	.000000	.633984-01	.000000	.410000-01	.717000-00	.242000-00
.308610-01	.432993+06	.000000	.000000	.000000	.000000	.000000	.000000	.000000
.340360-01	.423341+06	.000000	.000000	.000000	.000000	.000000	.000000	.000000
.372110-01	.395762+06	.000000	.000000	.000000	.000000	.000000	.000000	.000000
.407924-01	.335777+06	.000000	.000000	.000000	.000000	.000000	.000000	.000000
.414274-01	.326814+06	.000000	.000000	.000000	.000000	.000000	.000000	.000000
.439674-01	.275792+06	.000000	.000000	.000000	.000000	.000000	.000000	.000000
.465074-01	.231665+06	.000000	.000000	.000000	.000000	.000000	.000000	.000000
.503174-01	.186160+06	.000000	.000000	.000000	.000000	.000000	.000000	.000000
.534924-01	.155822+06	.000000	.000000	.000000	.000000	.000000	.000000	.000000
.566674-01	.134449+06	.000000	.000000	.000000	.000000	.000000	.000000	.000000
.639826-01	.113764+06	.000000	.000000	.000000	.000000	.000000	.000000	.000000

TABLE IV. - PROBE DATA - CONTINUED

LOW TEMPERATURE VITIATED NITROGEN

AXIAL LOCATION = 0.33 CM

Z-M	PP-N/M**2	Z-M	TT-DEG K	Z-M	Y-H2	Y-H2O	Y-N2	Y-O2
.000000	.314403+06	.000000	.755556+03	.000000	.100000+01	-.000000	-.000000	-.000000
.889000-03	.303371+06	.121920-01	.114444+04	.317500-02	.100000+01	-.000000	-.000000	-.000000
.723900-02	.292340+06	.165100-01	.153333+04	.635000-02	.100000+01	-.000000	-.000000	-.000000
.122174-01	.273034+06	.223520-01	.155556+04	.996950-02	.100000+01	.000000	.000000	.000000
.185674-01	.423341+06	.266700-01	.155556+04	.127000-01	.000000	.130000-00	.838000-00	.320000-01
.245110-01	.430236+06	.317500-01	.153889+04	.189484-01	.000000	.150000-00	.768000-00	.820000-01
.308610-01	.441267+06	.393700-01	.146667+04	.222504-01	.000000	.162000-00	.755000-00	.830000-01
.340360-01	.437130+06	.469900-01	.129444+04	.316484-01	.000000	.128000-00	.784000-00	.870000-01
.372110-01	.429546+06	.495300-01	.125556+04	.381000-01	.000000	.134000-00	.816000-00	.500000-01
.439674-01	.431614+06	.520700-01	.114444+04	.444500-01	.000000	.141000-00	.820000-00	.390000-01
.503174-01	.110317+06	.546100-01	.922222+03	.570484-01	.000000	.000000	.809000-00	.191000-00
.534924-01	.992851+05	.571500-01	.544444+03	.633984-01	.000000	.000000	.785000-00	.215000-00

LOW TEMPERATURE VITIATED NITROGEN

AXIAL LOCATION = 5.1 CM

Z-M	PP-N/M**2	Z-M	TT-DEG K	Z-M	Y-H2	Y-H2O	Y-N2	Y-O2
.000000	.304750+06	.000000	.316667+03	.000000	.100000+01	-.000000	-.000000	-.000000
.469900-02	.291650+06	.609600-02	.444444+03	.317500-02	.100000+01	-.000000	-.000000	-.000000
.840740-02	.278550+06	.104140-01	.156111+04	.635000-02	.100000+01	-.000000	-.000000	-.000000
.110490-01	.260623+06	.154940-01	.151667+04	.914400-02	.100000+01	.000000	.000000	.000000
.147574-01	.426788+06	.203200-01	.152778+04	.127000-01	.439000-00	.132000-00	.411000-00	.180000-01
.245110-01	.443336+06	.259080-01	.151111+04	.189484-01	.000000	.154000-00	.739000-00	.106000+00
.308610-01	.446094+06	.317500-01	.150556+04	.252984-01	.000000	.162000-00	.736000-00	.102000+00
.340360-01	.446783+06	.386080-01	.146667+04	.316484-01	.000000	.148000-00	.760000-00	.920000-01
.372110-01	.446783+06	.444500-01	.140556+04	.419100-01	.000000	.138000-00	.816000-00	.460000-01
.439674-01	.412999+06	.513080-01	.122778+04	.482600-01	.000000	.193000-00	.707000-00	.990000-01
.503174-01	.153065+06	.561340-01	.700000+03	.000000	.000000	.000000	.000000	.000000
.534924-01	.106869+06	.000000	.000000	.000000	.000000	.000000	.000000	.000000

LOW TEMPERATURE VITIATED NITROGEN

AXIAL LOCATION = 10.2 CM

Z-M	PP-N/M**2	Z-M	TT-DEG K	Z-M	Y-H2	Y-H2O	Y-N2	Y-O2
.000000	.322677+06	.000000	.511111+03	.127000-02	.100000+01	-.000000	-.000000	-.000000
.469900-02	.299924+06	.508000-02	.527778+03	.317500-02	.100000+01	-.000000	-.000000	-.000000
.840740-02	.277171+06	.101600-01	.118333+04	.584200-02	.100000+01	.000000	.000000	.000000
.110490-01	.284066+06	.147320-01	.167778+04	.635000-02	.937000-00	.270000-01	.360000-01	.000000
.147574-01	.395072+06	.203200-01	.152222+04	.127000-01	.485000-00	.131000-00	.362000-00	.220000-01
.153670-01	.415756+06	.254000-01	.151111+04	.152400-01	.000000	.175000-00	.767000-00	.590000-01
.168910-01	.432993+06	.317500-01	.150556+04	.202184-01	-.000000	.148000-00	.756000-00	.960000-01
.194310-01	.438509+06	.381000-01	.146667+04	.222504-01	-.000000	.146000-00	.755000-00	.990000-01
.219710-01	.435751+06	.444500-01	.143889+04	.316484-01	-.000000	.164000-00	.747000-00	.890000-01
.245110-01	.432304+06	.508000-01	.129444+04	.367284-01	-.000000	.147000-00	.759000-00	.940000-01
.308610-01	.428857+06	.584200-01	.733333+03	.419100-01	.000000	.111000+00	.836000-00	.530000-01
.339090-01	.429546+06	.000000	.000000	.482600-01	.000000	.174000-00	.723000-00	.103000+00
.348234-01	.428857+06	.000000	.000000	.608584-01	-.000000	.000000	.786000-00	.214000-00
.359410-01	.430236+06	.000000	.000000	.000000	.000000	.000000	.000000	.000000
.363474-01	.428857+06	.000000	.000000	.000000	.000000	.000000	.000000	.000000
.388874-01	.428857+06	.000000	.000000	.000000	.000000	.000000	.000000	.000000
.414274-01	.428857+06	.000000	.000000	.000000	.000000	.000000	.000000	.000000
.439674-01	.390246+06	.000000	.000000	.000000	.000000	.000000	.000000	.000000
.503174-01	.173749+06	.000000	.000000	.000000	.000000	.000000	.000000	.000000
.533654-01	.132380+06	.000000	.000000	.000000	.000000	.000000	.000000	.000000

TABLE IV. - PROBE DATA - CONCLUDED

LOW TEMPERATURE VITIATED NITROGEN

AXIAL LOCATION = 17.8 CM

Z-M	PP-N/M**2	Z-M	TT-DEG K	Z-M	Y-H2	Y-H2O	Y-N2	Y-O2
.000000	.319919+06	.000000	.522222+03	.127000-02	.943000-00	.150000-01	.380000-01	.400000-02
.482600-03	.306129+06	.508000-02	.100000+04	.330200-02	.928000-00	.180000-01	.470000-01	.700000-02
.586740-02	.292340+06	.104140-01	.131111+04	.635000-02	.917000-00	.230000-01	.550000-01	.500000-02
.723900-02	.307508+06	.152400-01	.174444+04	.127000-01	.540000-00	.123000+00	.319000-00	.170000-01
.122174-01	.307508+06	.203200-01	.156111+04	.152400-01	.287000-00	.152000-00	.527000-00	.340000-01
.135890-01	.325435+06	.259080-01	.152222+04	.177800-01	-.000000	.159000-00	.796000-00	.450000-01
.153670-01	.385419+06	.317500-01	.150556+04	.202184-01	-.000000	.162000-00	.743000-00	.950000-01
.168910-01	.406793+06	.381000-01	.147778+04	.252984-01	-.000000	.157000-00	.744000-00	.980000-01
.194310-01	.426099+06	.444500-01	.151111+04	.316484-01	-.000000	.150000-00	.748000-00	.102000+00
.199390-01	.424720+06	.513080-01	.135556+04	.444500-01	-.000000	.170000-00	.742000-00	.880000-01
.219710-01	.428857+06	.571500-01	.103333+04	.508000-01	-.000000	.182000-00	.748000-00	.710000-01
.245110-01	.428167+06	.637540-01	.811111+03	.633984-01	-.000000	.900000-01	.723000-00	.188000-00
.308610-01	.428167+06	.000000	.000000	.000000	.000000	.000000	.000000	.000000
.339090-01	.428167+06	.000000	.000000	.000000	.000000	.000000	.000000	.000000
.348234-01	.423341+06	.000000	.000000	.000000	.000000	.000000	.000000	.000000
.359410-01	.428167+06	.000000	.000000	.000000	.000000	.000000	.000000	.000000
.363474-01	.421272+06	.000000	.000000	.000000	.000000	.000000	.000000	.000000
.388874-01	.415067+06	.000000	.000000	.000000	.000000	.000000	.000000	.000000
.414274-01	.3812A2+06	.000000	.000000	.000000	.000000	.000000	.000000	.000000
.439674-01	.321298+06	.000000	.000000	.000000	.000000	.000000	.000000	.000000
.503174-01	.185470+06	.000000	.000000	.000000	.000000	.000000	.000000	.000000
.533654-01	.152375+06	.000000	.000000	.000000	.000000	.000000	.000000	.000000

LOW TEMPERATURE VITIATED NITROGEN

AXIAL LOCATION = 25.4 CM

Z-M	PP-N/M**2	Z-M	TT-DEG K	Z-M	Y-H2	Y-H2O	Y-N2	Y-O2
.000000	.338535+06	.000000	.655556+03	.127000-02	.918000-00	.250000-01	.530000-01	.500000-02
.482600-03	.315702+06	.508000-02	.727778+03	.330200-02	.924000-00	.170000-01	.530000-01	.500000-02
.586740-02	.293029+06	.101600-01	.100000+04	.635000-02	.879000-00	.280000-01	.840000-01	.800000-02
.586740-02	.297855+06	.152400-01	.151667+04	.127000-01	.566000-00	.148000-00	.273000-00	.130000-01
.723900-02	.306819+06	.203200-01	.170000+04	.152400-01	.275000-00	.185000-00	.512000-00	.280000-01
.723900-02	.311645+06	.254000-01	.154444+04	.177800-01	.212000-00	.185000-00	.582000-00	.210000-01
.122174-01	.317850+06	.317500-01	.154444+04	.202184-01	.000000	.156000-00	.768000-00	.760000-01
.122174-01	.322677+06	.381000-01	.150556+04	.341884-01	.000000	.134000-00	.771000-00	.950000-01
.135890-01	.343361+06	.444500-01	.139444+04	.444500-01	.000000	.229000-00	.683000-00	.880000-01
.135890-01	.335777+06	.508000-01	.113889+04	.444500-01	.000000	.190000-00	.725000-00	.860000-01
.153670-01	.382661+06	.571500-01	.827778+03	.508000-01	.000000	.134000-00	.725000-00	.140000-00
.168910-01	.401277+06	.635000-01	.555556+03	.508000-01	.000000	.168000-00	.726000-00	.107000+00
.194310-01	.428167+06	.000000	.000000	.571500-01	.000000	.100000+00	.752000-00	.147000-00
.199390-01	.432304+06	.000000	.000000	.633984-01	.000000	.180000-01	.802000-00	.179000-00
.219710-01	.435062+06	.000000	.000000	.000000	.000000	.000000	.000000	.000000
.245110-01	.435751+06	.000000	.000000	.000000	.000000	.000000	.000000	.000000
.308610-01	.433683+06	.000000	.000000	.000000	.000000	.000000	.000000	.000000
.340360-01	.426099+06	.000000	.000000	.000000	.000000	.000000	.000000	.000000
.348234-01	.419204+06	.000000	.000000	.000000	.000000	.000000	.000000	.000000
.359410-01	.417825+06	.000000	.000000	.000000	.000000	.000000	.000000	.000000
.363474-01	.411620+06	.000000	.000000	.000000	.000000	.000000	.000000	.000000
.388874-01	.379214+06	.000000	.000000	.000000	.000000	.000000	.000000	.000000
.414274-01	.337845+06	.000000	.000000	.000000	.000000	.000000	.000000	.000000
.439674-01	.283376+06	.000000	.000000	.000000	.000000	.000000	.000000	.000000
.503174-01	.195812+06	.000000	.000000	.000000	.000000	.000000	.000000	.000000
.533654-01	.164096+06	.000000	.000000	.000000	.000000	.000000	.000000	.000000
.553974-01	.147549+06	.000000	.000000	.000000	.000000	.000000	.000000	.000000
.639826-01	.111696+06	.000000	.000000	.000000	.000000	.000000	.000000	.000000

TABLE V

Static Temperature From Spectrophotometer Measurements - ^{o}K

	LOW TEMPERATURE VITIATED AIR			HIGH TEMPERATURE VITIATED AIR			HIGH TEMPERATURE VITIATED NITROGEN		
AXIAL POSITION	DISTANCE FROM CENTERLINE			DISTANCE FROM CENTERLINE			DISTANCE FROM CENTERLINE		
cm	1.90 cm	4.45 cm	5.08 cm	1.90 cm	4.45 cm	5.08 cm	1.90 cm	4.45 cm	5.08 cm
0.33	980	815	624	1058	893	670	1183	857	800
5.1	978	820	678	1116	919	675	1381	936	781
10.2	1001	821	678	1054	914	730	-	899	739
17.8	994	828	678	1098	929	705	-	890	732
25.4	1055	827	666	1117	1009	702	-	898	726

TABLE VI

Water Molar Concentrations from Spectrophotometer Measurements

	LOW TEMPERATURE VITIATED AIR			HIGH TEMPERATURE VITIATED AIR			HIGH TEMPERATURE VITIATED NITROGEN		
AXIAL POSITION cm	DISTANCE FROM CENTERLINE 1.90 cm	4.45 cm	5.08 cm	DISTANCE FROM CENTERLINE 1.90 cm	4.45 cm	5.08 cm	DISTANCE FROM CENTERLINE 1.90 cm	4.45 cm	5.08 cm
0.33	-	-	-	0.278	-	-	-	0.204	-
5.1	-	-	-	0.236	-	-	-	0.153	-
10.2	0.150	0.219	0.224	0.284	0.232	-	-	-	0.147
17.8	0.148	0.199	0.225	0.327	0.265	-	-	-	0.216
25.4	-	-	-	0.233	0.217	-	-	-	0.181

TABLE VII

Comparison of Water Molar Concentration Measurements for High Temperature Vitiated Air

AXIAL POSITION cm	DISTANCE FROM CENTERLINE cm	GAS CHROMATOGRAPH	SPECTRO-PHOTOMETER
0.33	1.90	0.217	0.278
5.1	1.90	0.200	0.236
10.2	1.90	0.261	0.284
	4.45	0.237	0.232
17.8	1.90	0.250	0.327
	4.45	0.208	0.265
25.4	1.90	0.163	0.233
	4.45	0.198	0.217

TABLE VIII

H_2/O_2 Reaction Mechanism

Reaction	K_f Rate Constant Units - cm^3, mole, sec, deg K, cal	Reference
1. $H_2 + O_2 \rightarrow 2OH$	$2.5 \times 10^{12} \exp\left(-\frac{19650}{T}\right)$	25
2. $H + O_2 \rightarrow OH + O$	$2.2 \times 10^{14} \exp\left(-\frac{8310}{T}\right)$	26
3. $O + H_2 \rightarrow OH + H$	$4.0 \times 10^{13} \exp\left(-\frac{5140}{T}\right)$	27
4. $H + H_2O \rightarrow OH + H_2$	$1.0 \times 10^{14} \exp\left(-\frac{10200}{T}\right)$	28
5. $O + H_2O \rightarrow 2OH$	$8.4 \times 10^{13} \exp\left(-\frac{9120}{T}\right)$	29
6. $H + OH + M \rightarrow H_2O + ITB$	$6.0 \times 10^{18}\ T^{-1}$	30
7. $H + H + M \rightarrow H_2 + ITB$	$3.0 \times 10^{18}\ T^{-1}$	31
8. $O + O + M \rightarrow O_2 + ITB$	$3.0 \times 10^{17}\ T^{-1}$	32
9. $H + O_2 + M \rightarrow HO_2 + ITB$	$8.6 \times 10^{14} \exp\left(\frac{645}{T}\right)$	33

Notes:

1. ITB is inert third body

2. Rate constants given above for reactions 6 and 9 are for the case of ITB = argon. The actual or effective rate constant for the third body present may be determined from:

$$K_{effective} = K_{argon}\left\{1 + Y_j\, \eta_j\right\}$$

where Y_j is the equilibrium mole fraction of species j and η_j is a weighting factor, e.g., $\eta_{H_2O} \simeq 30$. (Reaction 6)

$\eta_{H_2} \simeq 5$. (Reaction 7)

TABLE IX

Initial Mole Fractions of Free Radicals and Molecular Species Used in the Calculation of H_2/O_2 Reaction-Time Histories*

	Equivalence Ratio, ER			
	0.1	0.4	1.0	1.5
H_2	0.046	0.140	0.290	0.380
H_2O	0.217	0.195	0.161	0.1412
O_2	0.195	0.176	0.145	0.127
N_2	0.542	0.489	0.404	0.352
H	7.54×10^{-7}	6.80×10^{-7}	5.61×10^{-7}	4.9×10^{-7}
OH	8.09×10^{-4}	7.29×10^{-4}	6.02×10^{-4}	5.26×10^{-4}
O	2.98×10^{-5}	2.87×10^{-5}	2.22×10^{-5}	1.94×10^{-5}

* Calculated with Equilibrium Chemistry computer program, cf., Ref. 21.

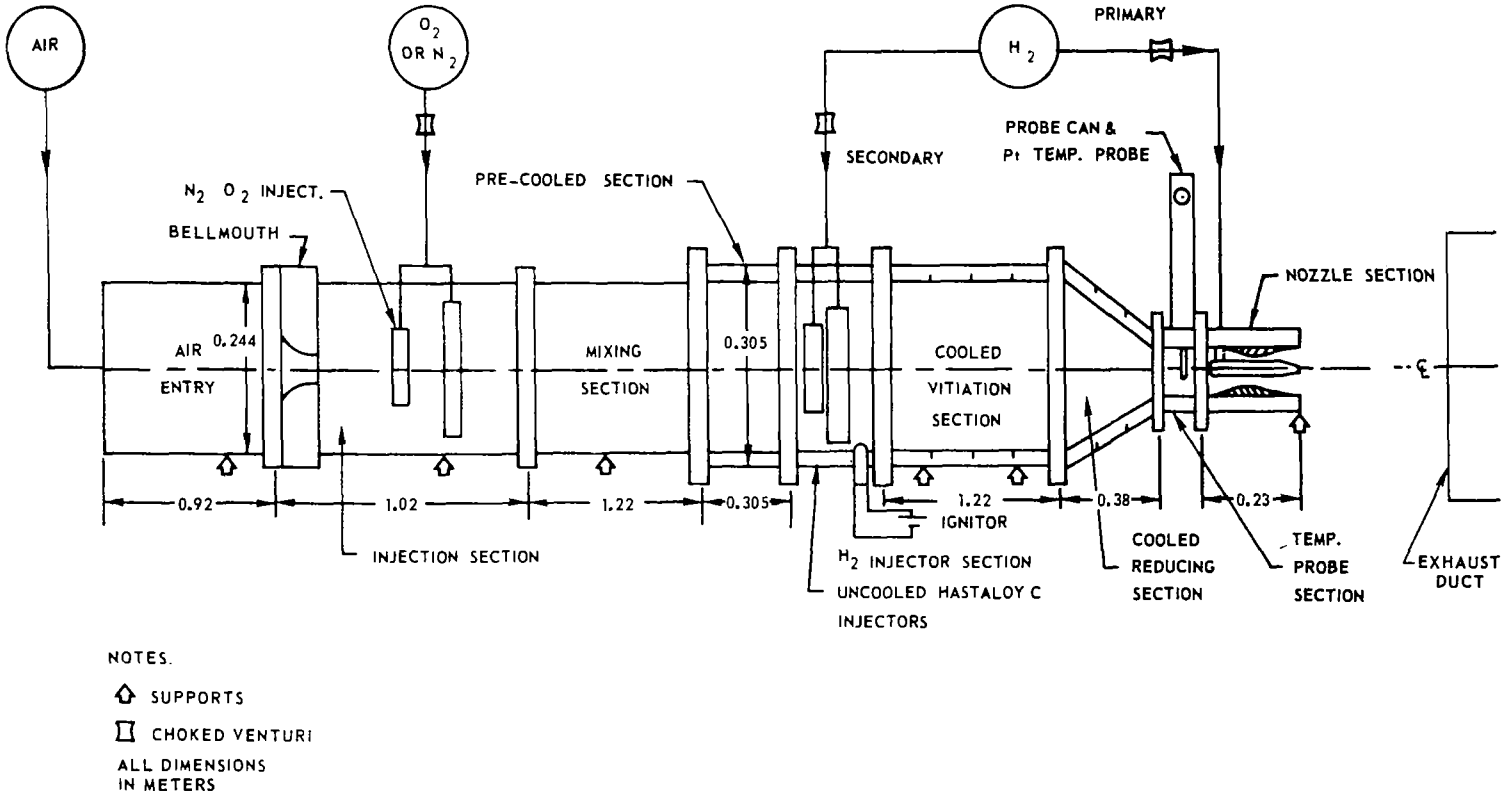

Figure 1. - TEST RIG - SCHEMATIC DIAGRAM

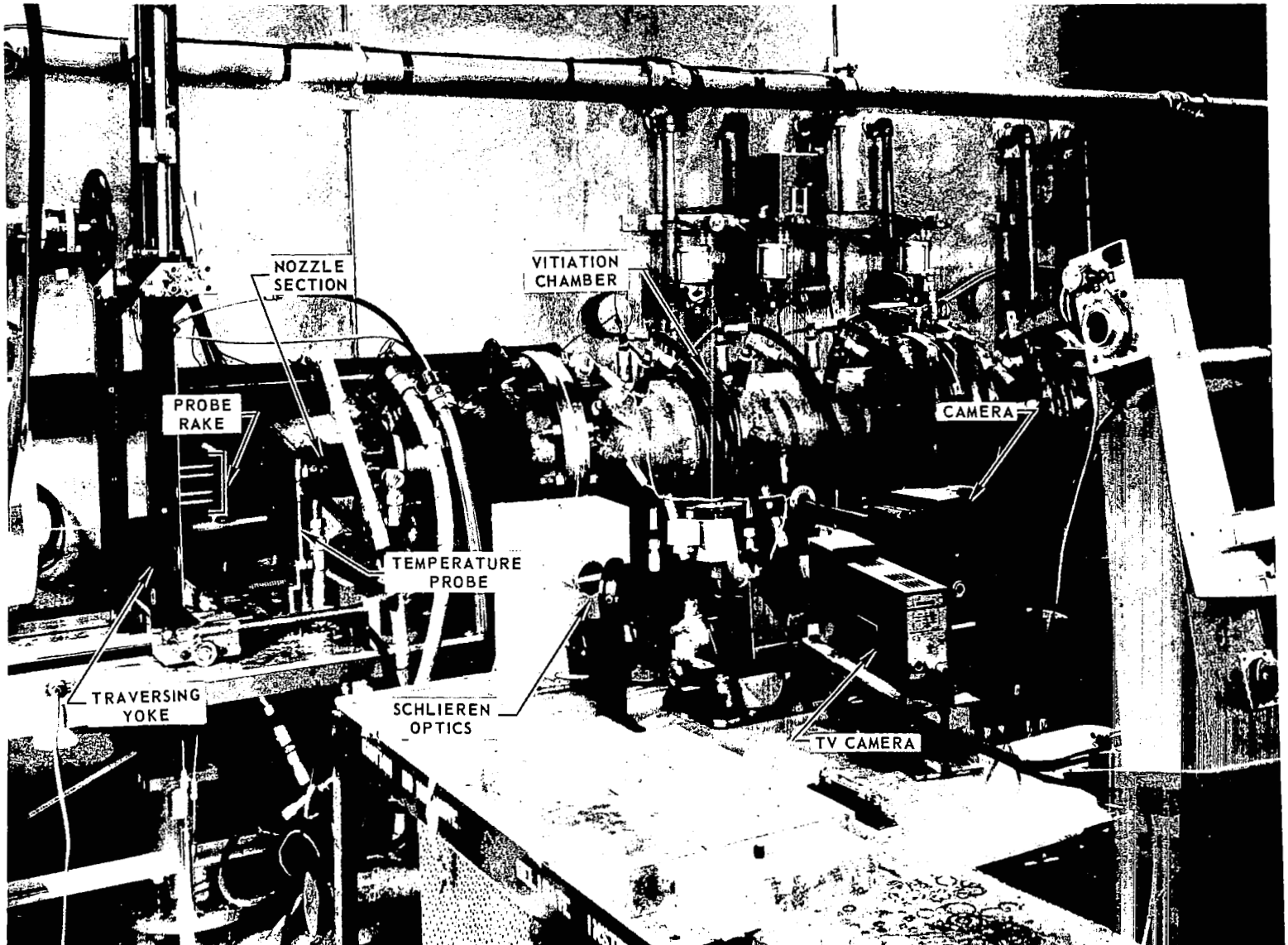

Figure 2. - PHOTOGRAPH OF TEST RIG

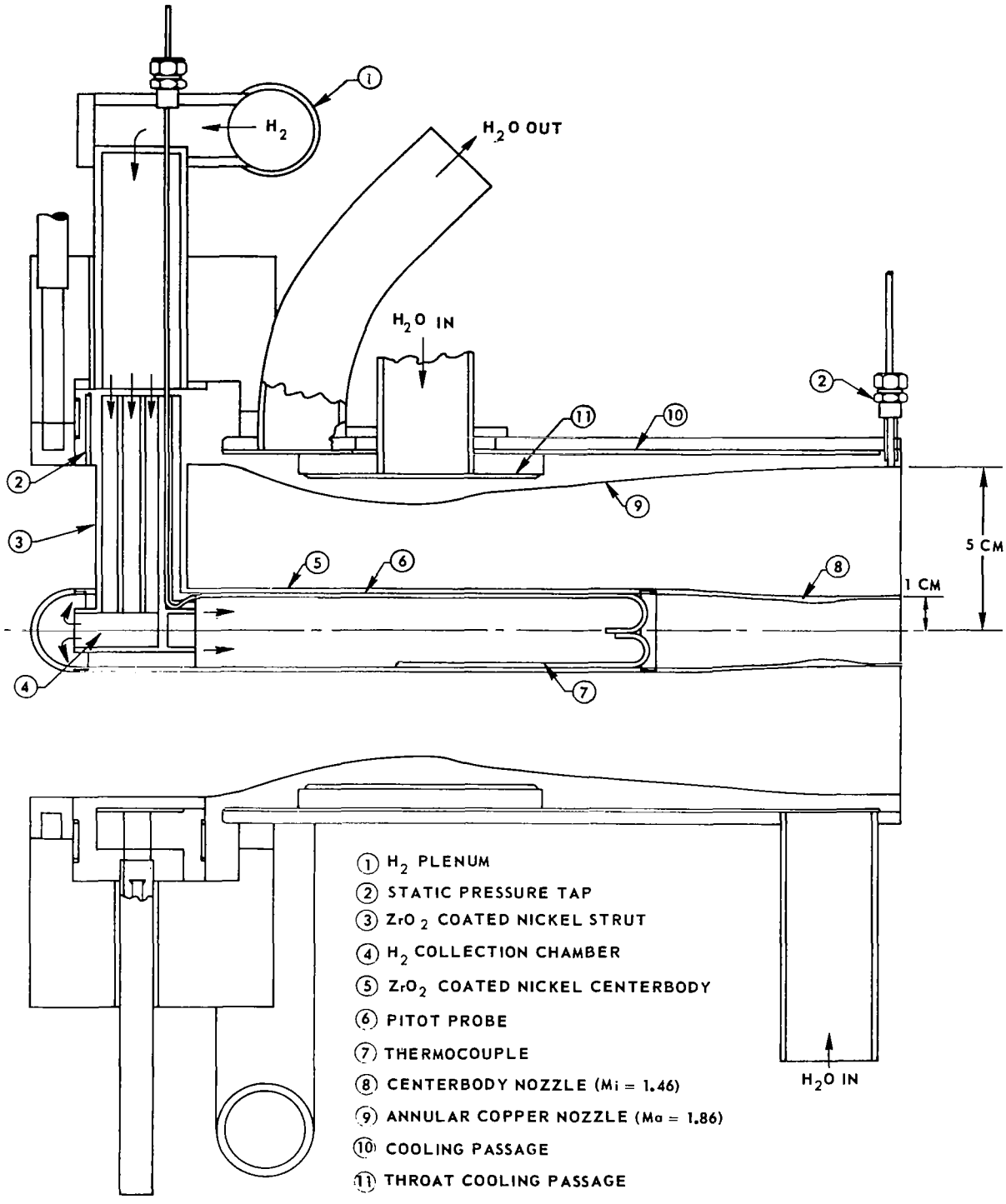

Figure 3. - NOZZLE SECTION DETAIL

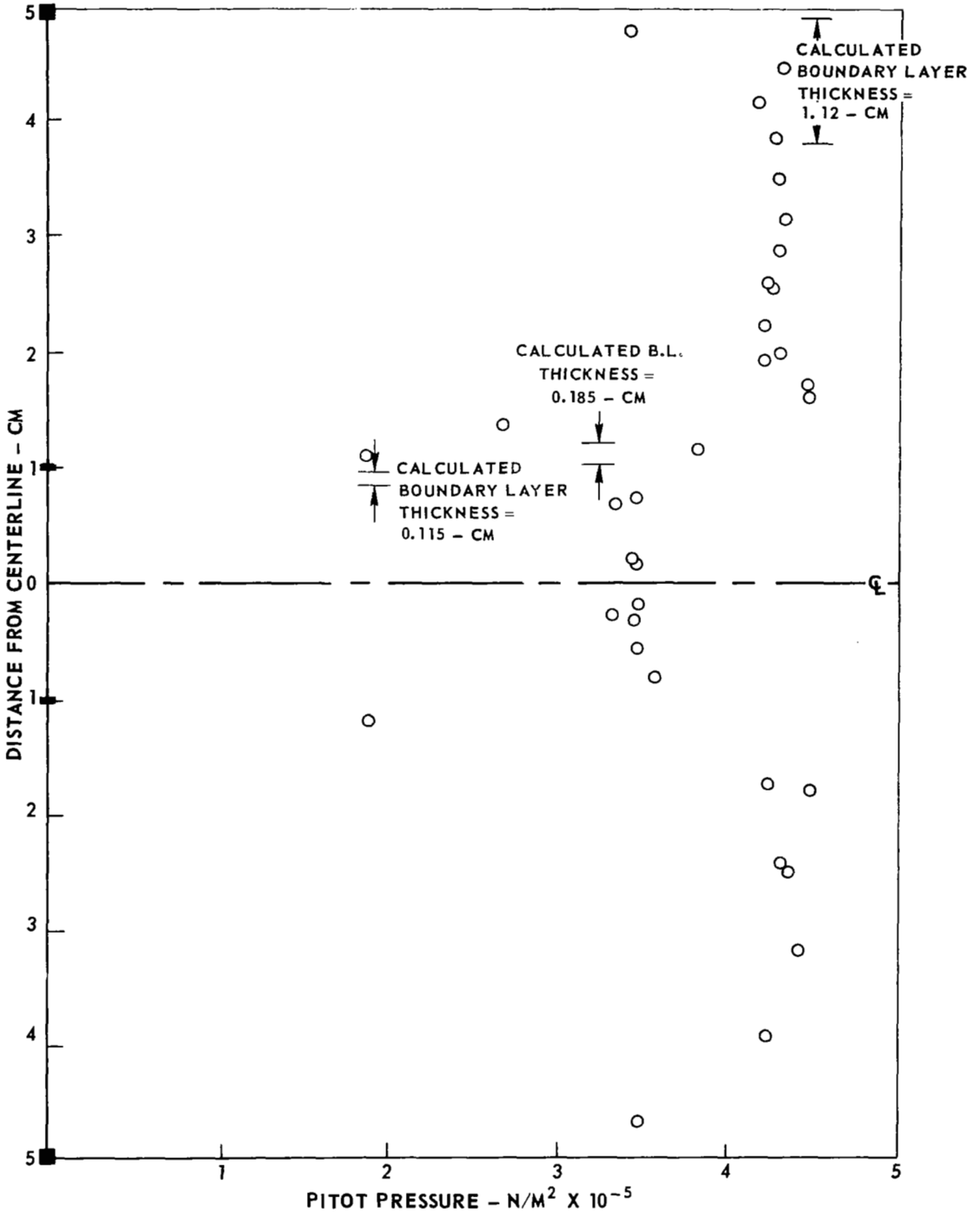

Figure 4. - PITOT PRESSURE PROFILE AT NOZZLE EXIT

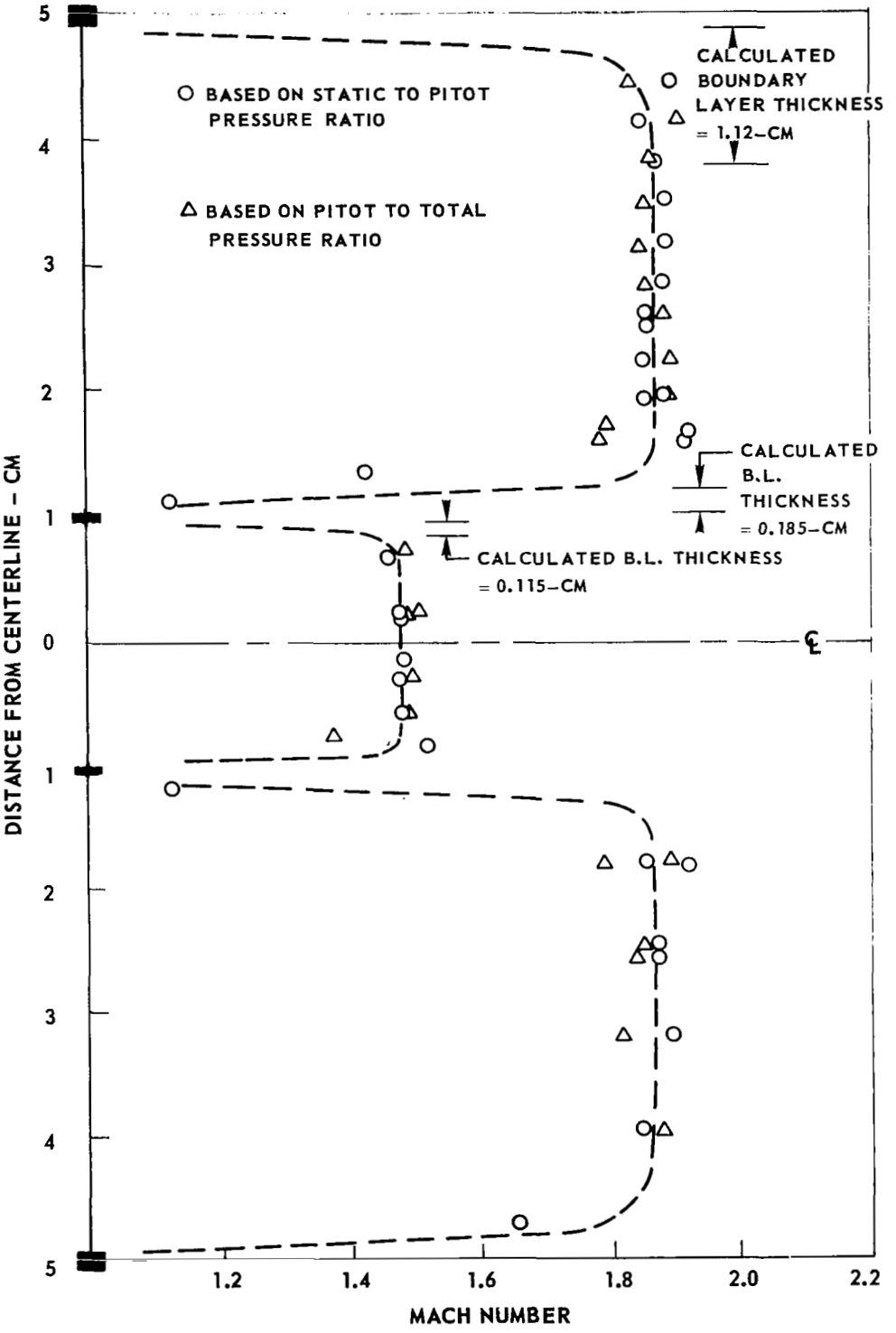

Figure 5. - MACH NUMBER DISTRIBUTION AT NOZZLE EXIT

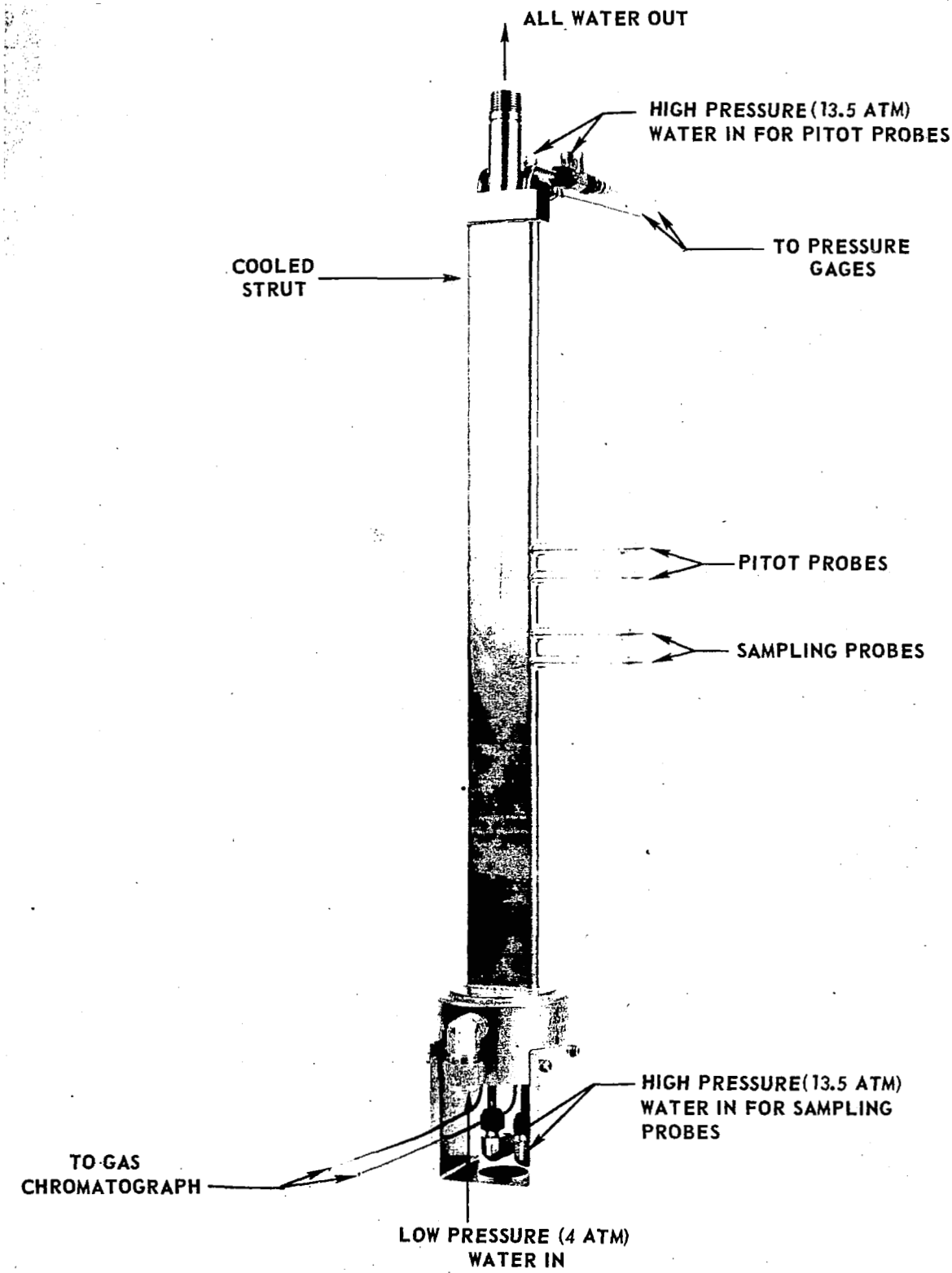

Figure 6. - PITOT - CONCENTRATION PROBE RAKE

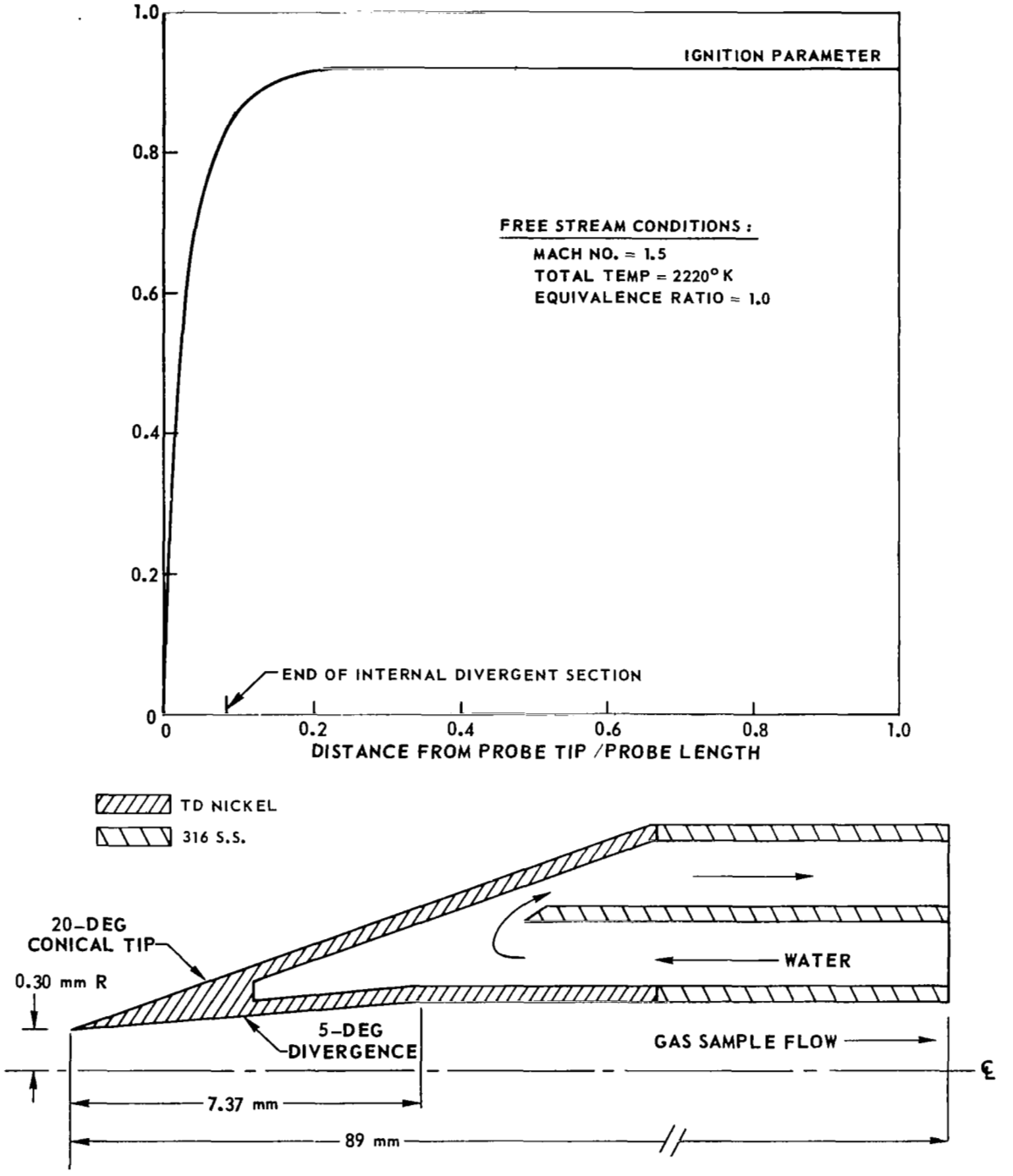

Figure 7. - QUENCHING PROBE SCHEMATIC DIAGRAM AND DESIGN FEATURES

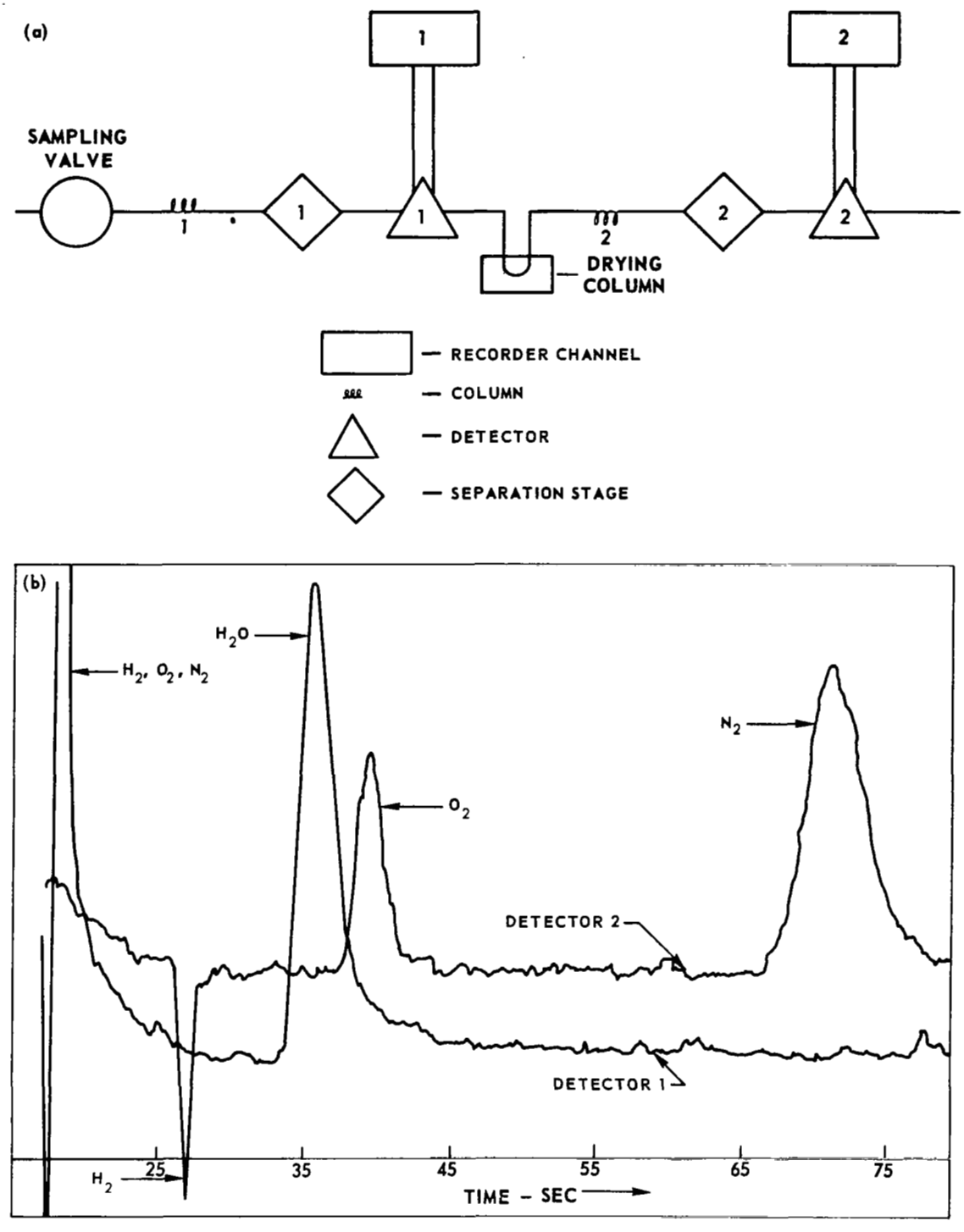

Figure 8. - GAS CHROMATOGRAPH SCHEMATIC DIAGRAM AND TRACE OF GC OUTPUT

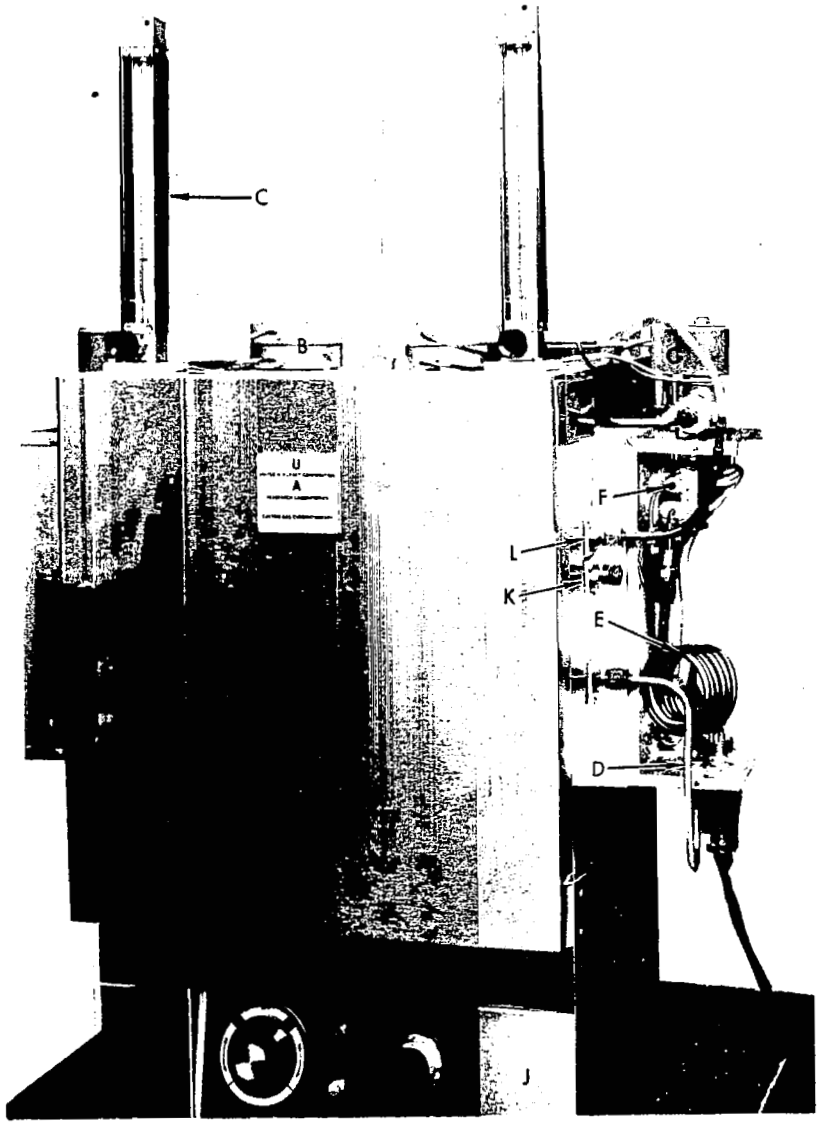

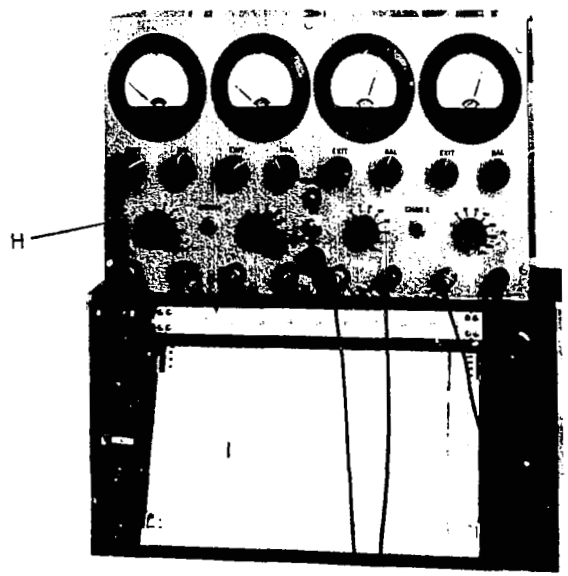

A – OVEN
B – GAS SAMPLING VALVES
C – FLOW METERS
D – H_2O ABSORBER
E – MOLECULAR SIEVE 13x
F – HOT WIRE DETECTOR
G – ACTUATOR FOR GAS SAMPLING VALVES
H – POWER SUPPLY AND ATTENUATORS
I – TWO PEN RECORDER
J – TEMPERATURE CONTROL
K – SAMPLE PROBE INLET
L – VACUUM PUMP INLET

FIGURE 9. GAS CHROMATOGRAPH SYSTEM.

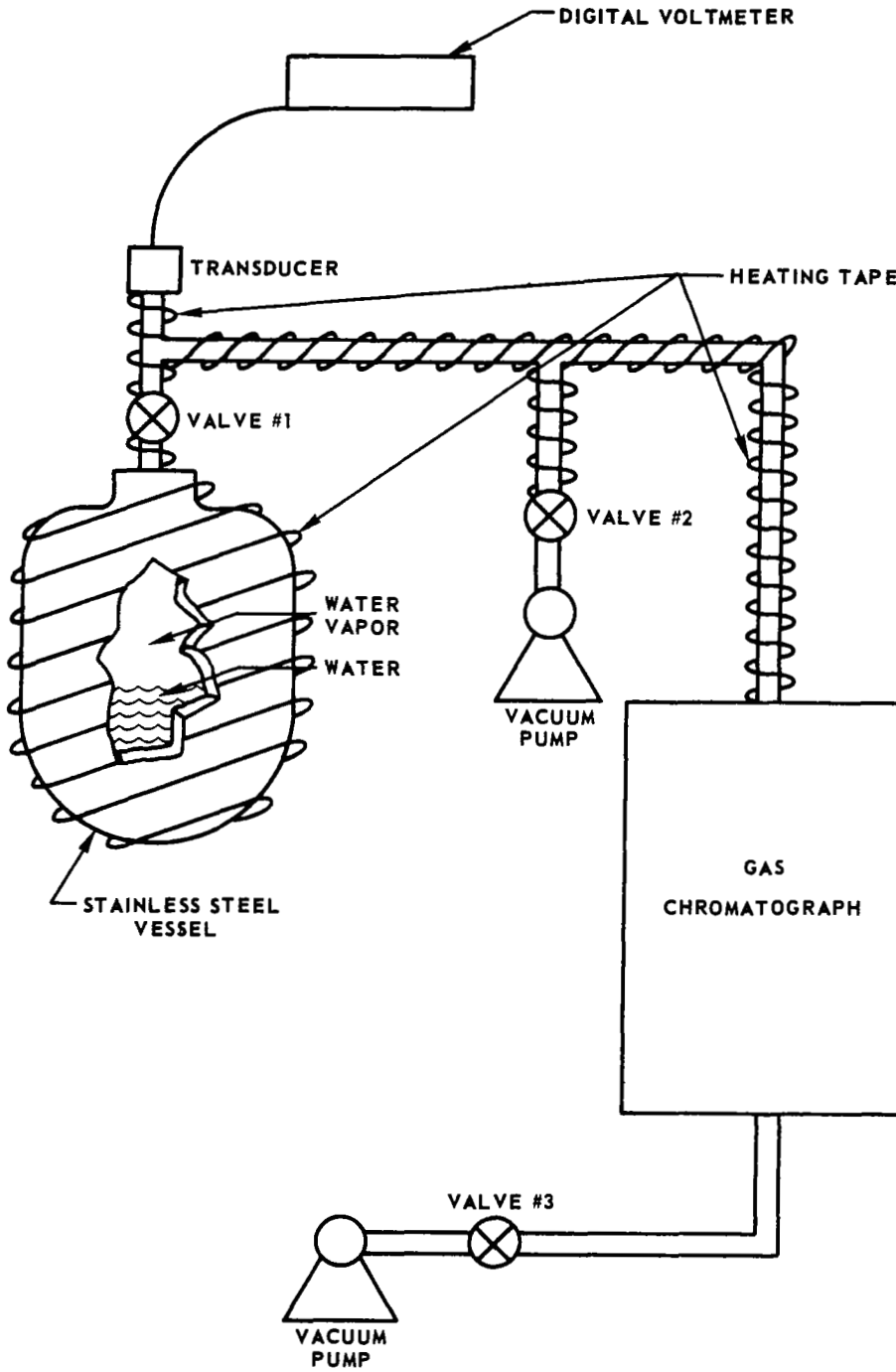

Figure 10. - SET-UP FOR WATER GC-CALIBRATION

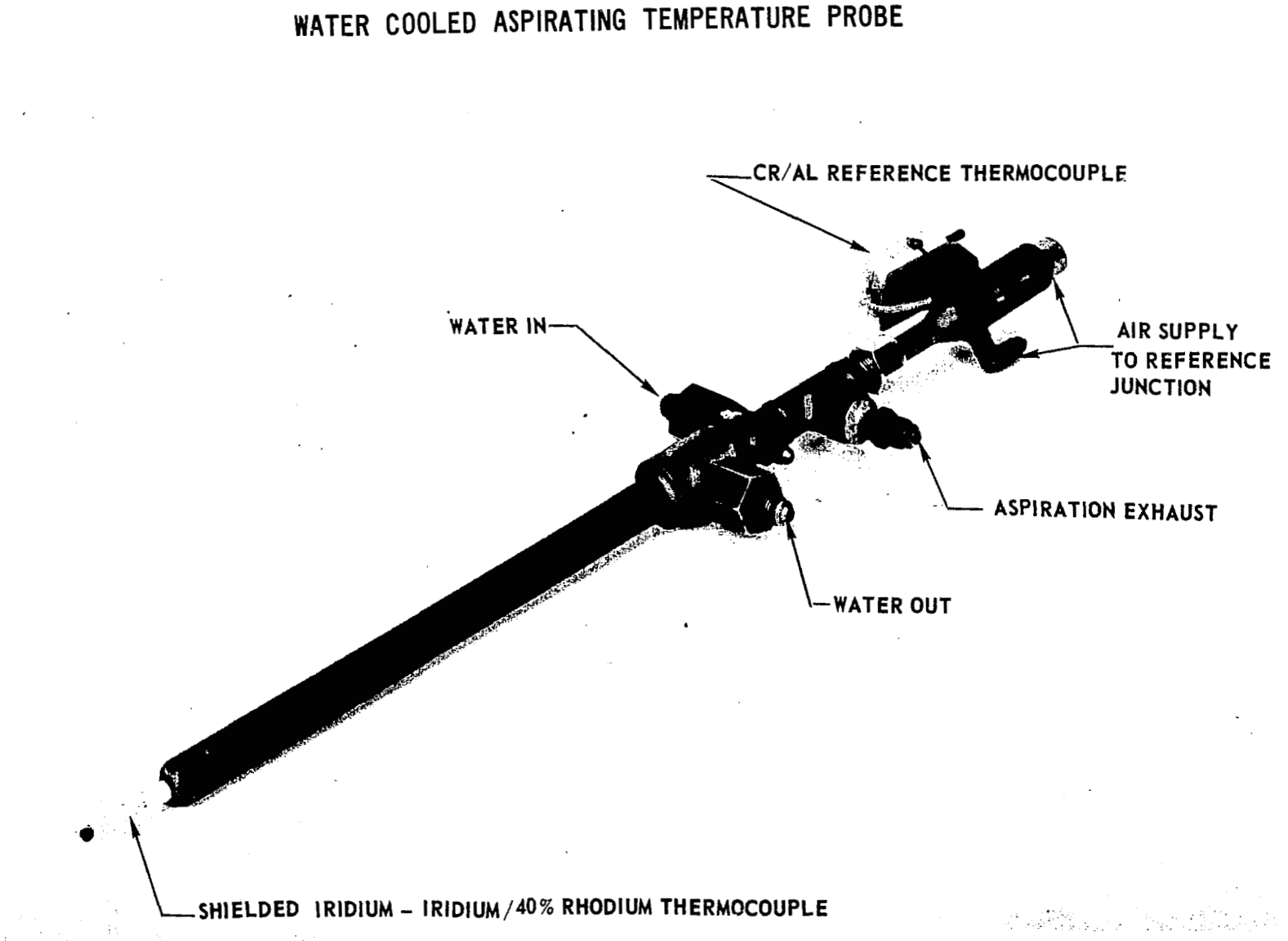

Figure 11. - ASPIRATING TOTAL TEMPERATURE PROBE

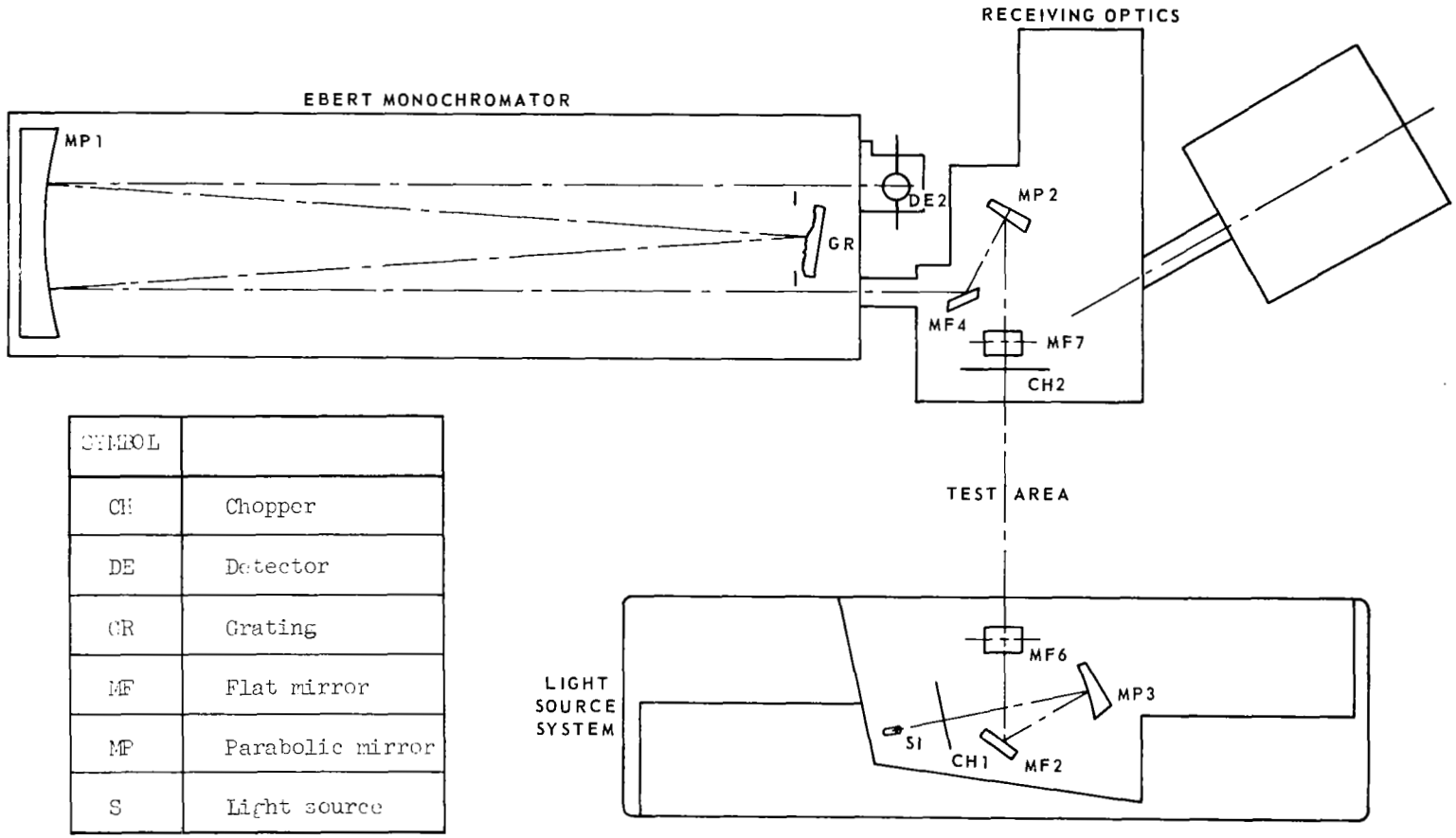

SYMBOL	
CH	Chopper
DE	Detector
GR	Grating
MF	Flat mirror
MP	Parabolic mirror
S	Light source

Figure 12. - EBERT SPECTROPHOTOMETER - SCHEMATIC DIAGRAM

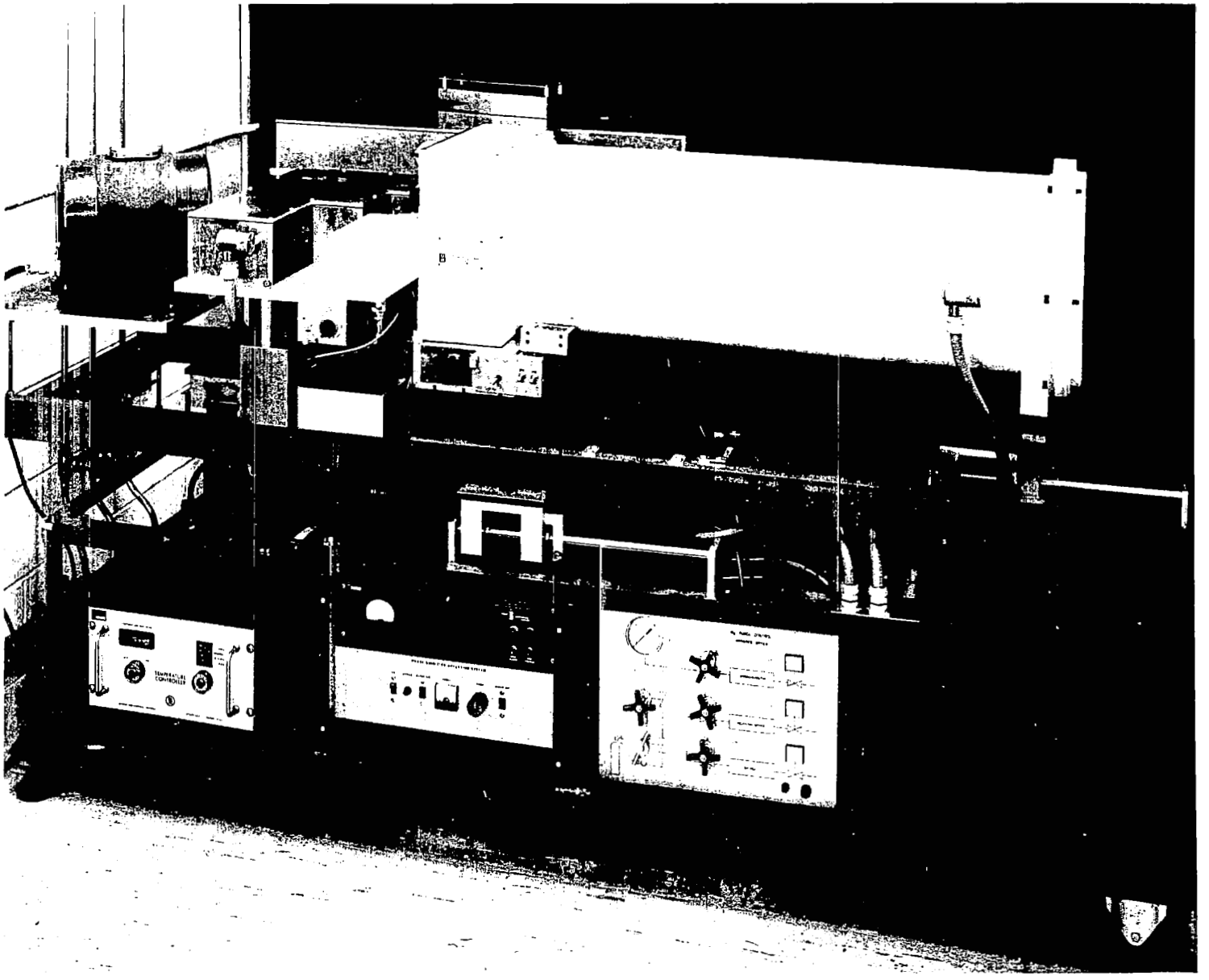

FIGURE 13. PHOTOGRAPH OF SPECTROPHOTOMETER SYSTEM

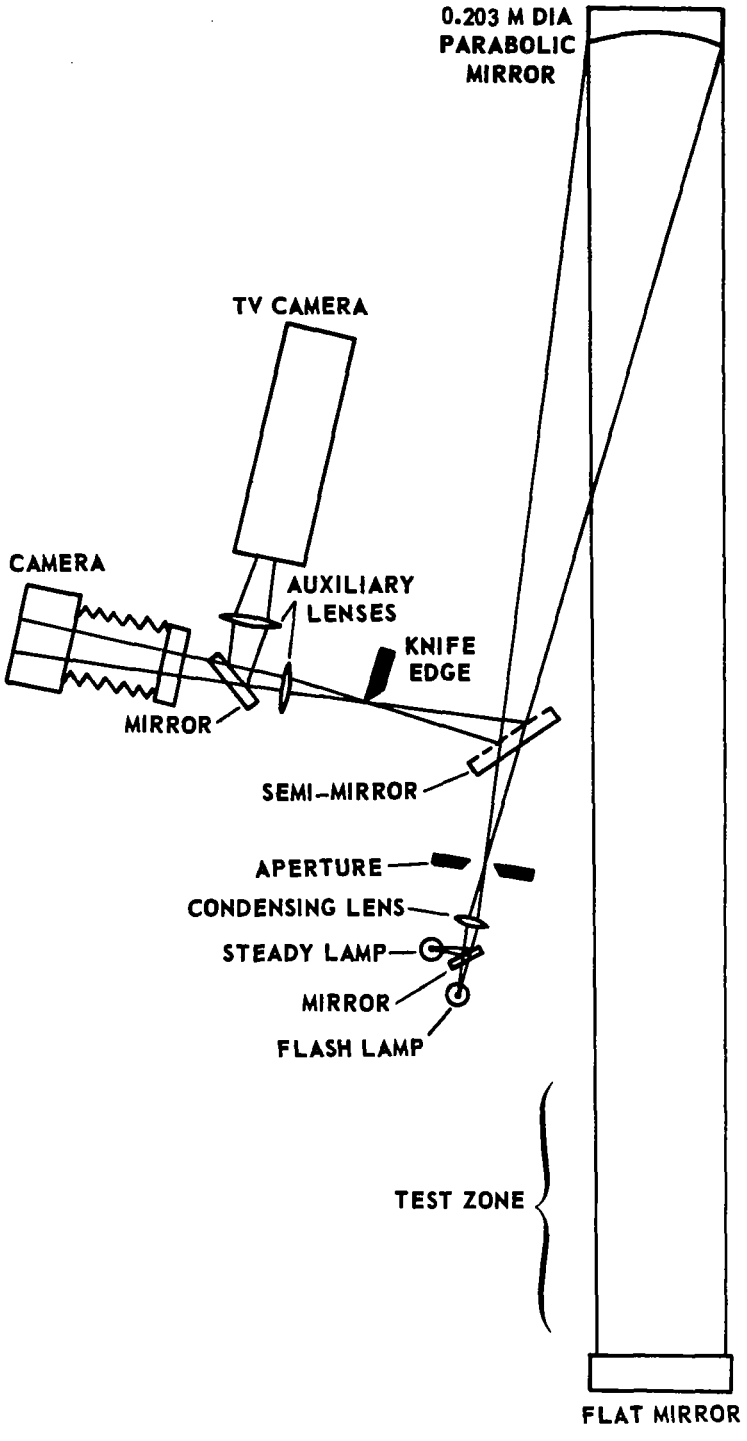

Figure 14. - 0.203-m DOUBLE-PASS SCHLIEREN - SCHEMATIC DIAGRAM

SYMBOL	WEIGHT FLOWS (KG/SEC)				
	H_2	AIR	O_2	N_2	TOTAL
□	0.0467	1.425	0.595	——	2.067
△	0.0463	1.680	——	0.426	2.152

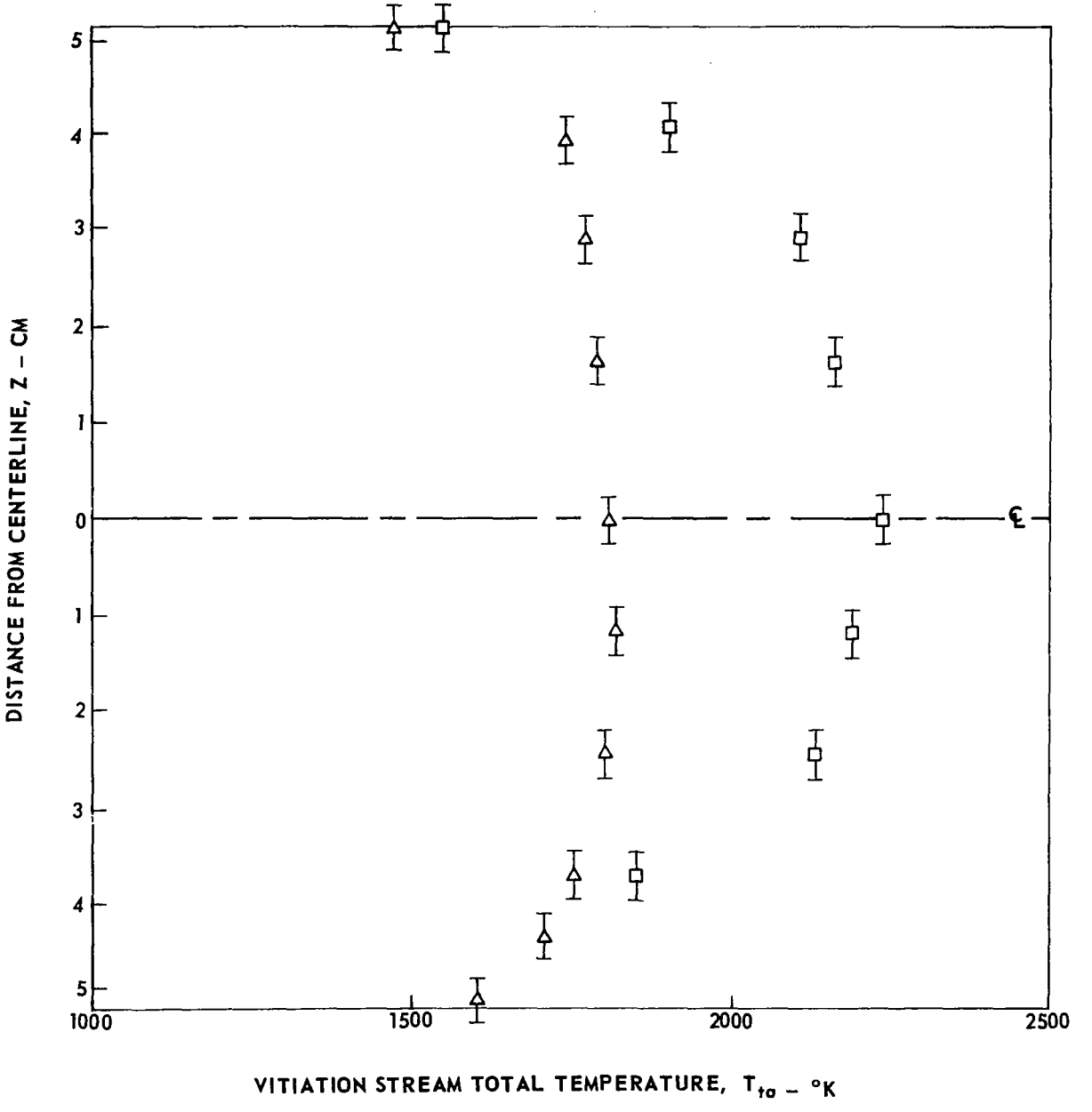

Figure 15. - TOTAL TEMPERATURE PROFILES AT ENTRANCE TO NOZZLE SECTION

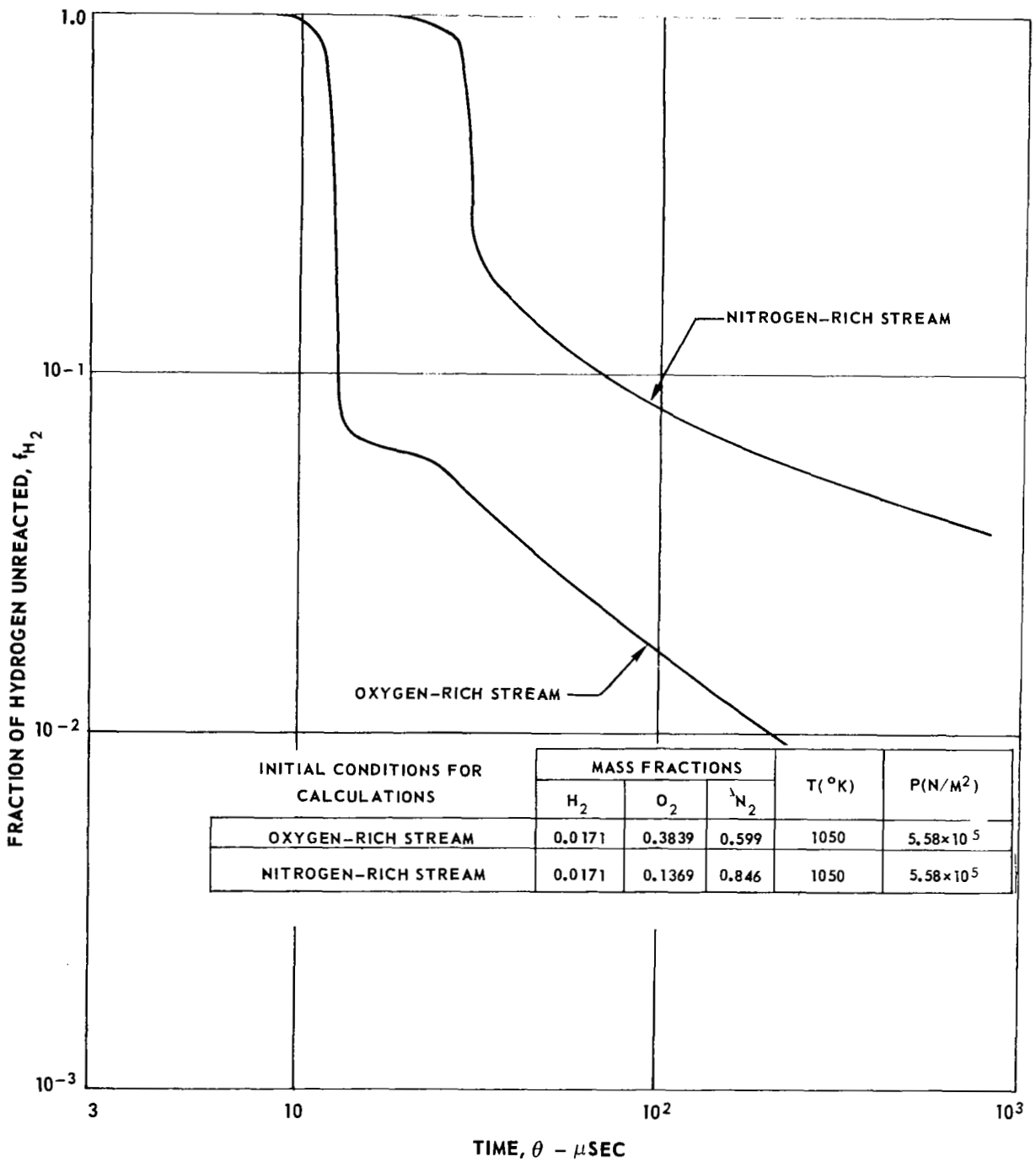

INITIAL CONDITIONS FOR CALCULATIONS	MASS FRACTIONS			T(°K)	P(N/M²)
	H_2	O_2	N_2		
OXYGEN-RICH STREAM	0.0171	0.3839	0.599	1050	5.58×10^5
NITROGEN-RICH STREAM	0.0171	0.1369	0.846	1050	5.58×10^5

Figure 16. - TIME-HISTORY OF FUEL CONSUMPTION IN VITIATION HEATER

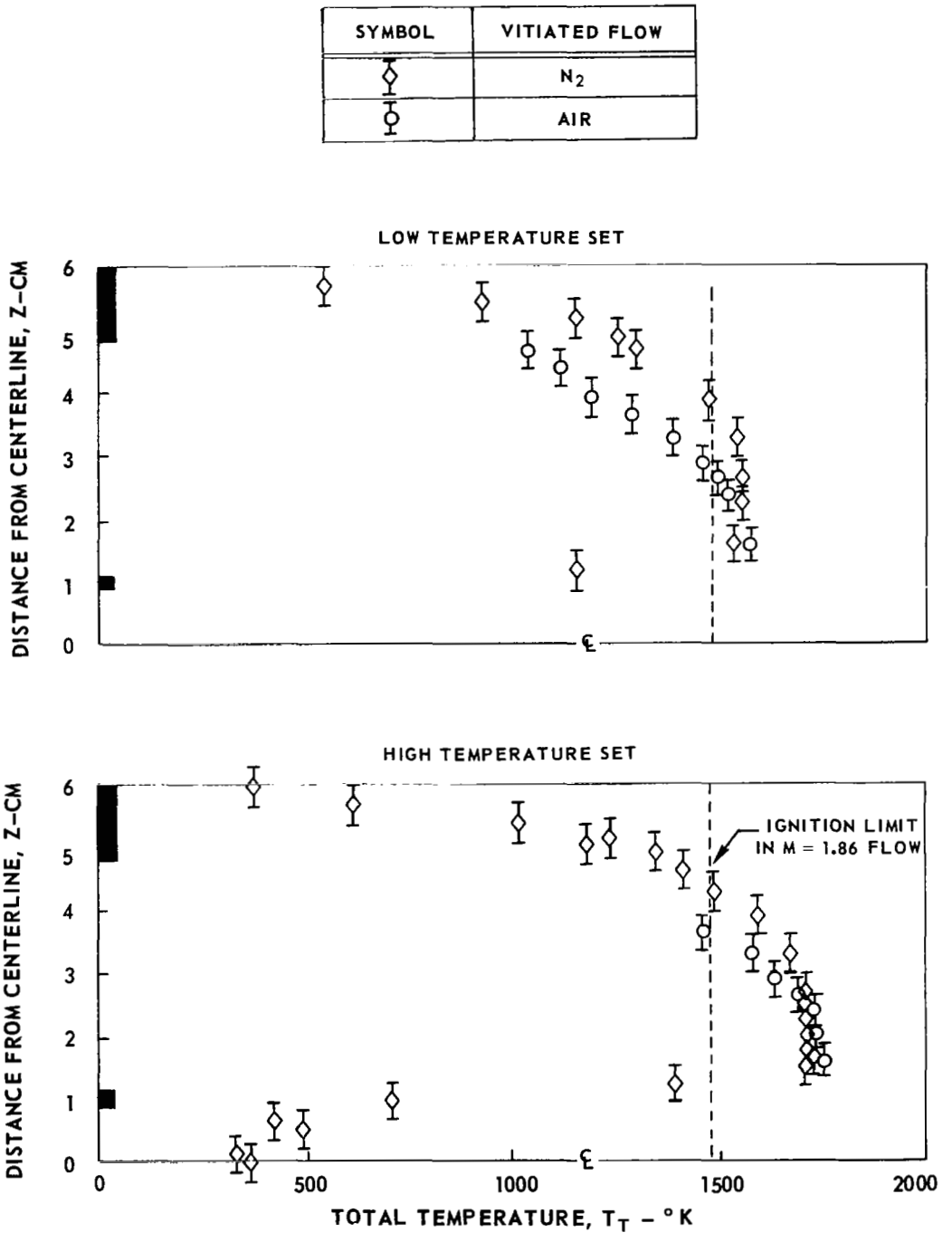

Figure 17. - TOTAL TEMPERATURE PROFILES AT NOZZLES EXIT PLANE

HIGH TEMPERATURE → DIRECTION OF FLOW → LOW TEMPERATURE

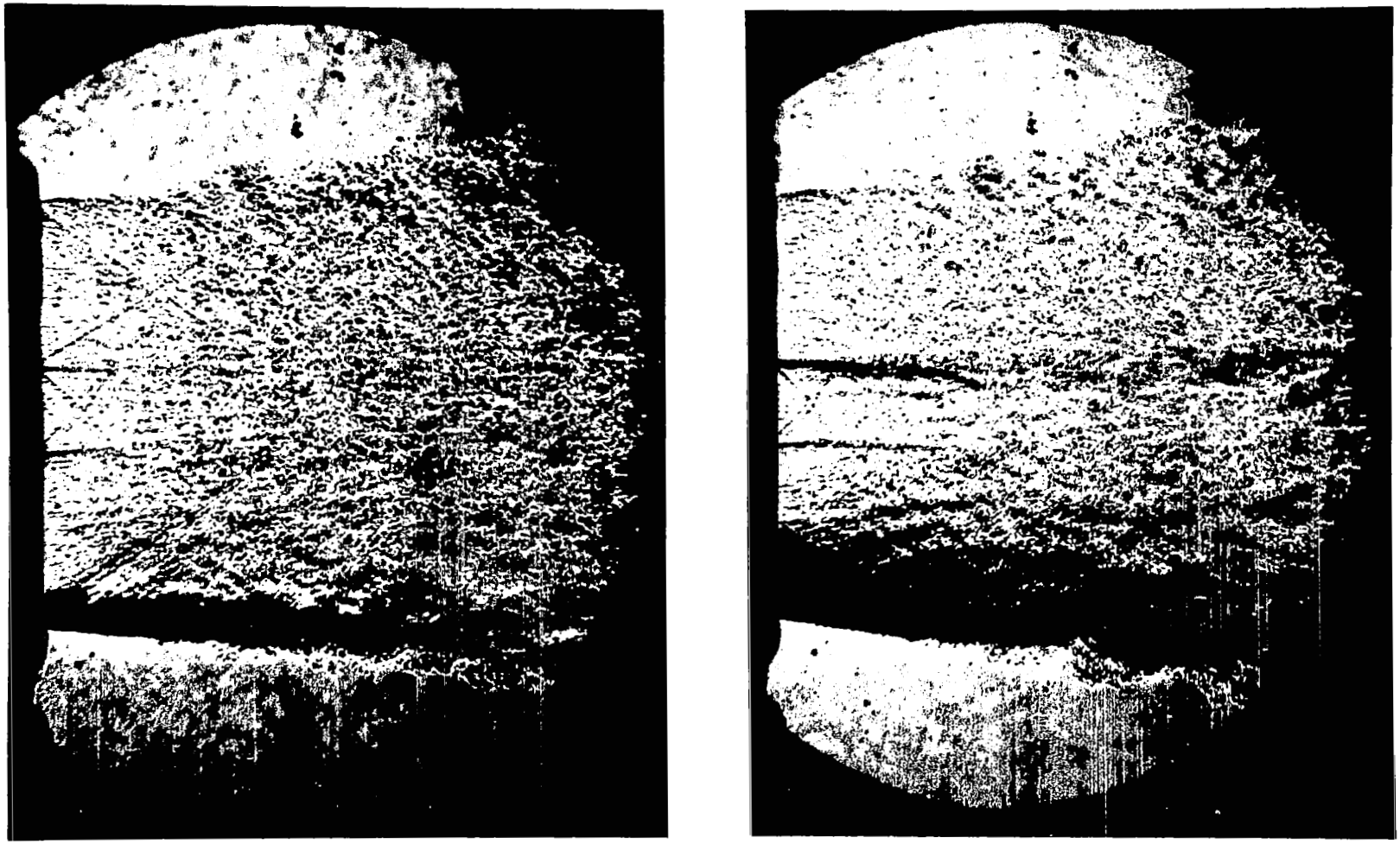

FIGURE 18. SCHLIEREN PHOTOGRAPH AT NOZZLE EXIT-VITIATED AIR

HIGH TEMPERATURE → DIRECTION OF FLOW → LOW TEMPERATURE

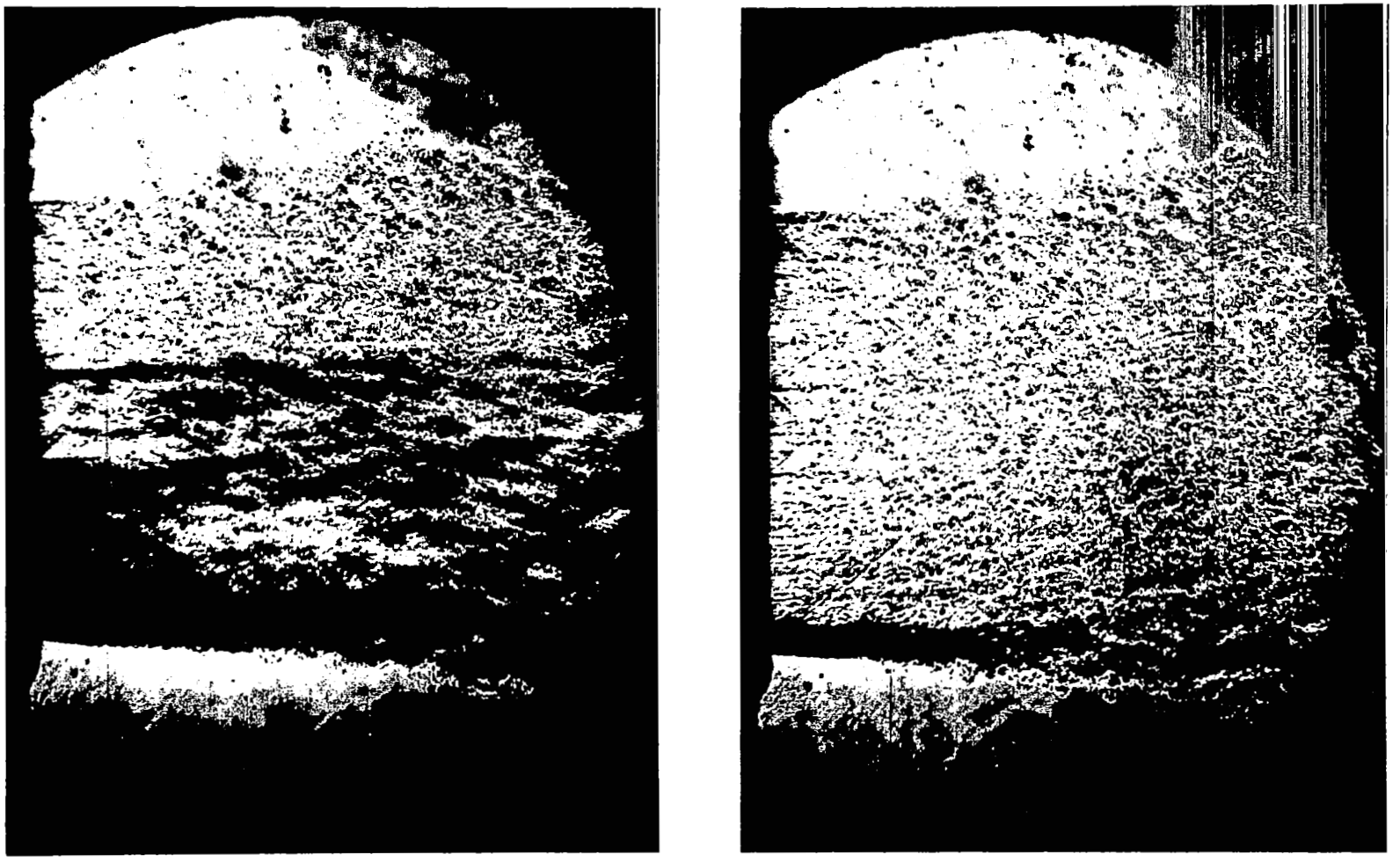

FIGURE 19. SCHLIEREN PHOTOGRAPHS AT NOZZLE EXIT-VITIATED NITROGEN

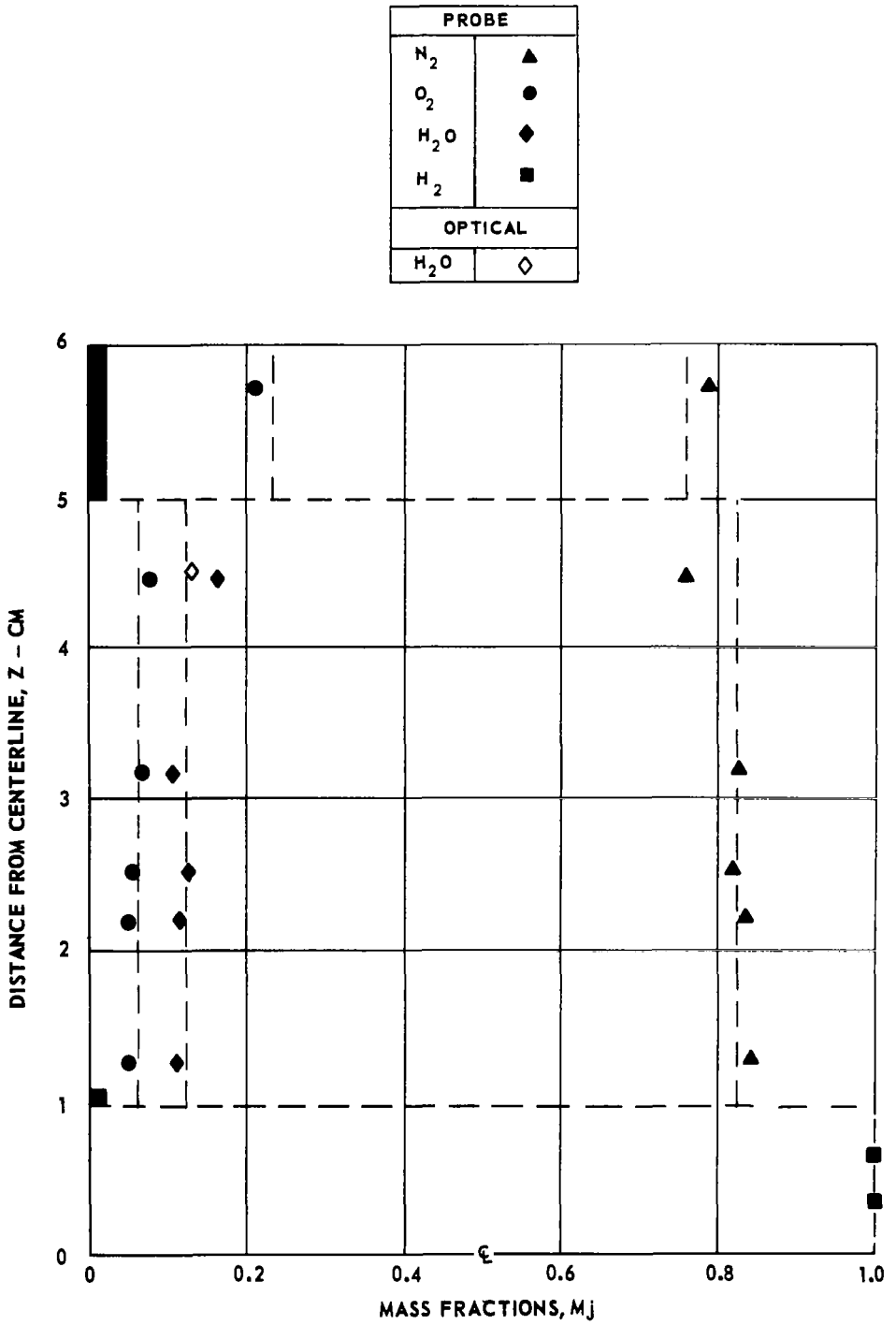

Figure 20. - CONCENTRATION PROFILES AT NOZZLES EXIT PLANE-HIGH TEMPERATURE VITIATED N_2

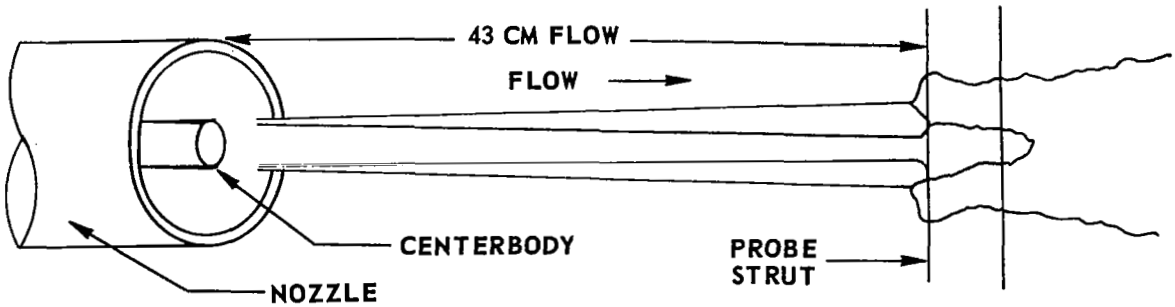

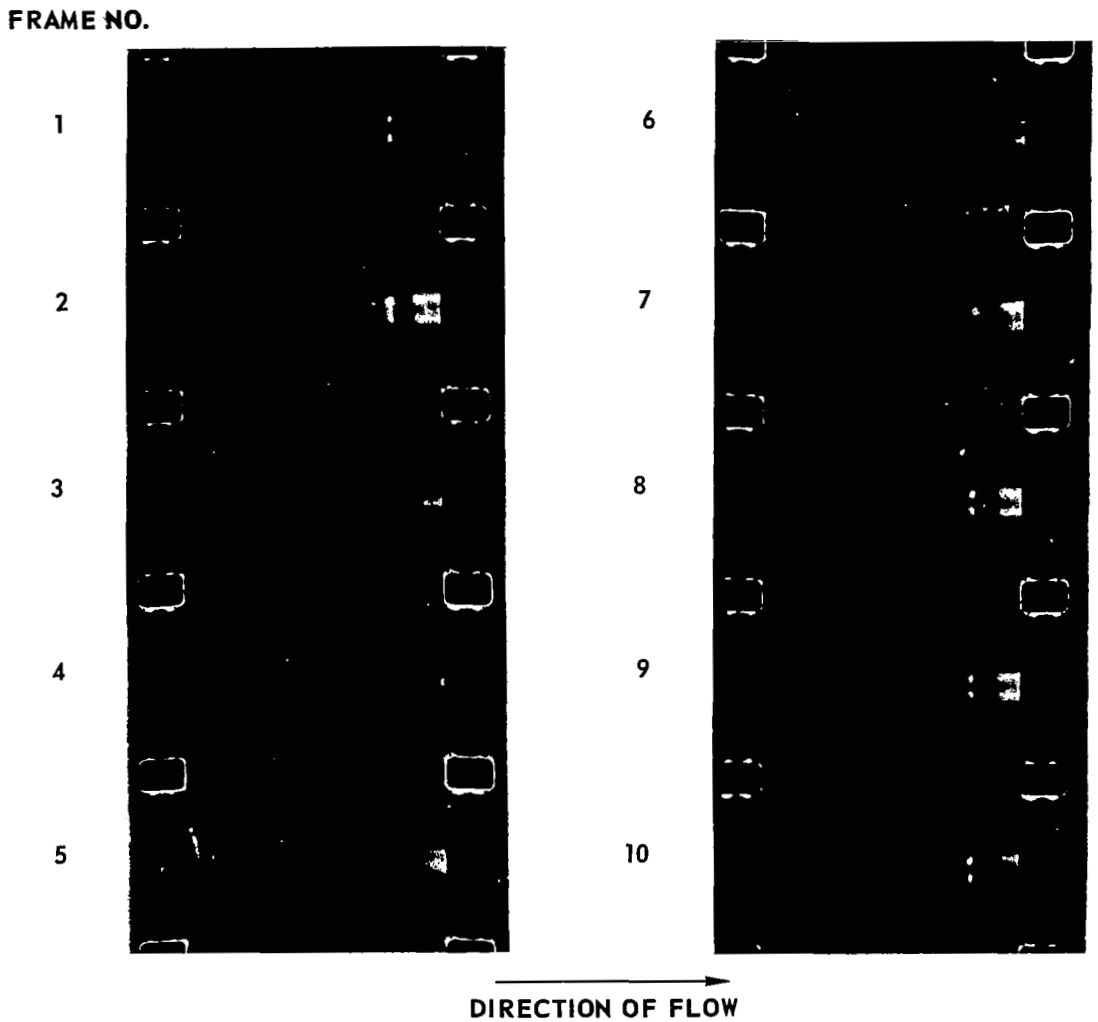

Figure 21. - FILM CLIP FROM 500 FPS MOTION PICTURE

(a) Ultraviolet

Flow Direction ⟶

Scale = 1/2

(b) Infrared

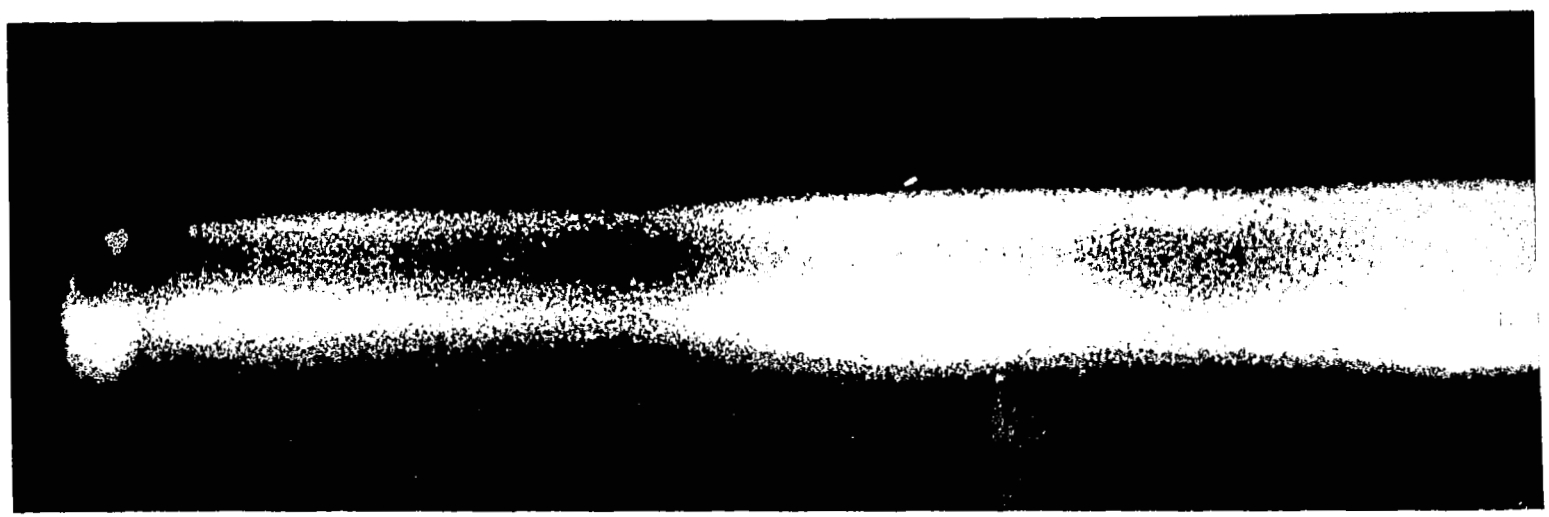

Figure 22. - HIGH TEMPERATURE AIR PHOTOGRAPHS

(a) Ultraviolet

Flow Direction ——————→

Scale = 1/2

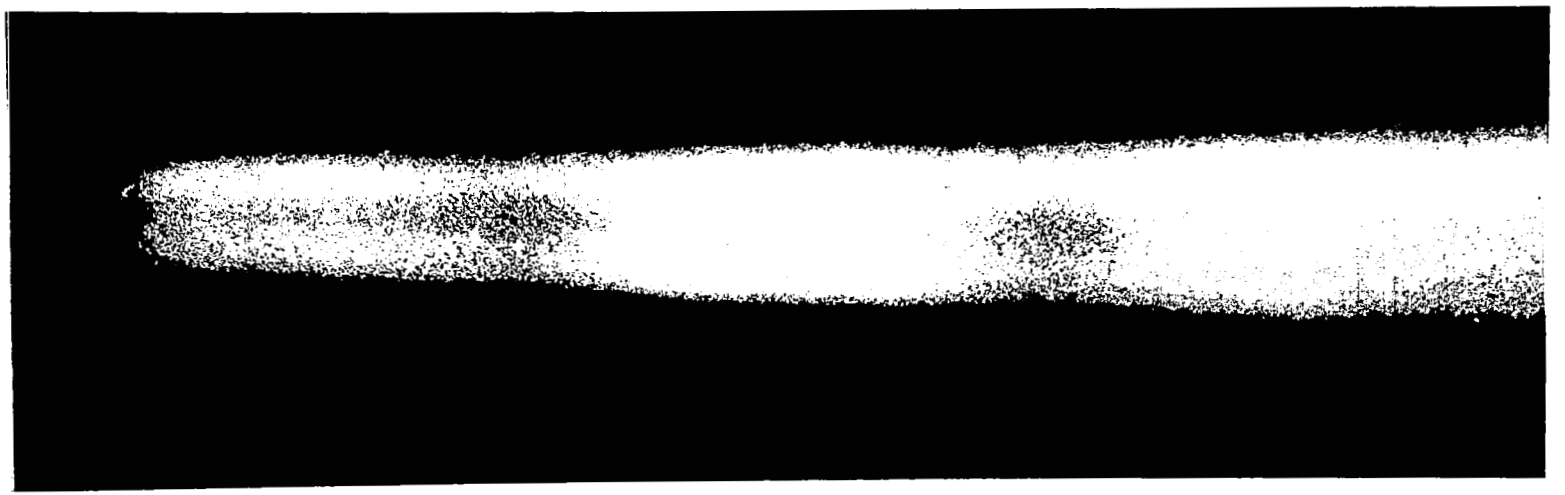

(b) Infrared

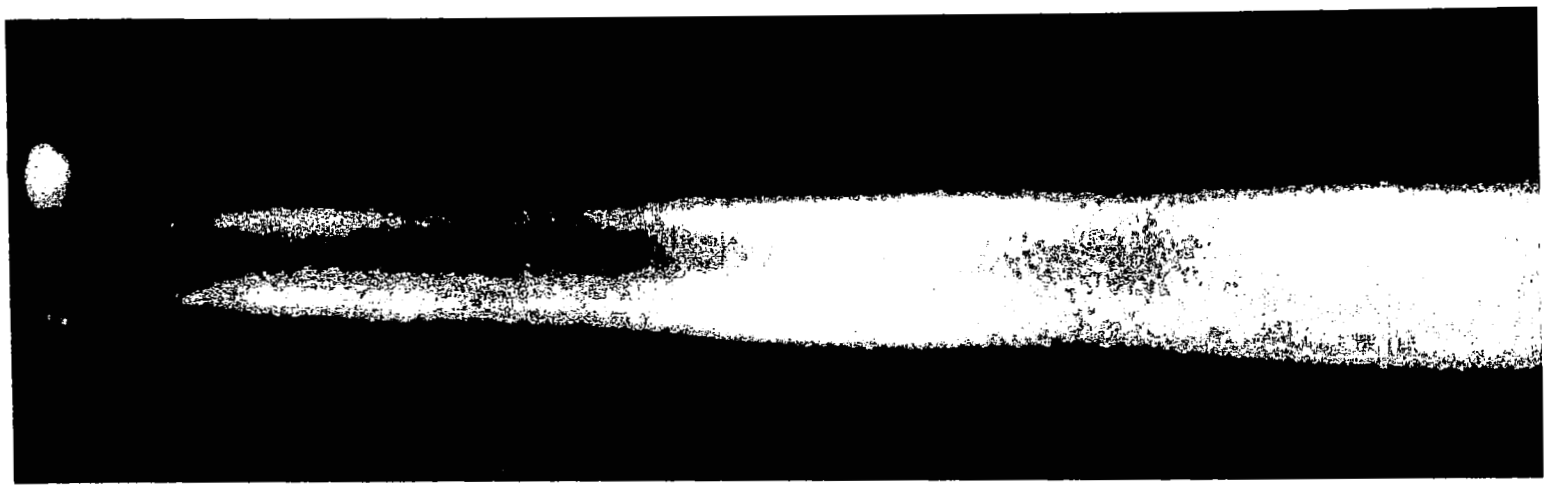

Figure 23. - LOW TEMPERATURE AIR PHOTOGRAPHS

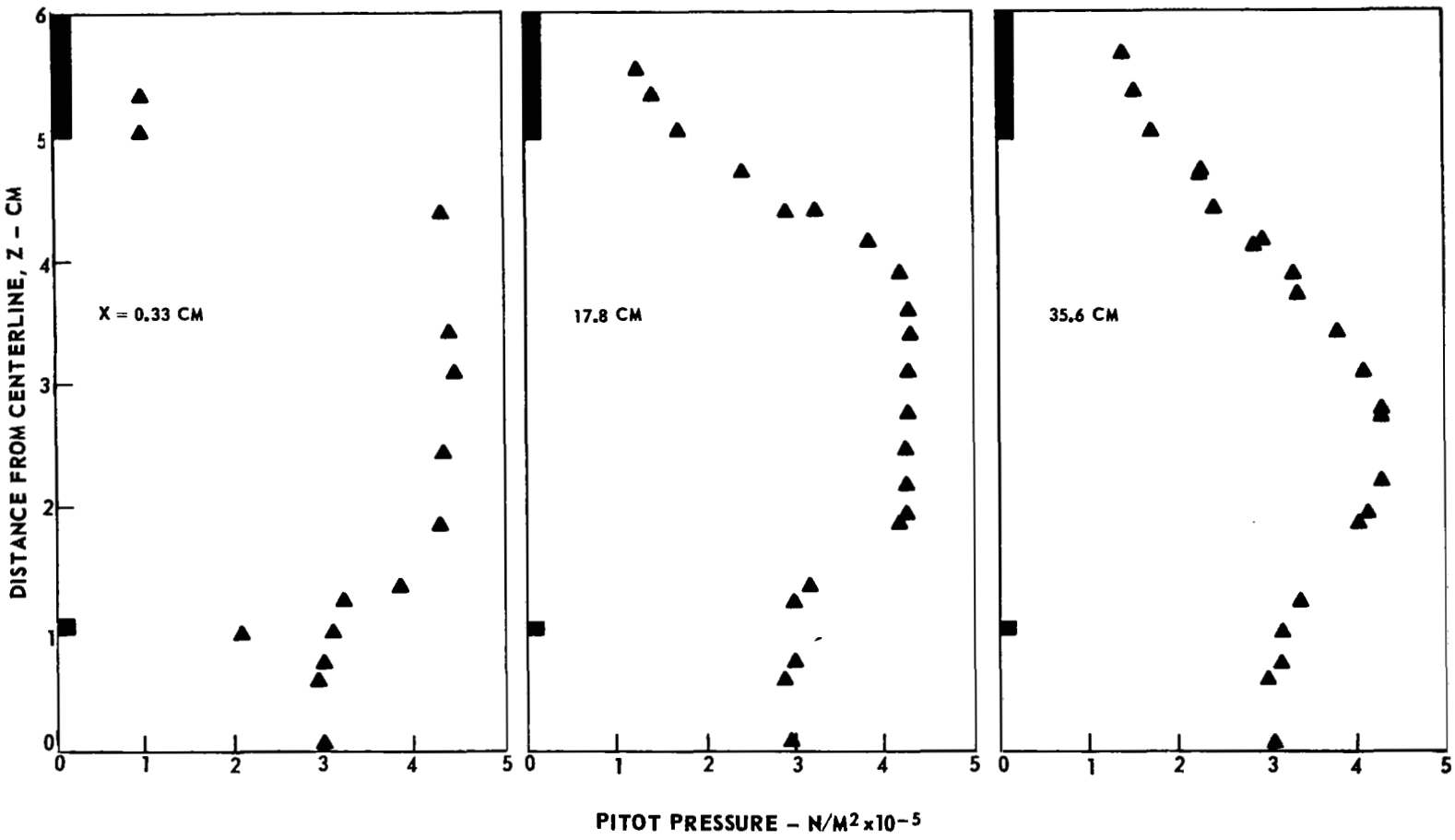

Figure 24. - PITOT PRESSURE PROFILES-HIGH TEMPERATURE VITIATED N_2

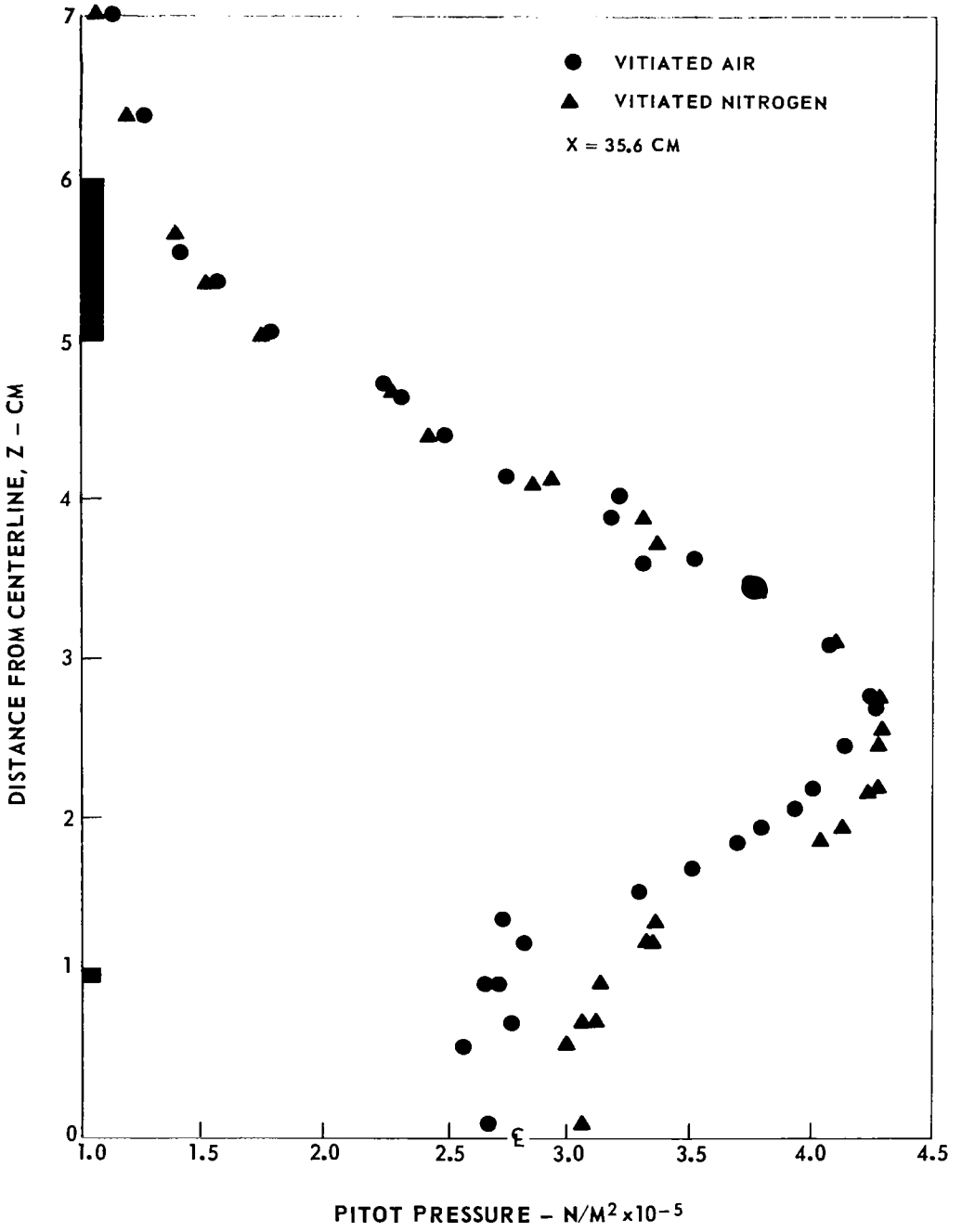

Figure 25. - COMPARISON OF PITOT PRESSURE PROFILES

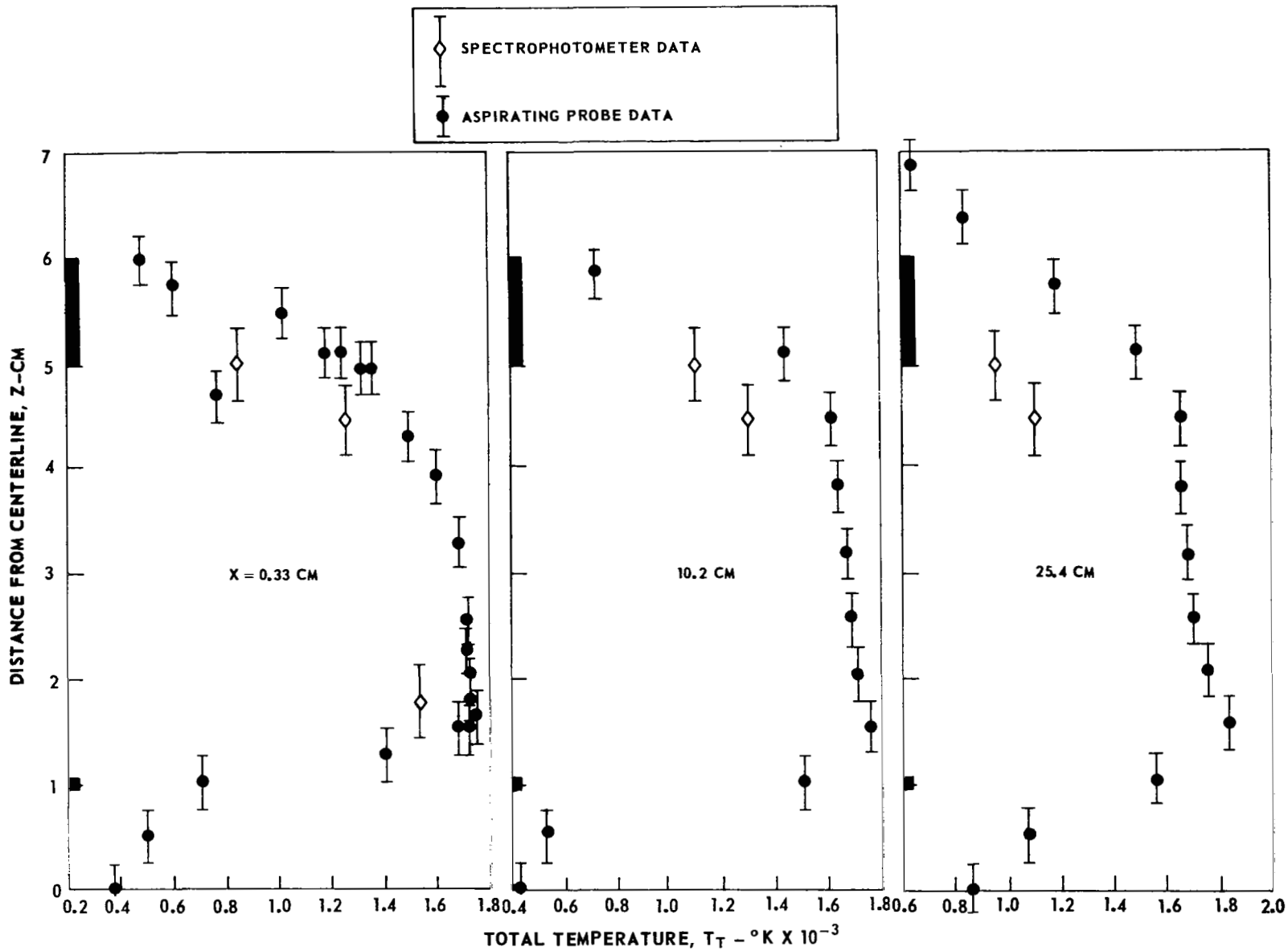

Figure 26. - TOTAL TEMPERATURE PROFILES - HIGH TEMPERATURE VITIATED N_2

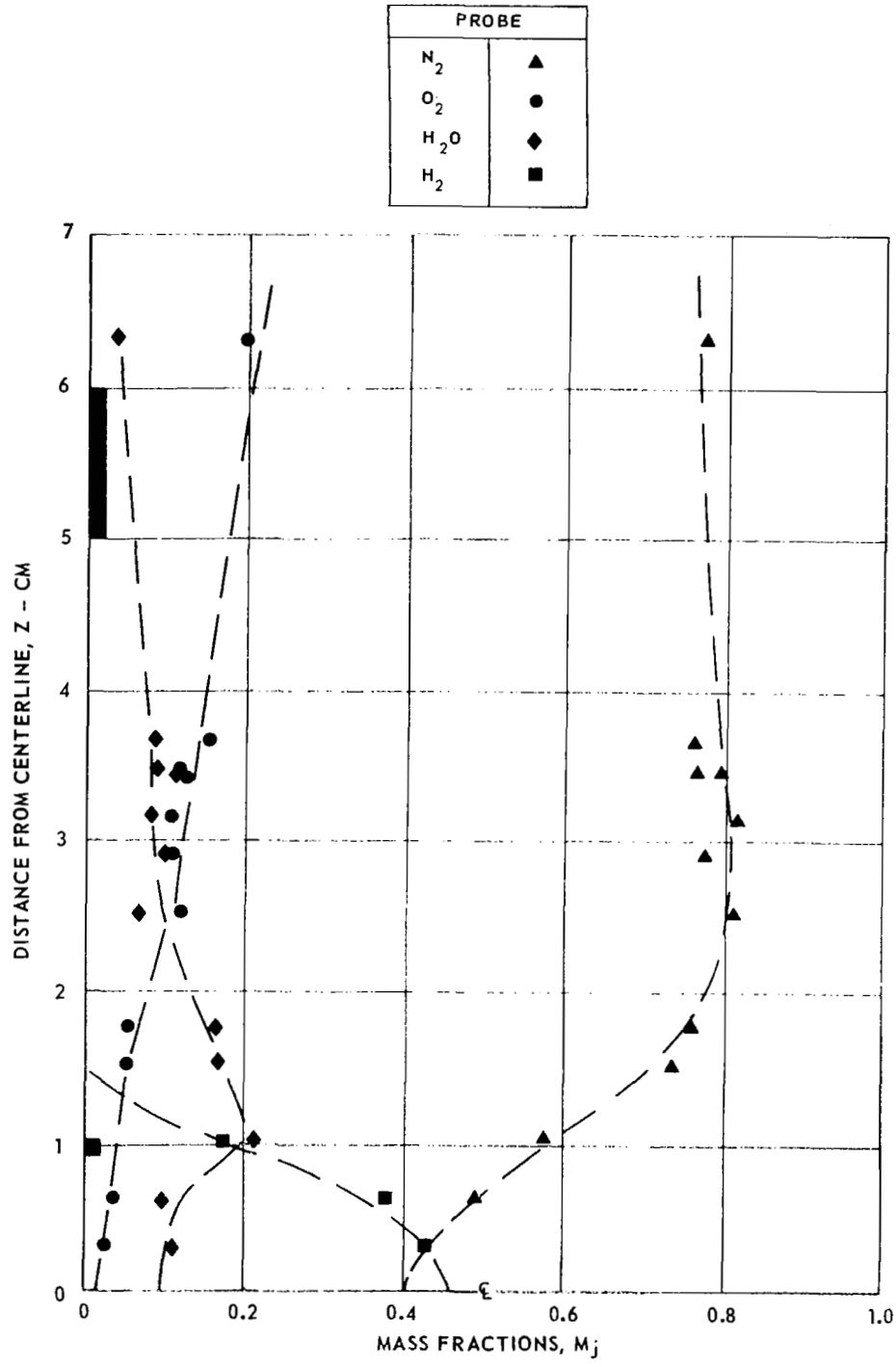

Figure 27. - CONCENTRATION PROFILES AT X = 35.6 cm - HIGH TEMPERATURE VITIATED N_2

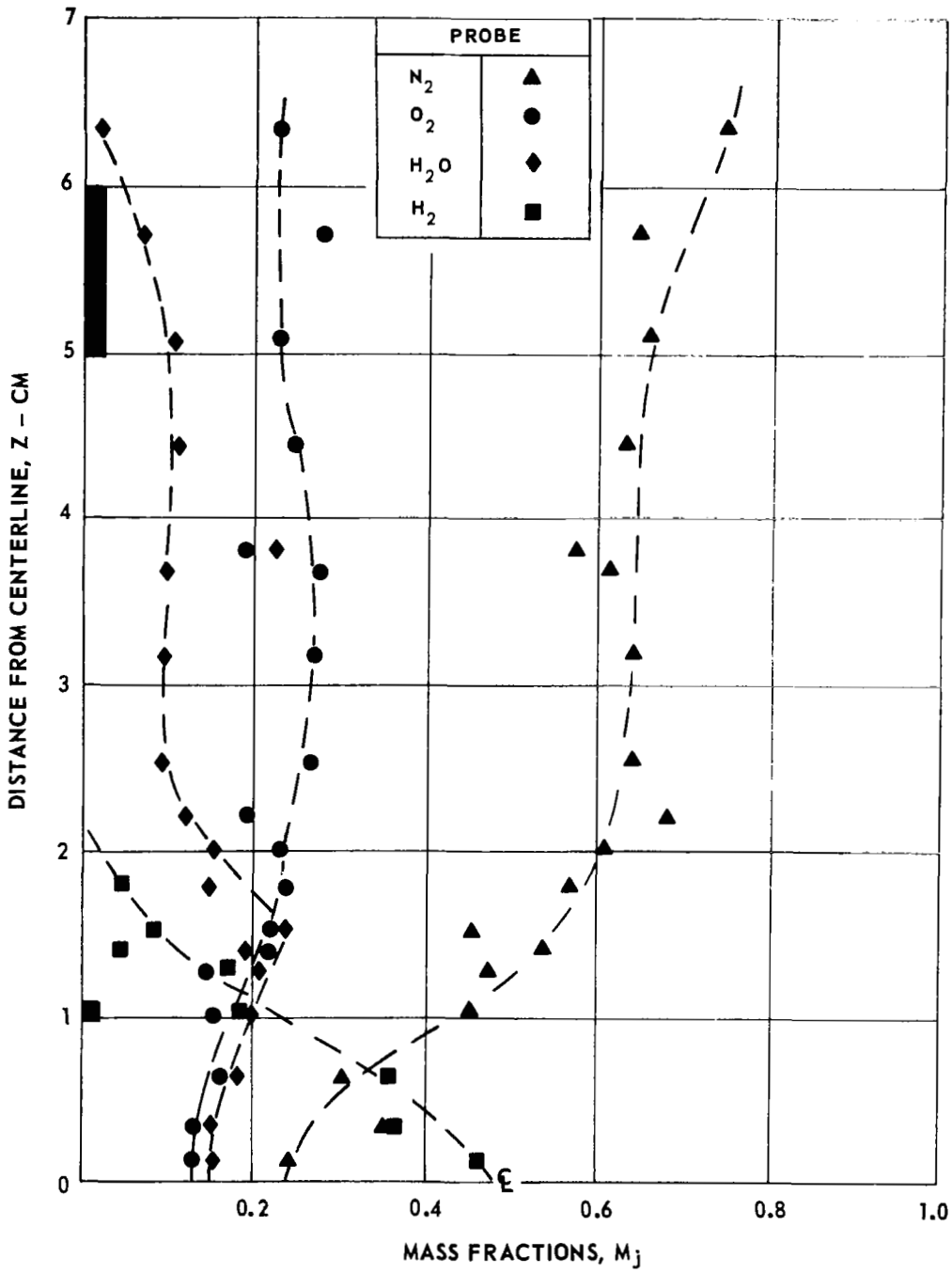

Figure 28. - CONCENTRATION PROFILES AT X = 35.6 cm - HIGH TEMPERATURE VITIATED AIR

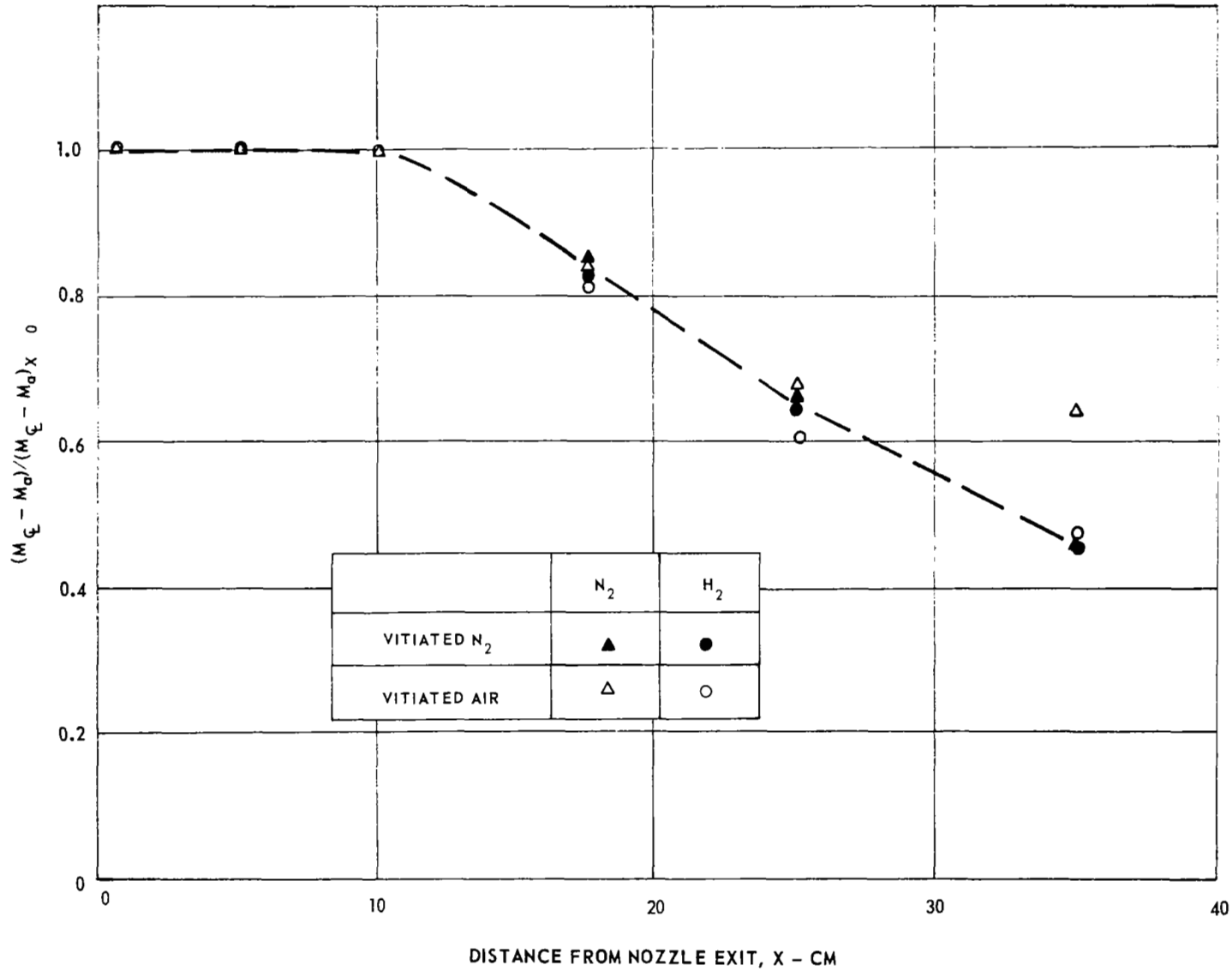

Figure 24. - CENTERLINE CONCENTRATION DECAY

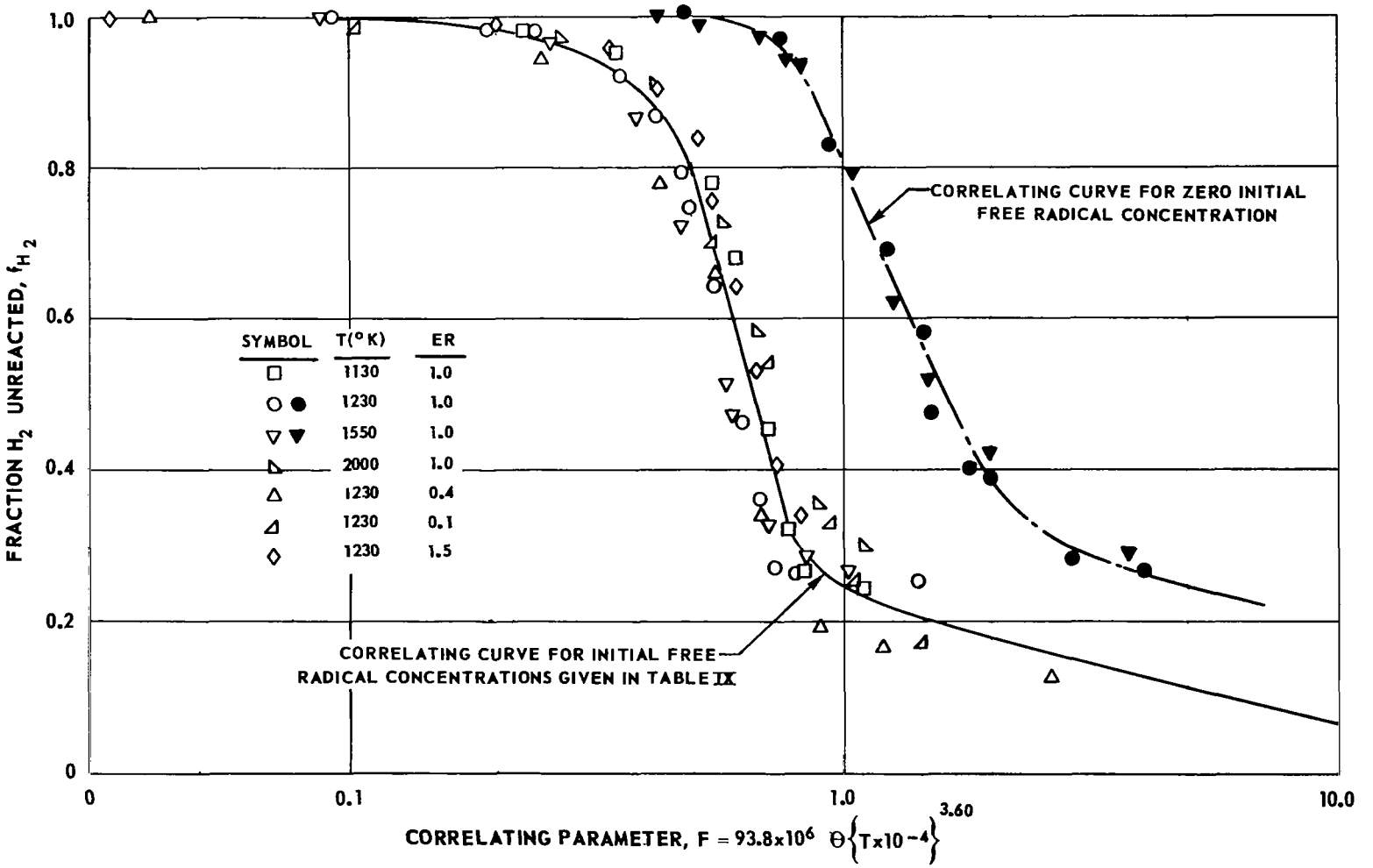

Figure 30. - CORRELATION OF CALCULATED REACTION-TIME HISTORIES FOR THE H_2-O_2 REACTION

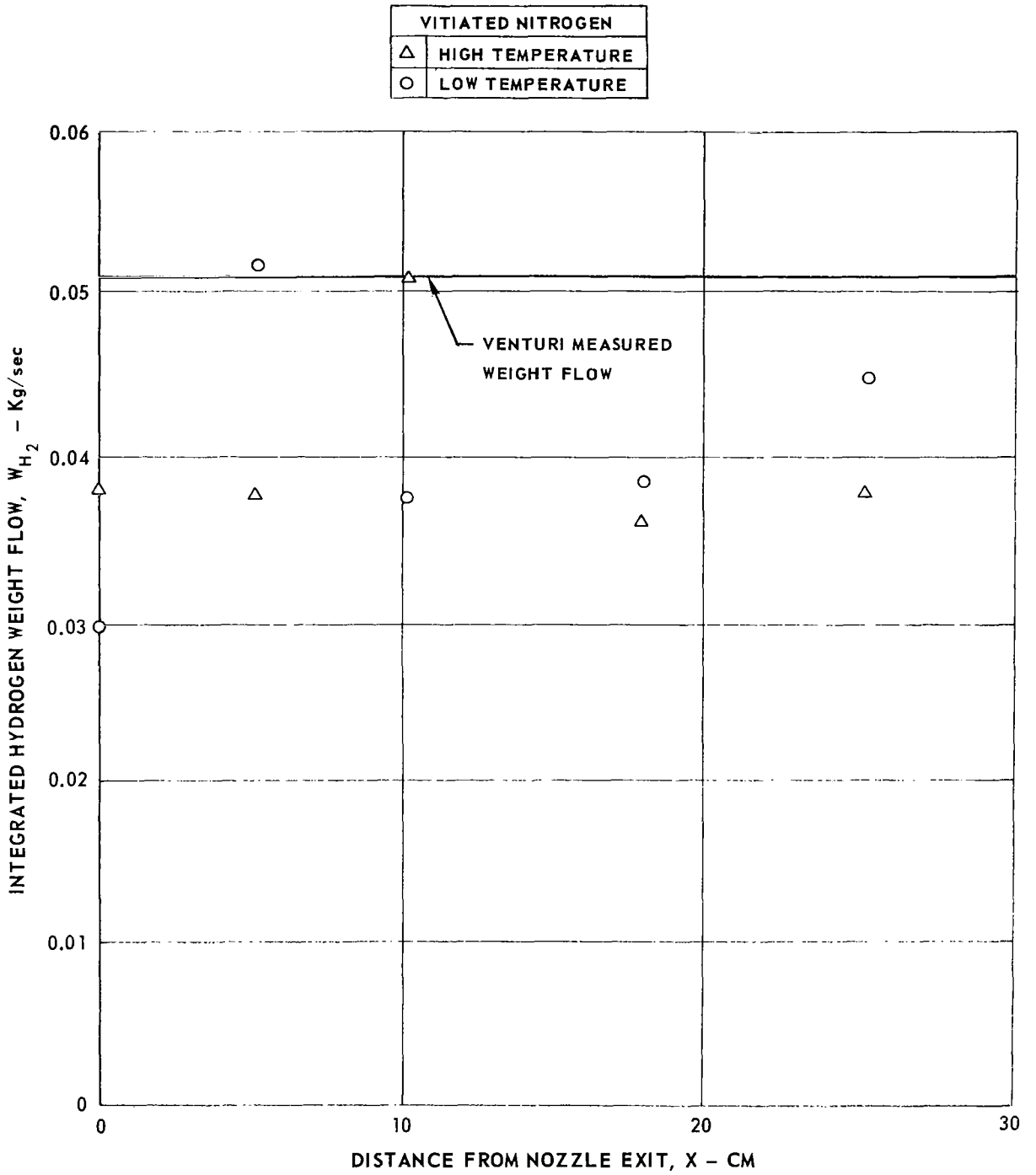

Figure 31. - HYDROGEN WEIGHT FLOWS AT VARIOUS AXIAL STATIONS

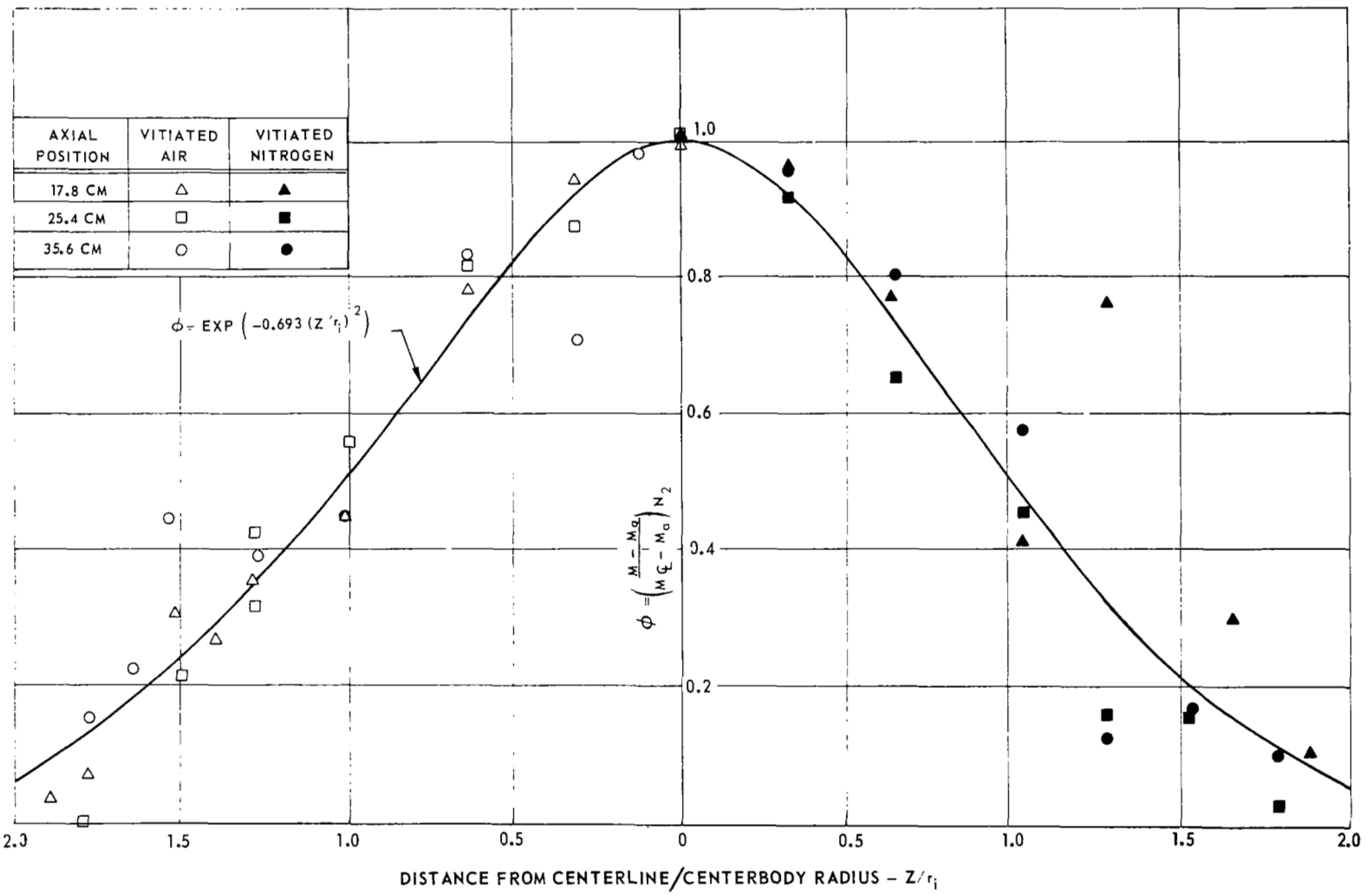

Figure 32. - NORMALIZED CONCENTRATION DISTRIBUTIONS

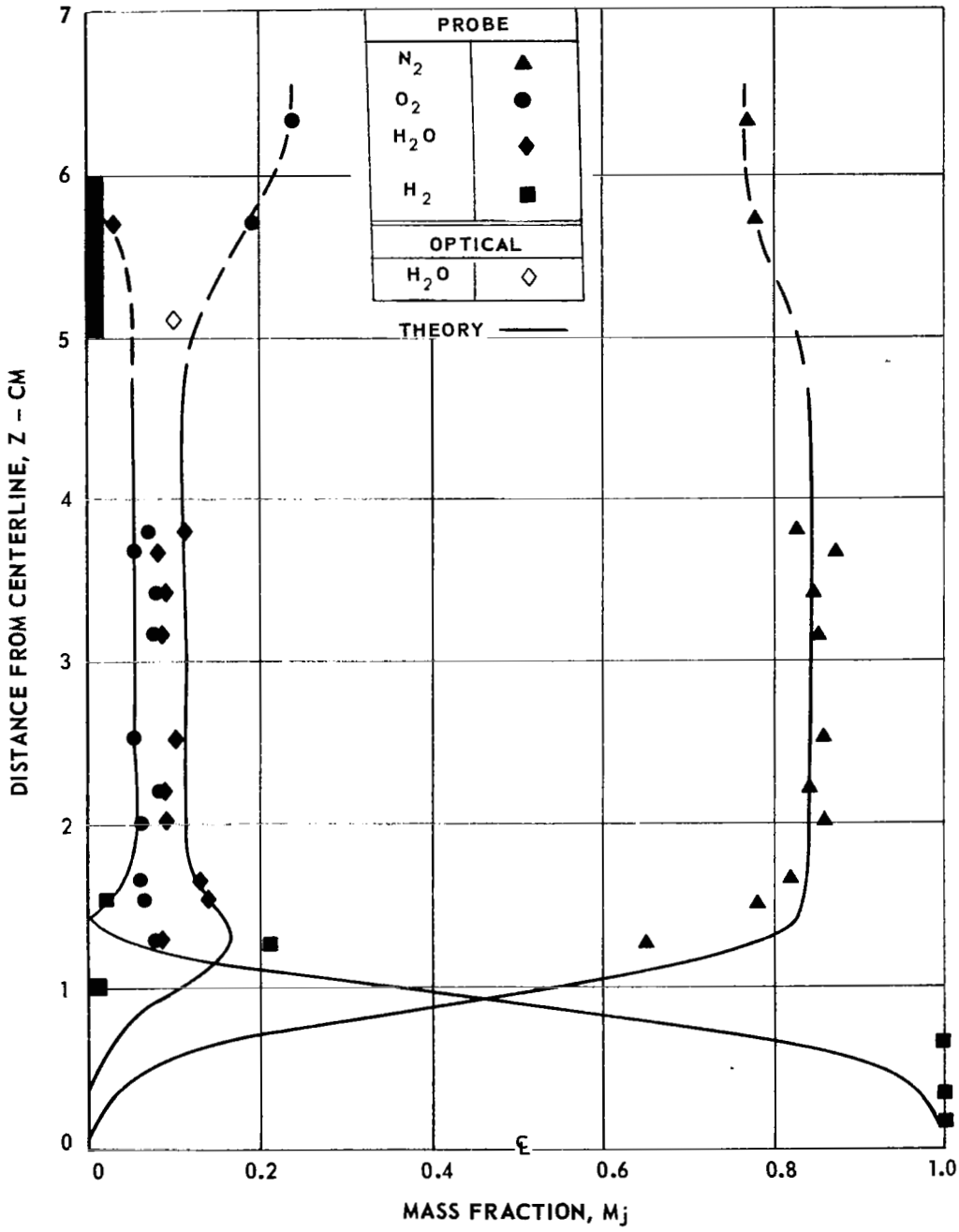

Figure 33. - PREDICTED CONCENTRATION PROFILES AT X = 10.2 cm COMPARED WITH DATA - HIGH TEMPERATURE VITIATED NITROGEN

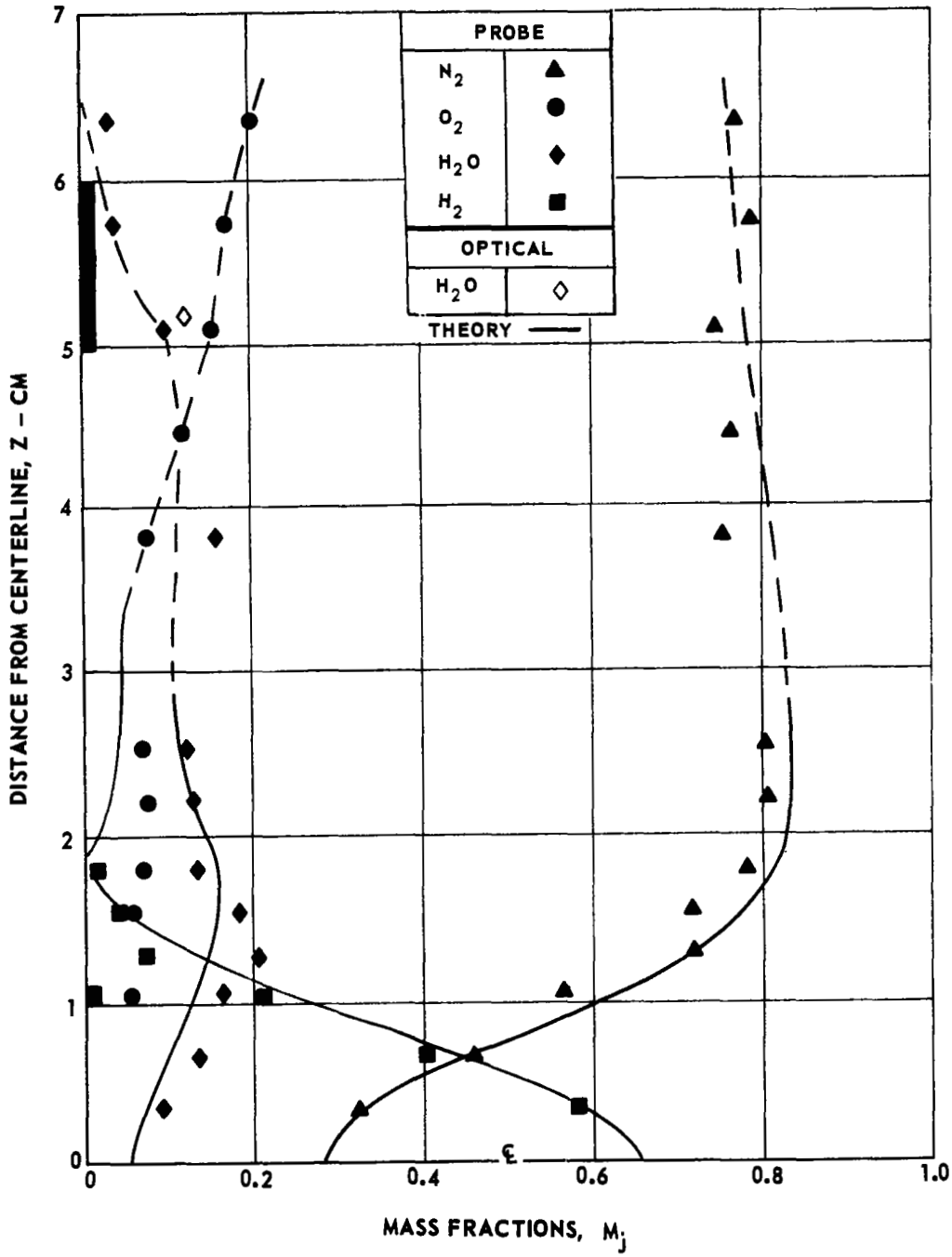

Figure 34. - PREDICTED CONCENTRATION PROFILES AT X = 25.4 cm COMPARED WITH DATA - HIGH TEMPERATURE VITIATED N_2

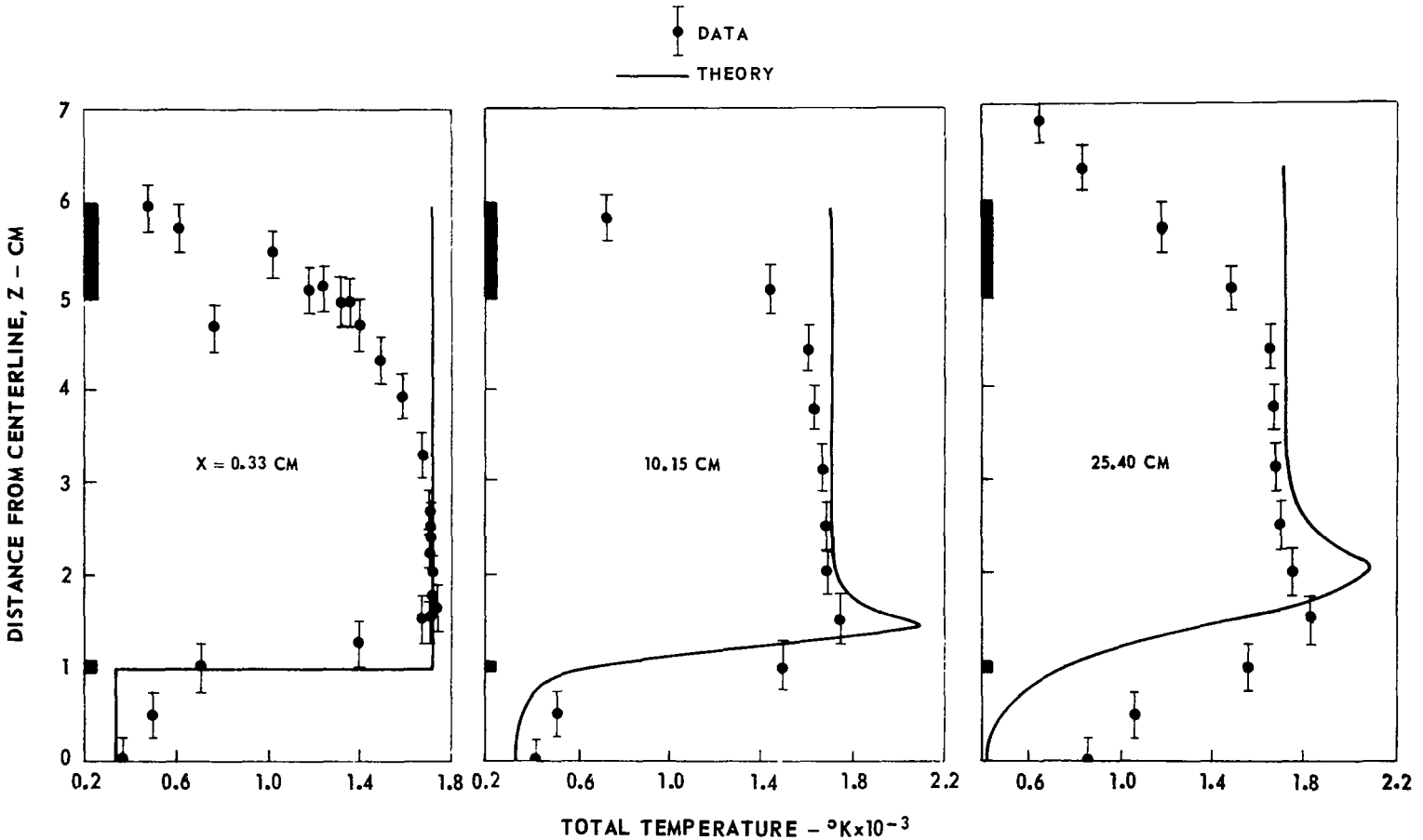

Figure 35. - PREDICTED TOTAL TEMPERATURE PROFILES COMPARED WITH DATA - HIGH TEMPERATURE VITIATED N_2

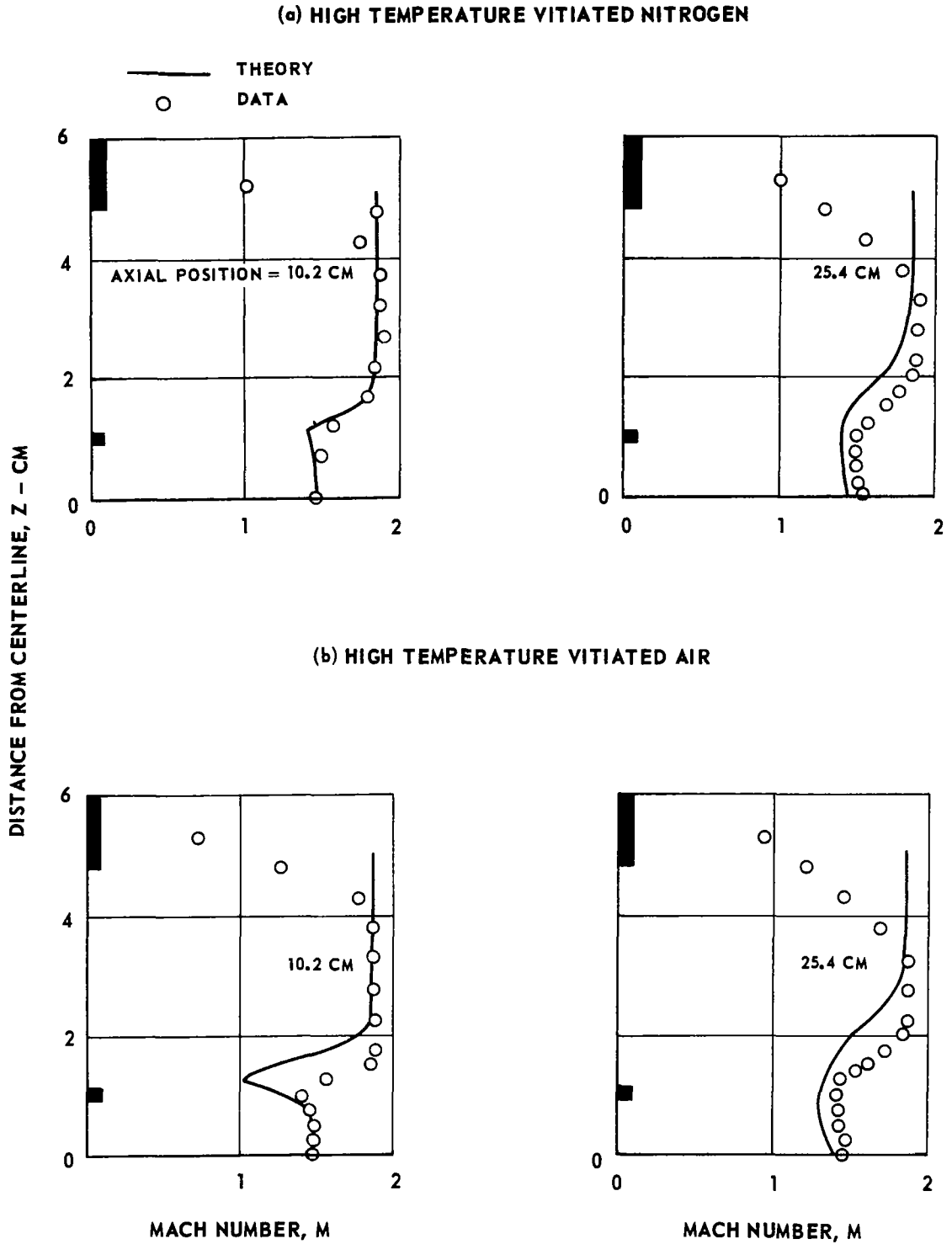

Figure 36. - COMPUTED MACH NUMBER PROFILES COMPARED WITH DATA

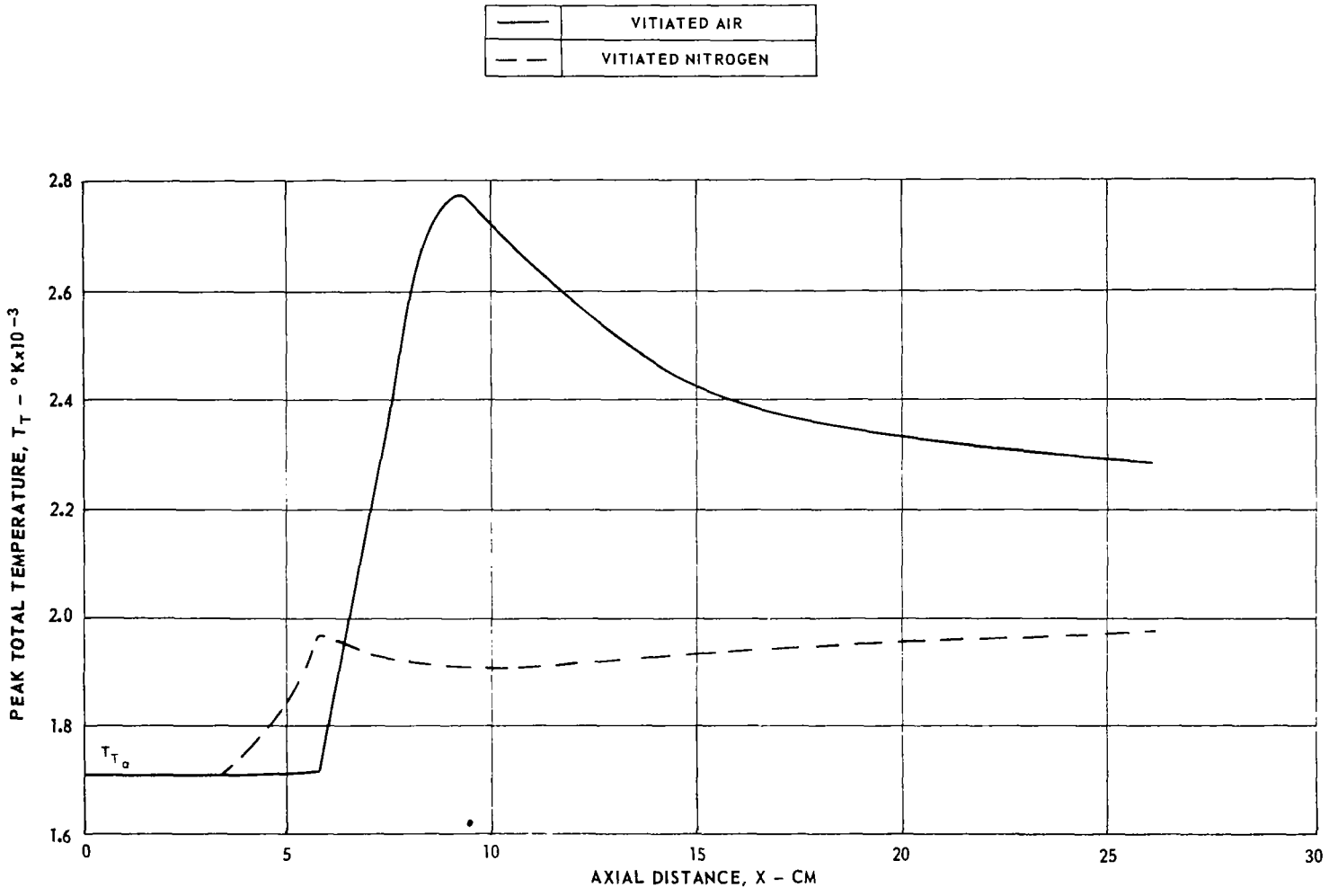

Figure 37. - PEAK TOTAL TEMPERATURES FOR THE HIGH TEMPERATURE CONDITIONS

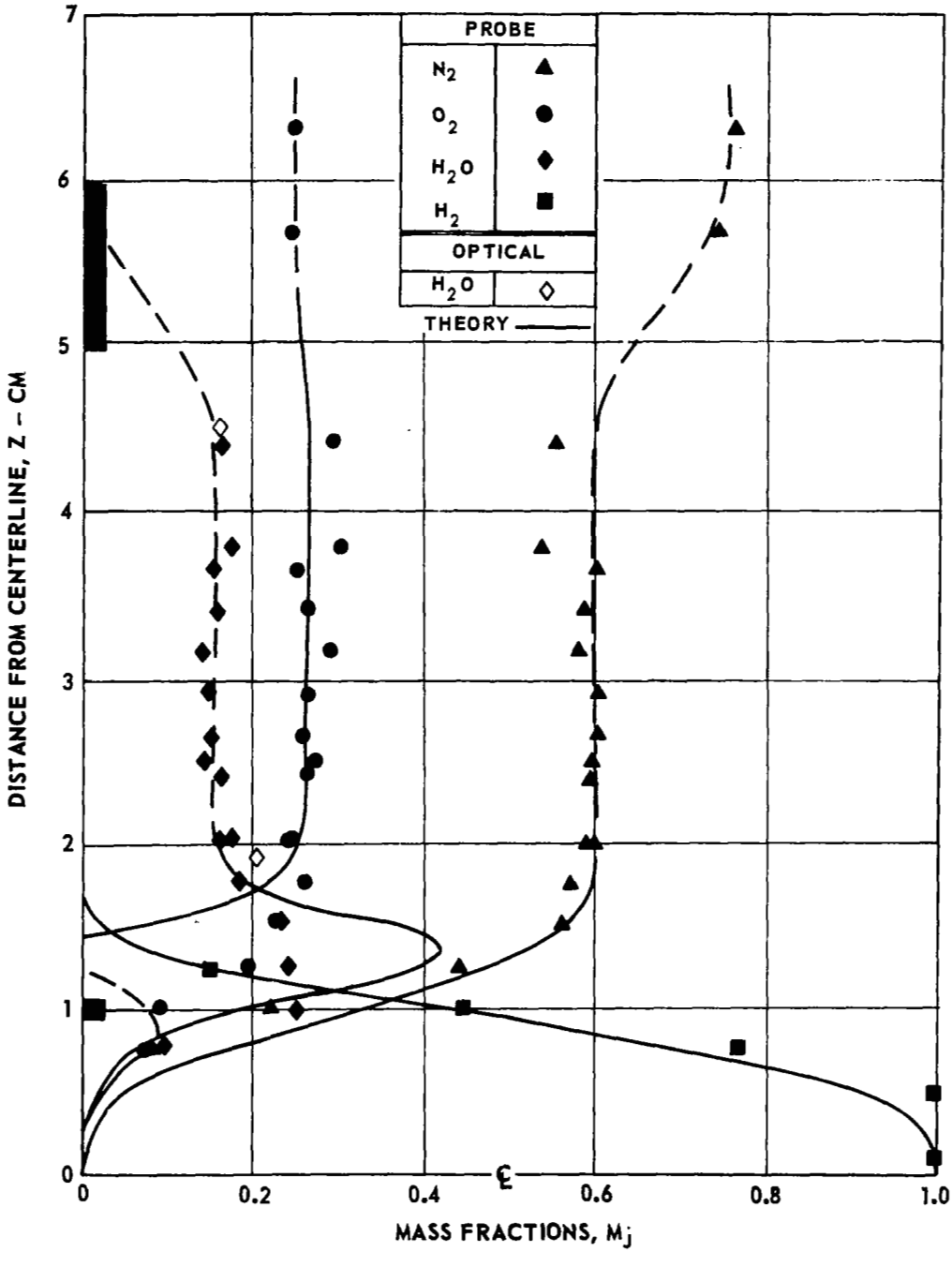

Figure 38. - PREDICTED CONCENTRATION PROFILES AT X = 10.2 cm COMPARED WITH DATA - HIGH TEMPERATURE VITIATED AIR

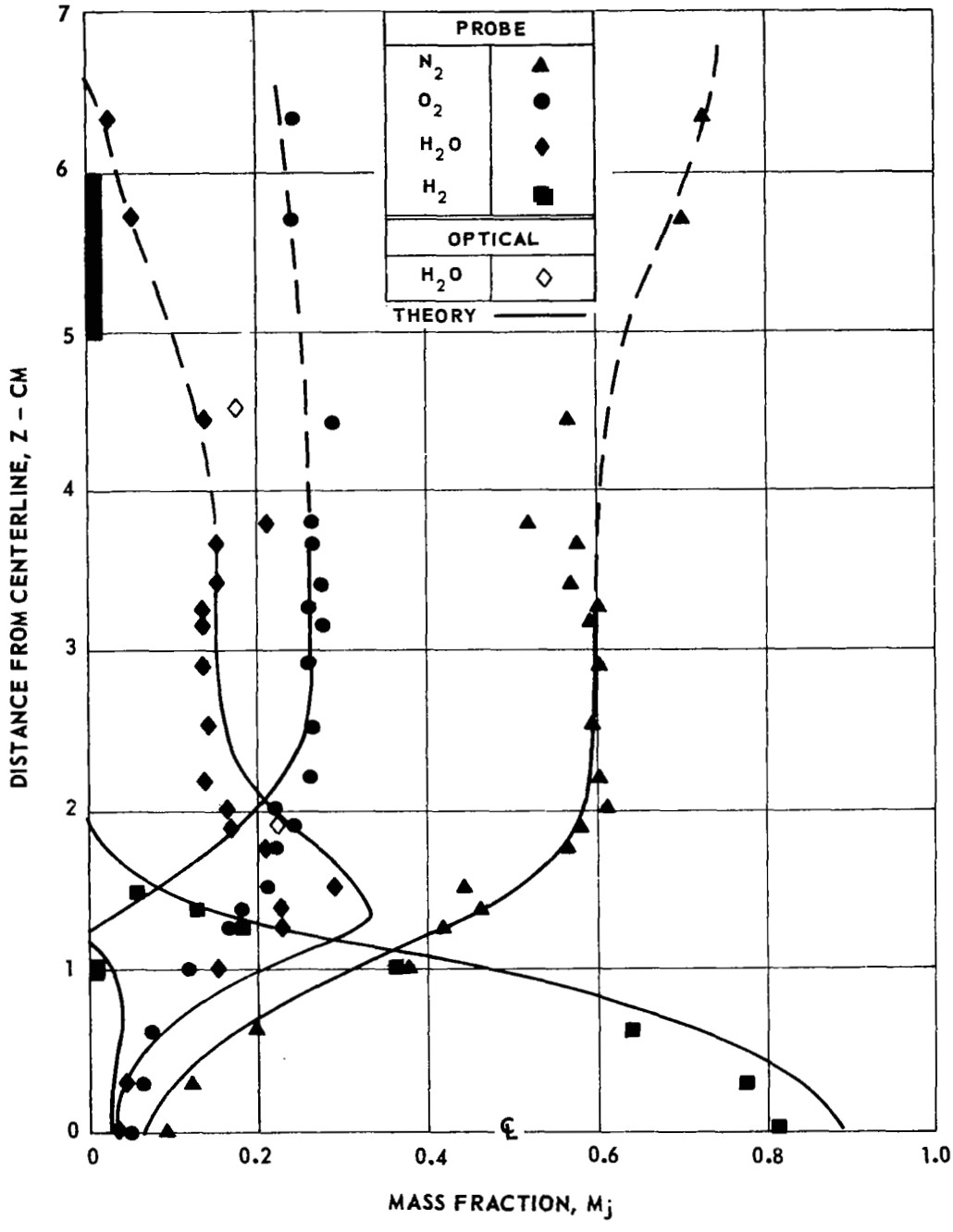

Figure 39. - PREDICTED CONCENTRATION PROFILES AT X = 17.8 cm COMPARED WITH DATA - HIGH TEMPERATURE VITIATED AIR

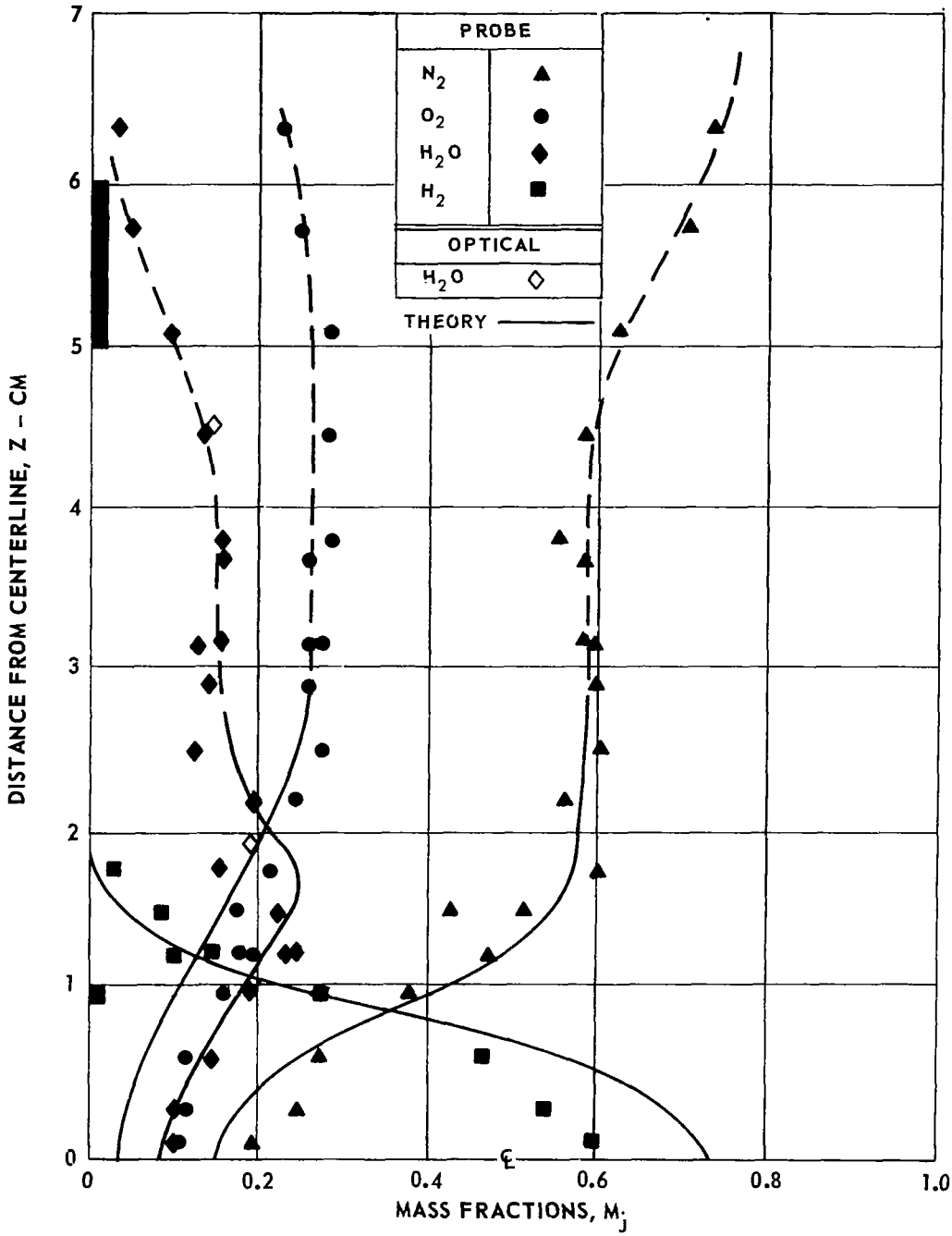

Figure 40. - PREDICTED CONCENTRATION PROFILES AT X = 25.4 cm COMPARED WITH DATA - HIGH TEMPERATURE VITIATED AIR

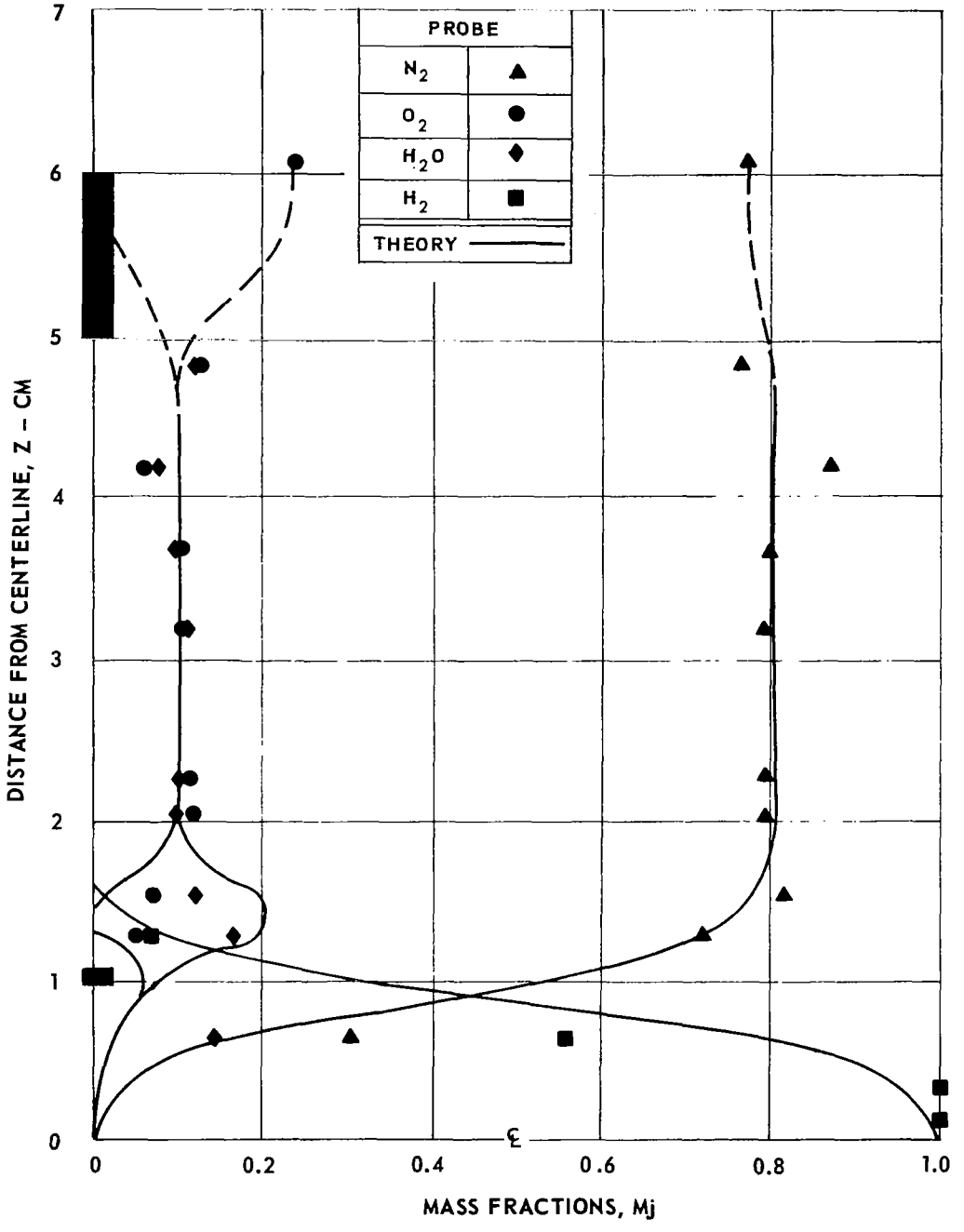

Figure 41. - PREDICTED CONCENTRATION PROFILES AT X = 10.2 cm COMPARED WITH DATA - LOW TEMPERATURE VITIATED N_2

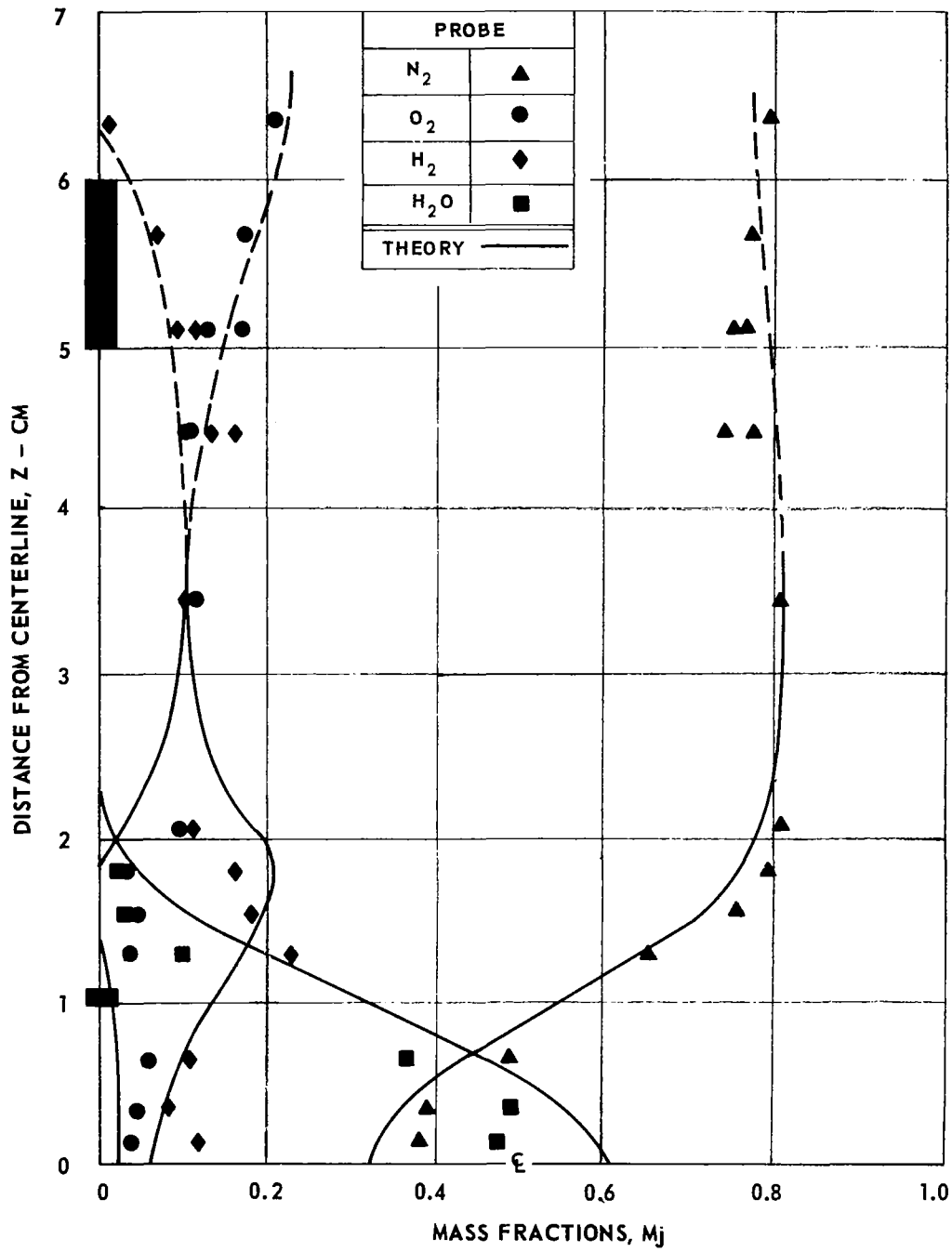

Figure 42. - PREDICTED CONCENTRATION PROFILES AT X = 25.4 cm COMPARED WITH DATA - LOW TEMPERATURE VITIATED N_2

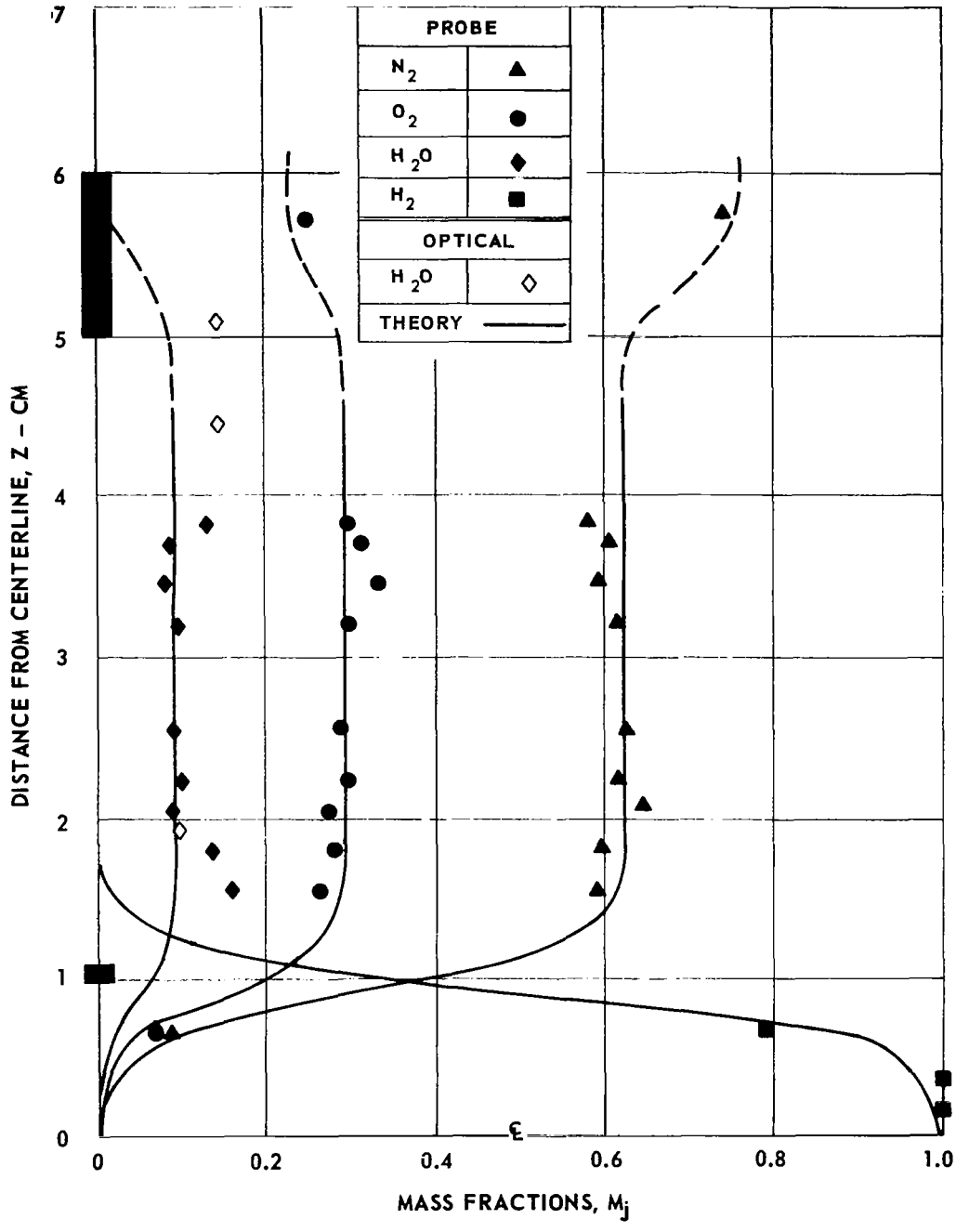

Figure 43. - PREDICTED CONCENTRATION PROFILES AT X = 10.2 cm COMPARED WITH DATA - LOW TEMPERATURE VITIATED AIR

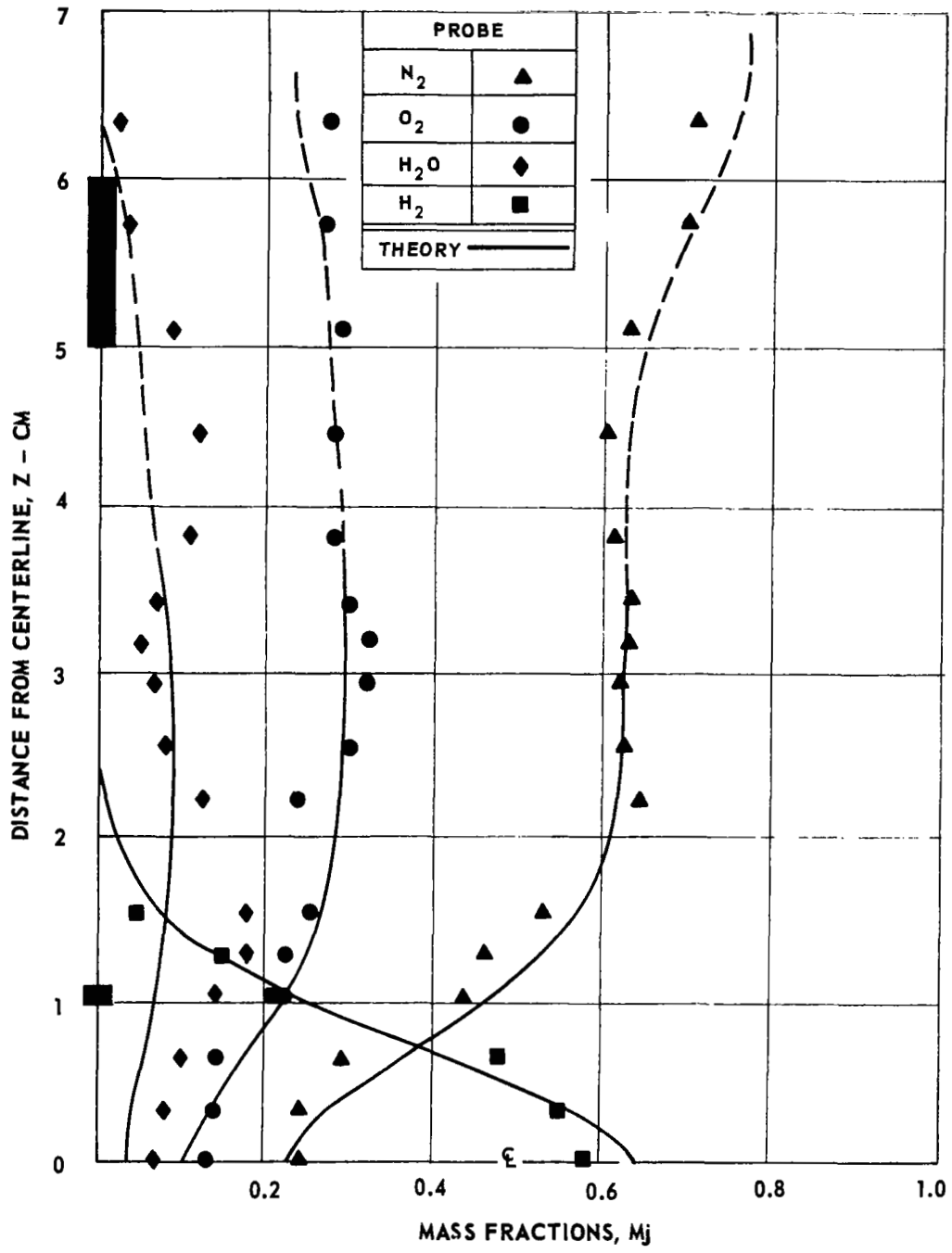

Figure 44. - PREDICTED CONCENTRATION PROFILES AT X = 25.4 cm COMPARED WITH DATA - LOW TEMPERATURE VITIATED AIR

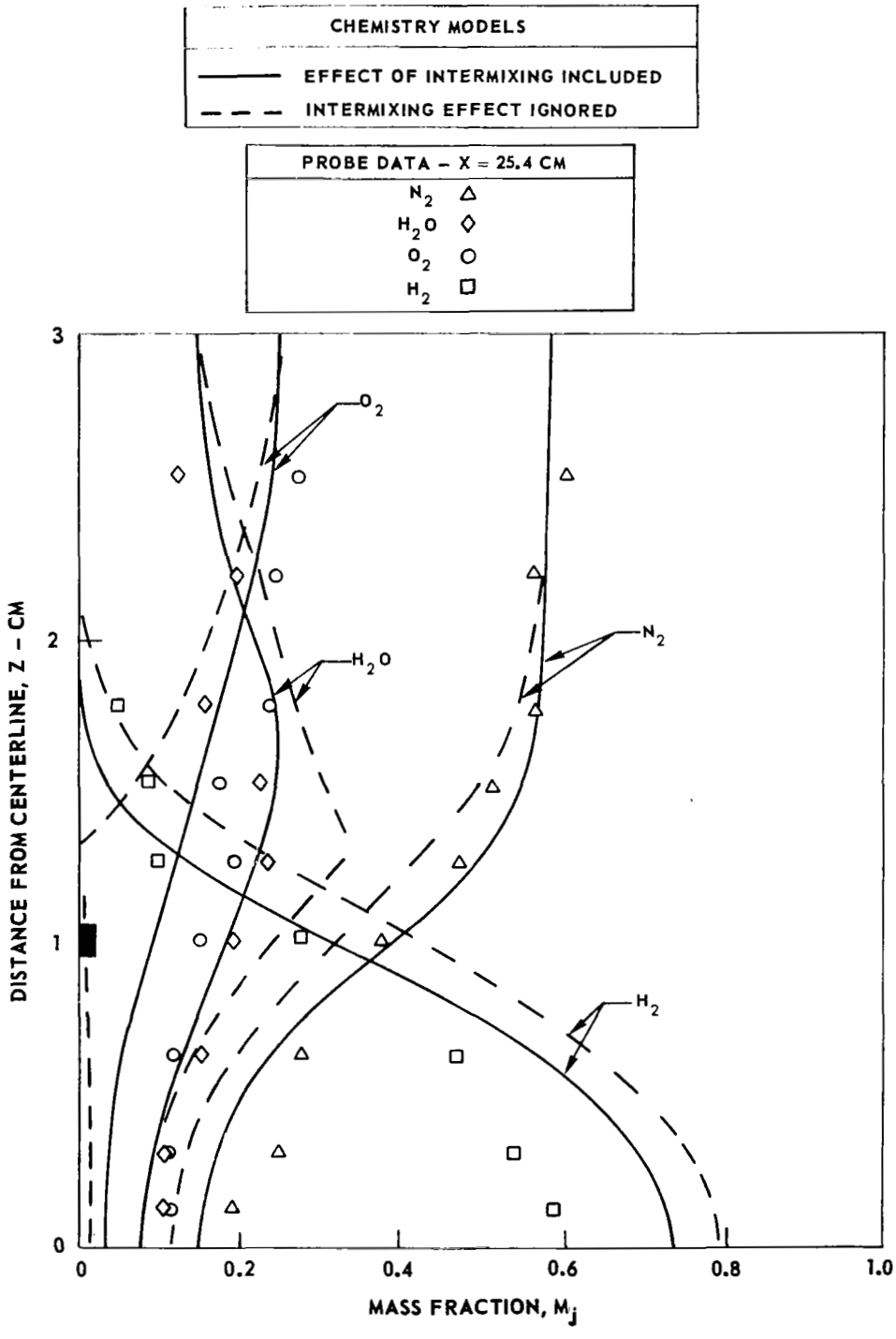

Figure 45. - THE INFLUENCE OF MIXING FLUID WITH DIFFERENT REACTION TIME HISTORIES ON PREDICTED SPECIES CONCENTRATIONS

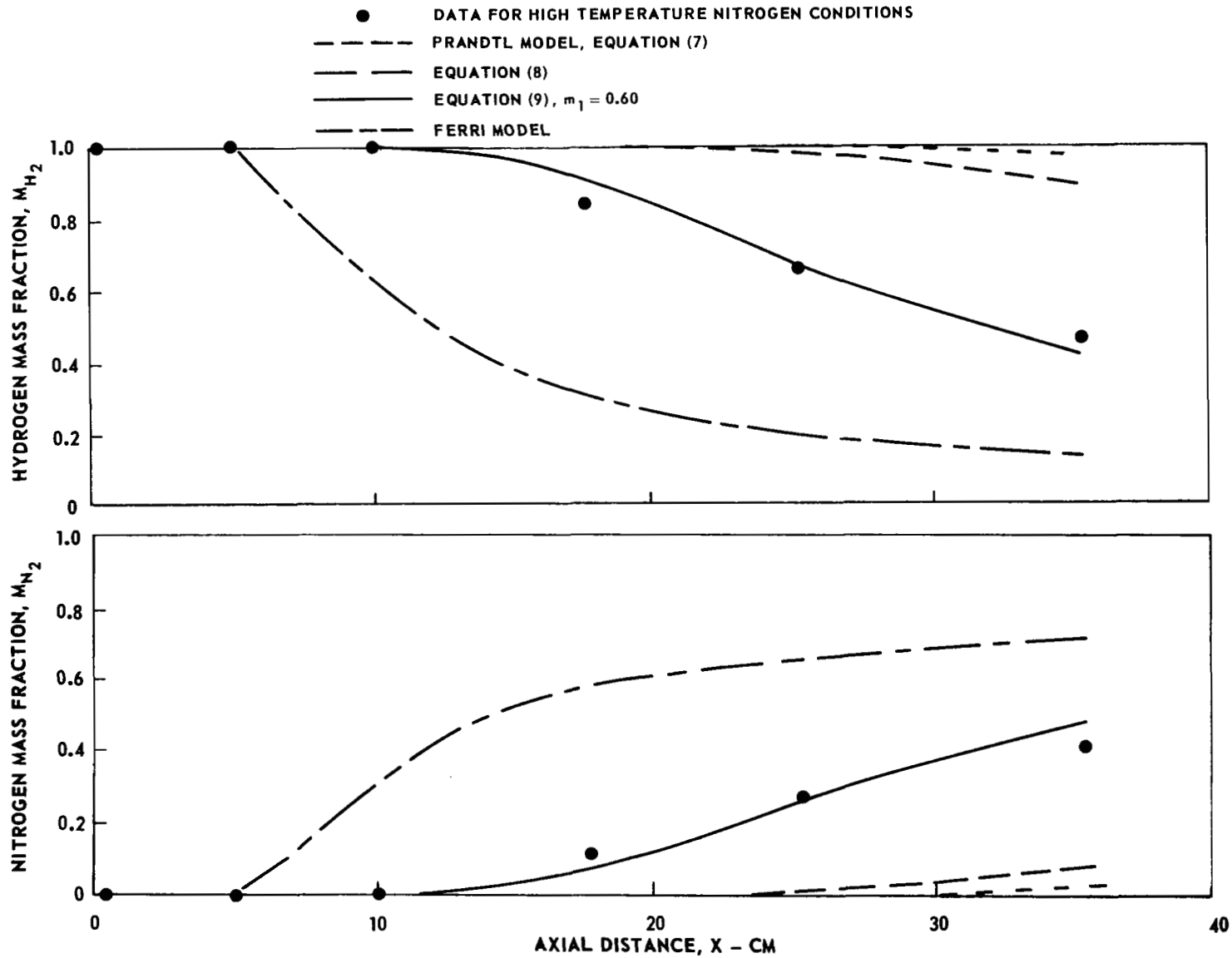

Figure 46. - CENTERLINE CONCENTRATION DECAY: COMPARISON OF DATA WITH DIFFERENT MIXING MODELS

NASA-Langley, 1969 — 33 CR-1473